ECF-200E-19-0003
Revision 0

# Groundwater Flow and Migration Calculations for Annual Assessment of the Final Status Monitoring Networks for the 200 East Area Dangerous Waste Management Units

Prepared for the U.S. Department of Energy
Assistant Secretary for Environmental Management

Contractor for the U.S. Department of Energy
under Contract DE-AC06-08RL14788

CH2MHILL
Plateau Remediation Company

**P.O. Box 1600**
**Richland, Washington 99352**

Approved for Public Release;
Further Dissemination Unlimited

This page intentionally left blank.

ECF-200E-19-0003
Revision 0

# Groundwater Flow and Migration Calculations for Annual Assessment of the Final Status Monitoring Networks for the 200 East Area Dangerous Waste Management Units

Date Published
July 2019

Prepared for the U.S. Department of Energy
Assistant Secretary for Environmental Management

Contractor for the U.S. Department of Energy
under Contract DE-AC06-08RL14788

CH2MHILL
Plateau Remediation Company
**P.O. Box 1600**
**Richland, Washington 99352**

APPROVED
By Janis D. Aardal at 2:51 pm, Jul 01, 2019

Release Approval | Date

Approved for Public Release;
Further Dissemination Unlimited

**TRADEMARK DISCLAIMER**

Reference herein to any specific commercial product, process, or service by tradename, trademark, manufacturer, or otherwise, does not necessarily constitute or imply its endorsement, recommendation, or favoring by the United States Government or any agency thereof or its contractors or subcontractors.

This report has been reproduced from the best available copy.

Printed in the United States of America

# ENVIRONMENTAL CALCULATION COVER PAGE

**SECTION 1 - Completed by the Responsible Manager**

| | |
|---|---|
| Project: 200 East Area- Annual Assessment of Final Status Monitoring Networks | **RELEASE / ISSUE** |
| Date: 6/4/2019 | DATE: Jul 01, 2019 HANFORD RELEASE |
| Calculation Title and Description: Groundwater Flow and Migration Calculations for Annual Assessment of the Final Status Monitoring Networks for the 200 East Area Dangerous Waste Management Units | |

**Qualifications Summary**

**Preparer(s):**

Name: Mashrur Chowdhury

Degree, Major, Institution, Year: MASc., Civil Engineering (Water), University of Waterloo, 2016
BASc., Environmental Engineering (Water Resources), University of Waterloo, 2014

Professional Licenses:

Brief Narrative of Experience: Mashrur Chowdhury provides expertise in the application and calibration of numerical groundwater flow models for use in regulatory hydrogeological assessments and remediation studies. He has experience working with large sites characterized by complex hydrogeology and interpreting data from hydrogeological investigations.

**Checker(s):**

Name: Marinko Karanovic

Degree, Major, Institution, Year: BS, Hydrogeology, University of Belgrade, 1999
MS, Hydrogeology, Ohio State University, 2005

Professional Licenses:

Brief Narrative of Experience: Mr. Karanovic has technical expertise in Hydrogeology, Numerical groundwater flow and contaminant transport modeling, programming and software development. His experience includes interpreting data from hydrogeologic investigations, creation and modification of groundwater flow and transport models, and assisting in remedial design and optimization. He is the developer of GroundWater Desktop, a fully three-dimensional (3D) interface for visualization and 3D analysis of groundwater models and their results and Environmental data such as water levels and chemistry. He has worked with groundwater flow models to assess flow and transport of contaminants at several Superfund Sites.

## ENVIRONMENTAL CALCULATION COVER PAGE (Continued)

**Senior Reviewer(s):**

Name: Charles W. Miller

Degree, Major, Institution, Year: BS, Soil Science, University of Idaho, 1983

Professional Licenses: Professional Geologist, Professional Hydrogeologist, Washington State

Brief Narrative of Experience: Charles Miller has 30 years combined experience in characterization and evaluation of environmental conditions. He has scoped, managed, implemented and reported investigations and remedial actions at a wide variety of industrial locations within the United States including military, nuclear and chemical industrial facilities. Particularly, industrial sites under DOD, NRC, and DOE management. He is experienced in RCRA RFI/CMS, CERCLA RI/FS, NRC Closure/License Termination actions and required remedial actions.

**SECTION 2 - Completed by Preparer**

Calculation Number: ECF-200E-19-0003 | Revision Number: 0

**Revision History**

| Revision No. | Description | Date | Affected Pages |
|---|---|---|---|
| | | | |

**SECTION 3 - Completed by the Responsible Manager**

**Document Control:**

Is the document intended to be controlled within the Document Management Control System (DMCS)? (●) Yes ( ) No

Does document contain scientific and technical information intended for public use? (●) Yes ( ) No

Does document contain controlled-use information? ( ) Yes (●) No

**SECTION 4 - Document Review and Approval**

| | | | |
|---|---|---|---|
| Preparer(s): | | | |
| Mashrur Chowdhury | S. Staff Scientist | | 6/4/19 |
| *Print First and Last Name* | *Position* | *Signature* | *Date* |
| Checker(s): | | | |
| Marinko Karanovic | S. Project Hydrogeo. | | 6/4/19 |
| *Print First and Last Name* | *Position* | *Signature* | *Date* |
| Senior Reviewer(s): | | | |
| Charles W. Miller | Associated Expert | | 6/4/19 |
| *Print First and Last Name* | *Position* | *Signature* | *Date* |
| Responsible Manager(s): | | | |
| William R. Faught | Manager | | 6-6-19 |
| *Print First and Last Name* | *Position* | *Signature* | *Date* |

| ENVIRONMENTAL CALCULATION COVER PAGE (Continued) | | |
|---|---|---|
| **SECTION 5 - Applicable if Calculation is a Risk Assessment or Uses an Environmental Model** | | |
| **Prior to Initiating Modeling:** | | |
| Required training for modelers completed:<br>Integration Lead: | | |
| *Print First and Last Name* | *Signature* | *Date* |
| Safety Software Approved:<br>Integration Lead: | | |
| *Print First and Last Name* | *Signature* | *Date* |
| **Calculation Approved:**<br>Risk/Modeling Integration Manager: | | |
| *Print First and Last Name* | *Signature* | *Date* |

This page intentionally left blank.

# Contents

**1 Purpose ..... 1-1**

**2 Background ..... 2-1**

2.1 200 East Area Groundwater ..... 2-1
2.2 Gradient and Flow Path Interpretation Overview ..... 2-2

**3 Calculation Methods ..... 3-1**

3.1 Water-Level Mapping Using the Tikhonov Regularized Inverse Method ..... 3-1
3.1.1 Data Used ..... 3-1
3.1.2 Method Description ..... 3-1
3.1.3 Implementation Using MODFLOW-USG and PEST ..... 3-3
3.2 Particle Tracking and Relative Detectability ..... 3-6
3.2.1 Particle Tracking ..... 3-7
3.2.2 Relative Detectability ..... 3-7
3.3 Evaluation of Vertical Migration Potential ..... 3-7

**4 Assumptions and Inputs ..... 4-1**

4.1 Assumptions ..... 4-1
4.1.1 Tikhonov Regularized Inverse Method of Water-Level Analysis ..... 4-1
4.1.2 Particle Tracking ..... 4-1
4.2 Input Data ..... 4-2
4.2.1 Water-Level Mapping Input ..... 4-2
4.2.2 Particle Starting Locations ..... 4-3

**5 Software Applications, Descriptions, Installation and Checkout, and Statements of Validity ..... 5-1**

5.1 Approved Software ..... 5-1
5.2 Software Description ..... 5-1
5.3 Support Software ..... 5-1
5.4 Software Installation and Checkout ..... 5-2
5.4.1 Statement of Valid Software Application ..... 5-2

**6 Calculations ..... 6-1**

6.1 Water-Level Analysis ..... 6-1
6.2 Particle Tracking ..... 6-5
6.3 Relative Detectability ..... 6-6

**7 Results ..... 7-1**

7.1 216-A-29 Ditch Input and Results ..... 7-1
7.1.1 Release Locations and Relative Detectability Grid for the 216-A-29 Ditch ..... 7-1

7.1.2 Results for the 216-A-29 Ditch ..... 7-6
7.2 216-A-36B Crib Input and Results ..... 7-9
7.2.1 Release Locations and Relative Detectability Grid for the 216-A-36B Crib ..... 7-9
7.2.2 Results for the 216-A-36B Crib ..... 7-9
7.3 216-A-37-1 Crib Input and Results ..... 7-12
7.3.1 Release Locations and Relative Detectability Grid for the 216-A-37-1 Crib ..... 7-16
7.3.2 Results for the 216-A-37-1 Crib ..... 7-16
7.4 216-B-3 Main Pond Input and Results ..... 7-20
7.4.1 Release Locations and Relative Detectability Grid for the 216-B-3 Pond ..... 7-20
7.4.2 Results for the 216-B-3 Pond ..... 7-23
7.5 216-B-63 Trench Input and Results ..... 7-23
7.5.1 Release Locations and Relative Detectability Grid for the 216-B-63 Trench ..... 7-26
7.5.2 Results for the 216-B-63 Trench ..... 7-26
7.6 Integrated Disposal Facility Input and Results ..... 7-31
7.6.1 Release Locations and Relative Detectability Grid for the Integrated Disposal Facility ..... 7-31
7.6.2 Results for the Integrated Disposal Facility ..... 7-31
7.7 Low-Level Burial Ground Waste Management Area-1 Input and Results ..... 7-37
7.7.1 Release Locations and Relative Detectability Grid for Low-Level Burial Ground Waste Management Area-1 ..... 7-37
7.7.2 Results for Low-Level Burial Ground Waste Management Area-1 ..... 7-37
7.8 Single-Shell Tank Waste Management Area A-AX Input and Results ..... 7-41
7.8.1 Release Locations and Relative Detectability Grid for Single-Shell Tank Waste Management Area A-AX ..... 7-44
7.8.2 Results for the Single-Shell Tank Waste Management Area A-AX ..... 7-44
7.9 Single-Shell Tank Waste Management Area B-BX-BY Input and Results ..... 7-48
7.9.1 Release Locations and Relative Detectability Grid for Single-Shell Tank Waste Management Area B-BX-BY ..... 7-48
7.9.2 Results for Single-Shell Tank Waste Management Area B-BX-BY ..... 7-48
7.10 Single-Shell Tank Waste Management Area C Input and Results ..... 7-52
7.10.1 Release Locations and Relative Detectability Grid for Single-Shell Tank Waste Management Area C ..... 7-55
7.10.2 Results for Single-Shell Tank Waste Management Area C ..... 7-55

**8 References ..... 8-1**

## Appendix

**A Measured Water Levels Used as Inputs to the Groundwater-Level Analysis ..... A-i**

# Figures

Figure 1-1. 200 East Area Facilities and Final Status Monitoring Networks Evaluated....1-2
Figure 3-1. L-Curve Example....3-2
Figure 3-2. Two-Dimensional Simulator Boundary Conditions and HSU Zones....3-5
Figure 6-1. Cumulative Relative Frequency of Absolute Residuals for 2018....6-4
Figure 6-2. Comparison of Observed Versus Simulated Groundwater Elevations....6-4
Figure 7-1. Mapped Groundwater Elevations and Calibration Residuals, 2018....7-2
Figure 7-2. Estimated Particle Pathlines, Advection, and Dispersion – 200 East Area, 2018....7-3
Figure 7-3. Final Status Monitoring Network for the 216-A-29 Ditch....7-4
Figure 7-4. Release Locations and Calculational Grid for the 216-A-29 Ditch....7-5
Figure 7-5. Groundwater Elevations and Particle Pathlines for the 216-A-29 Ditch, 2018....7-7
Figure 7-6. Relative Detectability Map for the 216-A-29 Ditch, 2018....7-8
Figure 7-7. Final Status Monitoring Network for the 216-A-36B Crib....7-10
Figure 7-8. Release Locations and Calculational Grid for the 216-A-36B Crib....7-11
Figure 7-9. Groundwater Elevations and Particle Pathlines for the 216-A-36B Crib, 2018....7-13
Figure 7-10. Relative Detectability Map for the 216-A-36B Crib, 2018....7-14
Figure 7-11. Final Status Monitoring Network for the 216-A-37-1 Crib....7-15
Figure 7-12. Release Locations and Calculational Grid for the 216-A-37-1 Crib....7-17
Figure 7-13. Groundwater Elevations and Particle Pathlines for the 216-A-37-1 Crib, 2018....7-18
Figure 7-14. Relative Detectability Map for the 216-A-37-1 Crib, 2018....7-19
Figure 7-15. Final Status Monitoring Network for the 216-B-3 Pond....7-21
Figure 7-16. Release Locations and Calculational Grid for the 216-B-3 Pond....7-22
Figure 7-17. Groundwater Elevations and Particle Pathlines for the 216-B-3 Pond, 2018....7-24
Figure 7-18. Relative Detectability Map for the 216-B-3 Pond, 2018....7-25
Figure 7-19. Final Status Monitoring Network for the 216-B-63 Trench....7-27
Figure 7-20. Release Locations and Calculational Grid for the 216-B-63 Trench....7-28
Figure 7-21. Groundwater Elevations and Particle Pathlines for the 216-B-63 Trench, 2018....7-29
Figure 7-22. Relative Detectability Map for the 216-B-63 Trench, 2018....7-30
Figure 7-23. Final Status Monitoring Network for IDF....7-33
Figure 7-24. Release Locations and Calculational Grid for IDF....7-34
Figure 7-25. Groundwater Elevations and Particle Pathlines for IDF, 2018....7-35
Figure 7-26. Relative Detectability Map for IDF, 2018....7-36
Figure 7-27. Final Status Monitoring Network for LLBG WMA-1....7-38
Figure 7-28. Release Locations and Calculational Grid for LLBG WMA-1....7-39
Figure 7-29. Groundwater Elevations and Particle Pathlines for LLBG WMA-1, 2018....7-40
Figure 7-30. Relative Detectability Map for LLBG WMA-1, 2018....7-42
Figure 7-31. Final Status Monitoring Network for SST WMA A-AX....7-43
Figure 7-32. Release Locations and Calculational Grid for SST WMA A-AX....7-45

Figure 7-33. Groundwater Elevations and Particle Pathlines for SST WMA A-AX, 2018 .....7-46
Figure 7-34. Relative Detectability Map for SST WMA A-AX, 2018 .....7-47
Figure 7-35. Final Status Monitoring Network for SST WMA B-BX-BY .....7-49
Figure 7-36. Release Locations and Calculational Grid for SST WMA B-BX-BY .....7-50
Figure 7-37. Groundwater Elevations and Particle Pathlines for SST WMA B-BX-BY, 2018.....7-51
Figure 7-38. Relative Detectability Map for SST WMA B-BX-BY, 2018 .....7-53
Figure 7-39. Final Status Monitoring Network for SST WMA C.....7-54
Figure 7-40. Release Locations and Calculational Grid for SST WMA C.....7-56
Figure 7-41. Groundwater Elevations and Particle Pathlines for SST WMA C, 2018.....7-57
Figure 7-42. Relative Detectability Map for SST WMA C, 2018.....7-58

## Tables

Table 4-1. Aquifer Transport Parameter Values .....4-2
Table 6-1. Calibration Targets for 2018.....6-1

# Terms

| | |
|---|---|
| ASCII | American Standard Code for Information Interchange |
| CCU | Cold Creek unit |
| CPGWM | Central Plateau Groundwater Model |
| DWMU | dangerous waste management unit |
| ECF | environmental calculation file |
| HSU | hydrostratigraphic unit |
| IDF | Integrated Disposal Facility |
| LLBG | low-level burial grounds |
| PUREX | Plutonium Uranium Extraction |
| RCRA | *Resource Conservation and Recovery Act of 1976* |
| Rwia | Ringold Formation member of Wooded Island – unit A |
| Rwie | Ringold Formation member of Wooded Island – unit E |
| SME | subject matter expert |
| SST | single-shell tank |
| TRIM | Tikhonov regularized inverse method |
| WMA | waste management area |

This page intentionally left blank.

# 1 Purpose

This environmental calculation file (ECF) describes calculations made to evaluate the continued suitability of the final status groundwater monitoring networks for various dangerous waste management units (DWMUs) in the 200 East Area of the Hanford Site Central Plateau (Figure 1-1). The following DWMUs are located in the 200 East Area:

- 216-A-29 Ditch
- 216-A-36B Crib
- 216-A-37-1 Crib
- 216-B-3 Main Pond
- 216-B-63 Trench
- Integrated Disposal Facility (IDF)
- Low-Level Burial Grounds (LLBG) Waste Management Area (WMA)-1
- Single-shell tank (SST) WMA A-AX
- SST WMA B-BX-BY
- SST WMA C

These DWMUs, shown in Figure 1-1, are collectively referred to as the 200 East Area facilities. This ECF re-evaluates the efficacy of the final status well networks using groundwater flow conditions calculated for calendar year 2018 to verify the continued suitability of the well locations for monitoring purposes. This ECF describes the conceptual and methodological basis for the calculations performed, describes the specific methods and codes used to perform the calculations, and presents calculation results that are applicable to the 200 East Area in general and to each individual 200 East Area facility specifically.

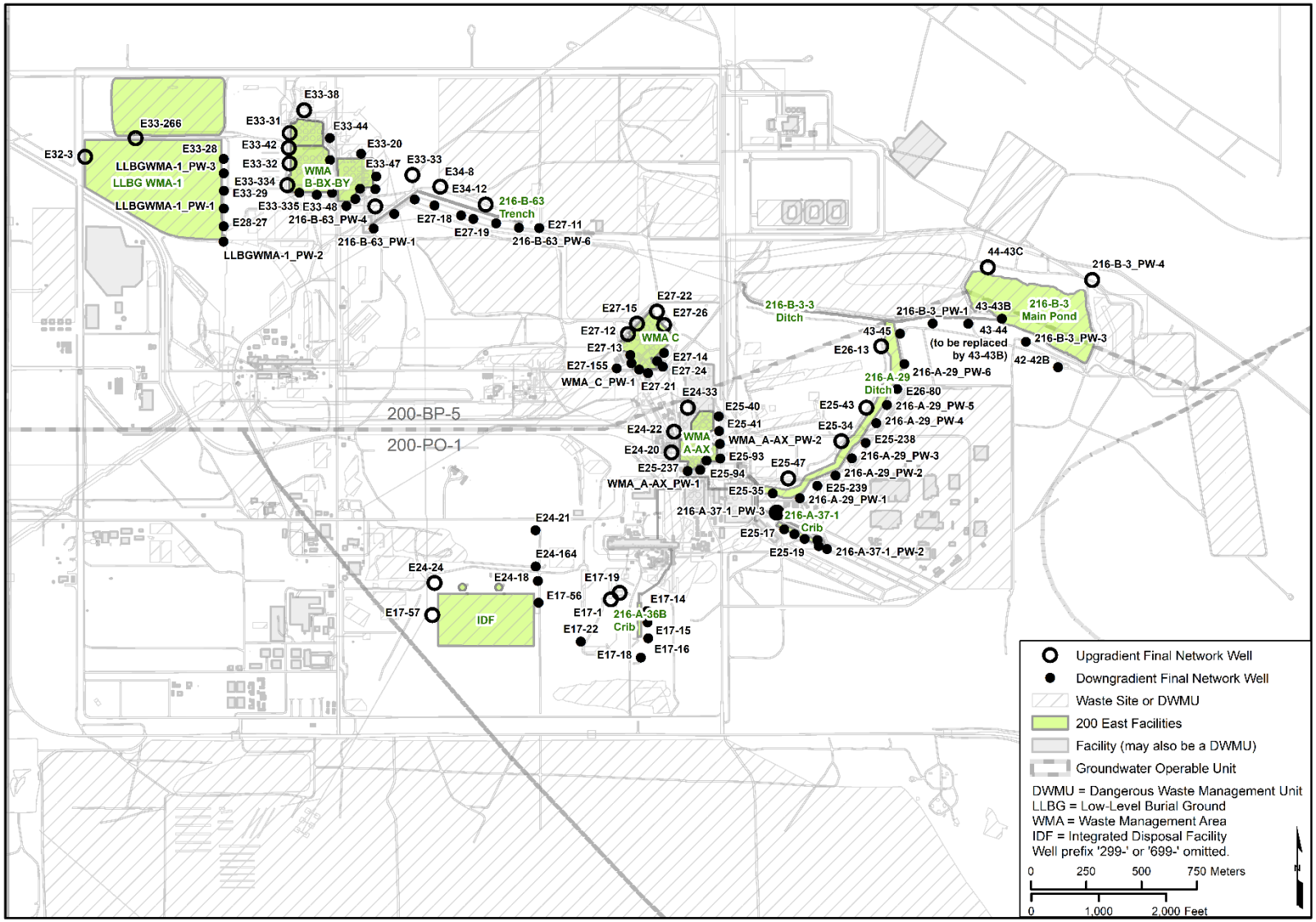


**Figure 1-1. 200 East Area Facilities and Final Status Monitoring Networks Evaluated**

# 2 Background

The final status groundwater monitoring network for each 200 East Area facility generally includes at least one upgradient well and a larger number of downgradient wells. The wells are typically screened at the top of the unconfined aquifer in order to detect significant increases in groundwater contamination that would result from a release at a facility that reaches the underlying water table from within the regulated unit. The final status monitoring networks for the 200 East Area facilities are shown in Figure 1-1. To support the assessment of the groundwater monitoring networks associated with each facility, the evaluation performed in this ECF required producing a piecewise, continuous (i.e., gridded) depiction of groundwater elevations and resulting hydraulic gradients encompassing all of the 200 East Area facilities.

## 2.1 200 East Area Groundwater

Groundwater elevations in the 200 East Area have historically varied greatly in response to water discharges from Hanford Site operations to many large wastewater-receiving features such as the 216-B-3 Pond. The 200 East Area groundwater elevation also responded to historical discharges in the 200 West Area. Most of the discharges ceased by the mid-1990s, and groundwater elevations in the 200 East Area have steadily decreased in areas where discharges formerly occurred. In recent years, changes in groundwater elevations and in corresponding hydraulic gradients and flow directions have been less evident from year to year as groundwater elevations asymptotically approach a quasi-steady-state condition.

The unconfined aquifer beneath the 200 East Area occurs in a buried paleochannel consisting of highly permeable sediments of the Hanford formation and Cold Creek unit (CCU). Because of the high permeabilities, the water table exhibits a low-magnitude hydraulic gradient (i.e., the water table is flat). In 2004, the hydraulic gradient magnitude in the 200 East Area vicinity was estimated using regional water-level measurement data to be $1.8\times10^{-5}$ m/m ($1.8\times10^{-5}$ ft/ft) (SGW-54165, *Evaluation of the Unconfined Aquifer Hydraulic Gradient Beneath the 200 East Area, Hanford Site*). At LLBG WMA-1, for example, this hydraulic gradient equates to a water table elevation change of 1.6 cm (0.63 in.) across the site; however, water-level measurements at LLBG WMA-1 typically exhibited variations of about 6 cm (2.4 in.). As a result of local variation occurring in a low-gradient setting, hydraulic gradient estimates for the water table are subject to a low signal-to-noise ratio (i.e., local variations in the data can obscure small differences in the true water table, making the determination of hydraulic gradients difficult). In addition, groundwater elevation in the 200 East Area also exhibits seasonal variability in response to changes in the discharge boundary elevation at the Columbia River.

To improve the accuracy of depth-to-groundwater measurements and corresponding groundwater elevation (i.e., water table) maps for the 200 East Area, a network of wells was established and steps were taken to reduce water-level measurement error. This was first done at LLBG WMA-1 and then later at the IDF/Plutonium Uranium Extraction (PUREX) Plant cribs area, LLBG WMA-2, and the Liquid Effluent Retention Facility. Previous work indicated that borehole deviation (i.e., nonverticality) was the most important source of error in the 200 East Area water-level measurements. To remedy this, gyroscope surveys were performed in the wells to correct for verticality error, and the tops of all well casings were resurveyed for elevation using a highly accurate leveling technique.

The initial results at the facilities were mixed (SGW-54165), with some areas still indicating uncertain flow directions. It was determined that larger study areas were needed to allow for water-level elevation differences between wells to be discerned. The well networks were expanded so eventually a single low-gradient well network was established that encompassed much of the 200 East Area. The collection of monthly water-level measurements from this network began in May 2013. The 200 East Area low-gradient network initially consisted of 56 wells and had expanded to 70 wells by 2018.

A groundwater pump-and-treat system is operating within the main unconfined aquifer in the 200 East Area to address groundwater contamination at the 200-BP-5 Groundwater Operable Unit. In 2018, this groundwater pump-and-treat system consisted of a single well, 299-E33-360, operating at an average flow rate of 617 L/min (163 gal/min). Due to the transmissivity of the Hanford formation (where the well is installed), the effects of groundwater extraction at the well only influence hydraulic gradients and corresponding groundwater flow directions and rates in the immediate vicinity of the well.

## 2.2 Gradient and Flow Path Interpretation Overview

The groundwater head and gradient calculation approach and tools developed for ECF-200E-18-0085, *Water Level Mapping and Hydraulic Gradient Calculations for 200 East Area RCRA Sites, 2018*, were used to meet the objectives of this ECF. The method discussed in ECF-200E-18-0085 combined a simplified groundwater flow simulator with statistical methods to obtain a best estimate of groundwater flow patterns near each facility. The parameters of the underlying flow simulator were determined through a regularized inverse interpolation technique referred to as the Tikhonov regularized inverse method (TRIM). TRIM (summarized here and detailed in Chapter 3) is founded upon a formal mathematical method that seeks a tradeoff between the complexity of the method or parameterization used to interpret measured data versus the “fit” to the data that the chosen method or parameterization attains. As described by Menke, 2018, *Geophysical Data Analysis: Discrete Inverse Theory*, and others, the calibration process is a tradeoff between method or parameter complexity and data fit. The more complex the method or its parameterization, the more closely the outputs from that method or parameterization can be expected to fit the data. However, a better fit does not guarantee a better estimator or predictor. Particularly in cases such as the 200 East Area, where there is low signal-to-noise ratio in the data, “overfitting” can occur with parameters responding to the noise rather than signal (Doherty, 2015, *Calibration and Uncertainty Analysis for Complex Environmental Models, PEST: Complete Theory and What it Means for Modelling the Real World*). Without constraints that recognize the presence of a low signal-to-noise ratio, overfitting can attain a very good data fit by inferring high parameter or method complexity such as exaggerated heterogeneity in a homogeneous system. In contrast, underfitting can occur when the method or parameterization used is too simple because it does not reasonably approximate the underlying physics or reflect the dominant physical characteristics of the system. A result of underfitting is insufficient capability to reproduce measured data. In either case of overfitting or underfitting, the results often do not agree well with subject matter expert (SME) knowledge of the system or with independent information.

TRIM was used to obtain a piecewise, continuous grid of groundwater elevations using a simplified groundwater flow simulator as the mechanism to interpolate between measured water levels in 2018 to prepare ECF-200E-18-0085. This was accomplished by developing a single-layer (i.e., two-dimensional), steady-state simulation approximating dominant groundwater flow characteristics over an area encompassing the 200 East Area facilities, and then using Tikhonov regularization (Tikhonov and Arsenin, 1977, *Solutions of Ill-Posed Problems*) (discussed in Chapter 3) to constrain parameter complexity and prevent overfitting to the measured water-level data. The hydraulic conductivity field determined through TRIM analysis for ECF-200E-18-0085 was then used in the steady-state simulations to interpolate between measured water levels for the purposes of this ECF. The advantage of using

a simplified groundwater flow simulator as the mechanism to interpolate between the measured water levels is that the resulting groundwater elevation grids conserve flow and are suitable for tracking particles to evaluate likely paths of groundwater and any contaminants that may reach the water table beneath the 200 East Area facilities.

This page intentionally left blank.

# 3 Calculation Methods

Calculations were completed to re-evaluate the final status groundwater monitoring networks at each of the 200 East Area facilities. The objective of the calculations was to determine whether interpreted groundwater flow conditions in 2018 continue to support the suitability of the final status groundwater monitoring wells locations that were originally proposed.

This chapter describes the calculation methods used to support this ECF. Some aspects of the evaluation described (specifically, the hydraulic conductivity field for the simplified two-dimensional groundwater flow simulator used in the TRIM analysis work) were developed for and are described in ECF-200E-18-0085. The work completed herein used the underlying groundwater flow simulator documented in ECF-200E-18-0085 to create water-level maps representing the average groundwater elevation conditions for 2018 for use in particle tracking and gradient calculations. The data, calculations, and output for 2018 are described in this chapter.

## 3.1 Water-Level Mapping Using the Tikhonov Regularized Inverse Method

Using the data and methods described in the following sections, regularized inverse water-level mapping was performed to produce continuous, gridded depictions of groundwater elevations encompassing the 200 East Area facilities to represent groundwater elevations throughout the 200 East Area.

### 3.1.1 Data Used

Maps of groundwater levels in the 200 East Area rely on measurements obtained from the wells in the low-gradient network. To prepare a piecewise, continuous grid of groundwater elevations that conserves flow throughout the area of interest and is consistent with measured groundwater levels for 2018, the annual average value of measured groundwater elevations obtained during 2018 were calculated for each monitoring well and evaluated for inclusion in assessing the monitoring networks.

### 3.1.2 Method Description

The method used to obtain the groundwater elevation grids (i.e., TRIM) is a formal mathematical technique that is used to trade the complexity of a method or parameterization that is being used to analyze measured data against the “fit” obtained to those data. When used with a deterministic model, Tikhonov regularization is used to constrain the parameters of the model while attempting to attain a satisfactory fit to the measured data that agrees with independent SME knowledge and information.

TRIM implements a common application of Tikhonov regularization by supplementing the measurement data set (in this case, annually averaged water-level measurements from 2018) with other information derived from SME knowledge. This knowledge is cast as “prior information” representing an anticipated system condition (e.g., understanding of distribution and variability of hydraulic conductivity within the study area). The addition of this information results in a mathematical technique referred to as penalized least squares regression, because a penalty is incurred when parameters deviate from the anticipated system condition specified by SMEs. The size of the penalty incurred during the regression is controlled using a weight parameter (Tikhonov and Arsenin, 1977), referred to as the global regularization weight parameter that is commonly denoted by “μ” (Doherty, 2015). The size of this penalty is “traded” against the degree to which the simulation matches the measurement data. To attain a better fit to the measurement data, a larger penalty is usually incurred by deviating further from the anticipated system condition.

This method of specifying the anticipated system condition can take many forms. It is commonly specified as either a "preferred value" (e.g., it is desired that the best fit to the data be attained while attaining parameter values that are close to a value of $X$) or a "preferred difference" condition (e.g., it is desired that the best fit be obtained to the data while obtaining parameter values that show minimal difference between each other). In the context of groundwater data analysis, particularly for clastic sedimentary aquifer materials such as those encountered in the unconfined aquifer in the 200 East Area, the preferred system condition is typically homogeneity (i.e., that the regression should seek as good of a fit as can be obtained while keeping parameters as homogeneous as possible). This approach, also referred to as smoothness regularization, is used to prevent the regression from inferring parameter values that are considered by SMEs to be unlikely.

The tradeoff between the complexity of the simulator or its parameterization versus the fit obtained to the measurement data can be plotted graphically. This often results in a shape similar to an uppercase letter "L" (i.e., concave upward to the right) and is referred to as an L-curve (Hansen, 2000, *The L-curve and its use in the numerical treatment of inverse problems*). L-curves are used to evaluate the relationship between two related or competing terms in many different analyses, providing a graphical method to select an acceptable solution that does not over-fit nor under-fit the data. In the context of Tikhonov regularization, the L-curve depicts the tradeoff between a sum of squared weighted residuals (or least squares) measurement objective function (usually shown on the X-axis) and a regularization objective function that is calculated as the sum of squared deviations from the preferred system condition. The manner in which this plot changes with different values of the global regularization weight parameter, $\mu$, traces the tradeoff between these two objectives.

Figure 3-1 provides an example of an L-curve. The figure shows that as the value of the global regularization weight parameter increases, greater emphasis is placed on honoring the preferred system condition, which keeps the regularization objective function low but results in a larger measurement objective function (penalizing the fit achieved to the measured data). Conversely, as the value of the global regularization weight parameter decreases, less emphasis is placed on honoring the preferred system condition, which results in a larger regularization objective function but provides the regression the ability to attain a better fit to the measurement data.

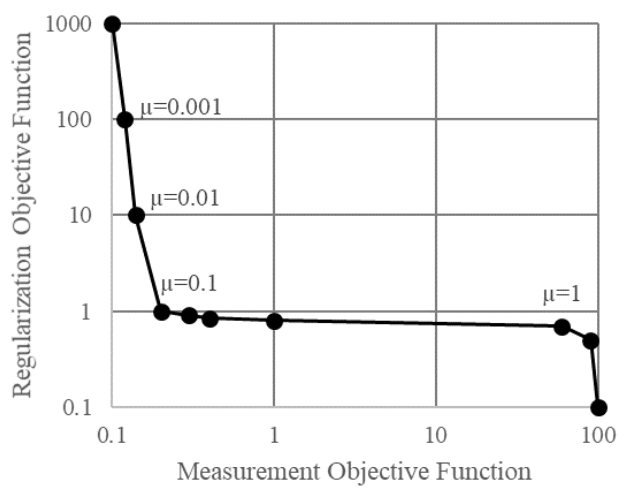


Source: Hansen, 2000, *The L-curve and its use in the numerical treatment of inverse problems.*

**Figure 3-1. L-Curve Example**

### 3.1.3 Implementation Using MODFLOW-USG and PEST

Two linked calculation tools are needed to obtain the necessary piecewise grid for 2018:

- A method for calculating groundwater elevations throughout the area
- A method for implementing the Tikhonov regularization technique to evaluate the tradeoff between complexity and data fit

The calculations described in this section were completed for and are described in ECF-200E-18-0085. The underlying groundwater simulator that was developed was used with the average water-level data for 2018 (described in Chapter 6) to complete the calculations for this ECF.

#### *3.1.3.1 Groundwater Elevations*

Throughout the 200 East Area, the predominant factors that affect area-wide groundwater flow patterns are (1) the high-hydraulic conductivity sediments that comprise the Hanford formation and the CCU; (2) the location of lower hydraulic conductivity sediments and basalts that are lateral to or a subcrop within the high-conductivity sediments; and (3) lateral sources and sinks (inflows and outflows) of water, particularly along the northwest and southeast extents of the 200 East Area. As detailed in ECF-200E-18-0085, these predominant factors have previously been represented by developing and parameterizing a simplified single-layer (two-dimensional), steady-state simulator of groundwater flow using the unstructured grid release of the MODFLOW program, MODFLOW-USG (Panday et al., 2013, "MODFLOW-USG Version 1: An Unstructured Grid Version of MODFLOW for Simulating Groundwater Flow and Tightly Coupled Processes Using a Control Volume Finite-Difference Formulation).

The MODFLOW-USG simulation code is a control-volume, finite-difference formulation of the commonly used finite-difference U.S. Geological Survey MODFLOW groundwater flow simulator. A disadvantage of the regular rectangular grids that result from the use of regular finite-difference methods is that when small cells are used to represent an area of interest, a very large number of cells is created throughout the domain. When used together with Tikhonov regularization, this can produce a number of relationships between model cells that can render the problem mathematically intractable. An advantage of the unstructured grid formulation implemented in MODFLOW-USG is that it can support irregular (nonrectangular) grids. In particular, MODFLOW-USG can support a Voronoi grid, which is well suited for this purpose because a smaller number of cells is needed to discretize the area encompassing the 200 East Area facilities, and a correspondingly smaller number of regularization (prior information) equations is needed to specify relations between the parameter value in each cell and that of neighboring cells.

As discussed in ECF-200E-18-0085, the simplified two-dimensional simulator of groundwater flow conditions was constructed as follows:

1. A single-layer grid was constructed using a Voronoi mesh. The Voronoi mesh was designed using the software program AlgoMesh® (HydroAlgorithmics, 2016, *AlgoMesh User Guide*) that enables the user to adjust the number of cells, their geometry, aspect ratios, and density in focused areas of the domain. AlgoMesh writes a file that defines the Voronoi mesh in a format that can be read by the Groundwater Vistas™ program (Rumbaugh and Rumbaugh, 2017, *Groundwater Vistas Version 7*),

AlgoMesh® is a registered trademark of HydroAlgorithmics Pty Ltd, Canberra, Australia.
Groundwater Vistas™ is a trademark of Environmental Simulations, Inc., Reinholds, Pennsylvania.

from which the MODFLOW-USG specific input files are generated and through which initial parameters and boundary conditions were developed.

2. Lateral boundary conditions were specified using (a) specified-flux boundaries to represent the flow between the 200 East and 200 West Areas, Gable Gap to the north, the basalt to the north, and the Treated Effluent Disposal Facility to the east; and (b) a specified-head boundary to represent the region to the southeast where groundwater flows eastward toward the Columbia River.

3. Based on SME knowledge, the hydraulic conductivity of the sediments within which the water table resides was discretized into three hydrostratigraphic unit (HSU) zones representing the Hanford formation, CCU, and Ringold Formation member of Wooded Island – unit E (Rwie). Delineation of HSUs at the elevation of the water table was prepared by intersecting the Central Plateau Groundwater Model (CPGWM) water table grid with a three-dimensional geological model (ECF-HANFORD-13-0029, *Development of the Hanford South Geologic Framework Model, Hanford Site, Washington*). Within each of these delineated HSU zones, the hydraulic conductivity was defined as homogeneous for purposes of defining initial parameter values (this represents the preferred system condition at the commencement of the Tikhonov regularization that followed).

The resulting simplified groundwater flow simulator is two-dimensional (i.e., a single layer), with the resolution of the mesh refined in areas of particular interest (e.g., near groups of monitoring wells). Figure 3-2 shows the resulting grid, boundaries, and hydraulic conductivity zones.

#### *3.1.3.2 Tikhonov Regularization*

The method of Tikhonov regularization is used in several software packages and programming environments. One of these programs is PEST (Doherty, 2015), which implements Tikhonov regularization as a constrained parameter estimation or calibration procedure. PEST is used widely at the Hanford Site to assist with calibrating groundwater models and other models, using utilities to link PEST to groundwater models and other programs. For this reason, PEST was selected for use in preparing this ECF. When incorporating Tikhonov regularization in a calibration using PEST, the sum of squared weighted residuals measurement objective function (which is sought to minimize during traditional parameter estimation) is augmented with a second term that quantifies the degree of deviation from the preferred system condition. A sum of squared weighted differences is calculated between the preferred condition and the condition that is represented by the value of the parameters (Tonkin and Doherty, 2005, "A Hybrid Regularized Inversion Methodology for Highly Parameterized Environmental Models"; Doherty, 2015; Doherty, 2016, *PEST Model-Independent Parameter Estimation User Manual Part I: PEST, SENSAN, and Global Optimisers*). This sum of squared weighted deviations from the preferred conditions constitutes the regularization objective function that is shown in the example L-curve figure (Figure 3-1).

The PEST software can implement Tikhonov regularization in two modes of operation. When operating in the first of these modes (regularization mode), the PEST program calculates updates to the values of the parameters that provide an improved fit to the measured values. The program also determines a global regularization weight parameter that enables the measurement component of this composite objective function to meet a target value ascribed by the user as representing an "acceptable" fit (Doherty, 2015). When operating in the second of these modes (Pareto mode), the PEST program calculates updates to the values of the parameters by conducting a form of line search that describes a line exploring the relationship between the regularization objective function, the global regularization weight parameter, and measurement objective function in a manner that can be used to plot an L-curve (e.g., as shown in Figure 3-1).

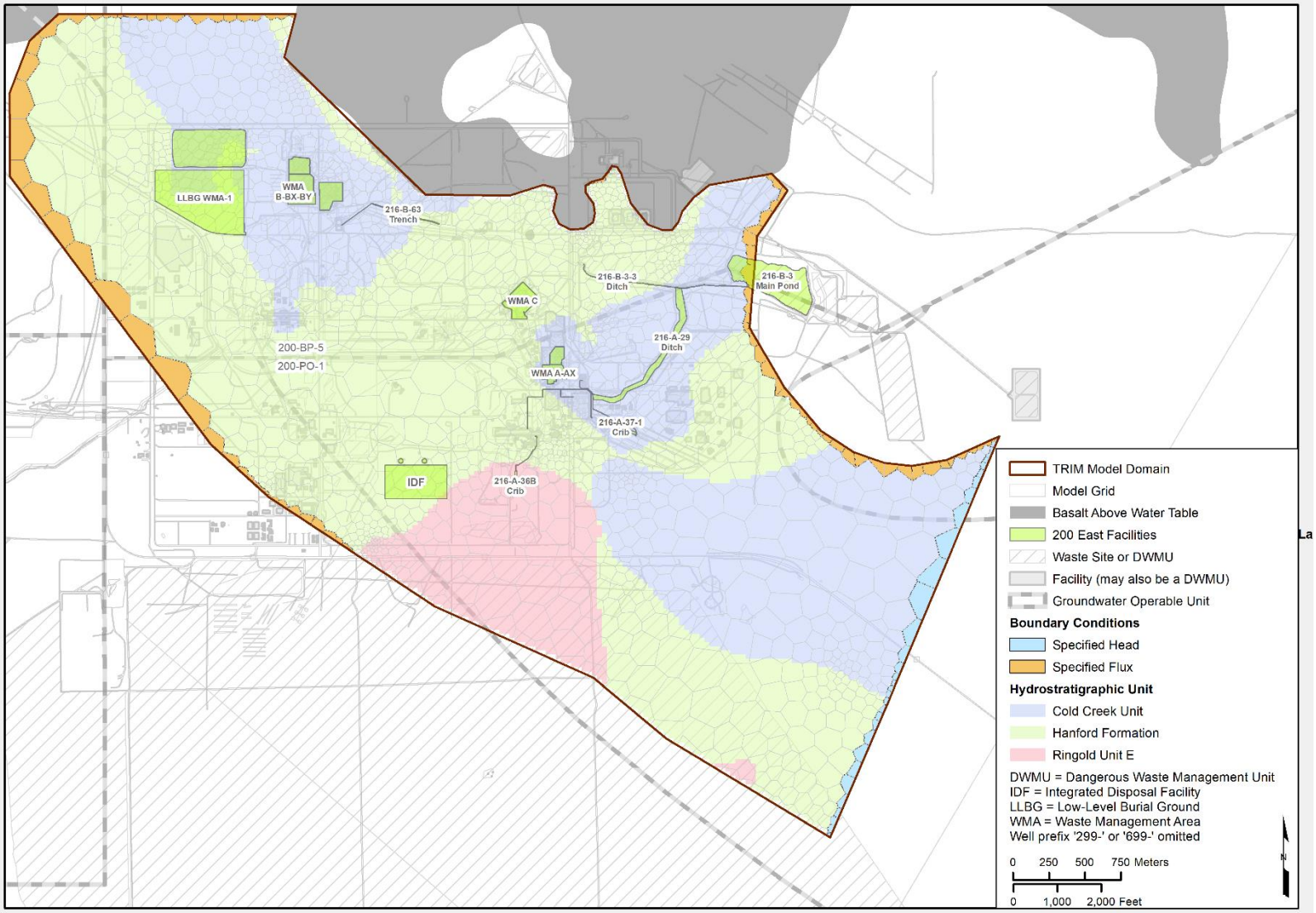


**Figure 3-2. Two-Dimensional Simulator Boundary Conditions and HSU Zones**

#### *3.1.3.3 Limitations*

The simplified two-dimensional groundwater flow simulator that underlies TRIM (developed using the MODFLOW-USG code for this ECF) was used specifically to provide a mechanism to interpret groundwater-level data and obtain groundwater elevation contours depicting directions of groundwater flow and potential migration pathways based upon the measured data. The groundwater elevation contours are obtained by trading off the complexity of the groundwater simulator parameterization versus the fit that is obtained to the measured groundwater elevation data, effectively using the groundwater simulator as an alternative to distance-weighted interpolation (e.g., kriging) to interpolate between the measured groundwater-level data. Because the resulting piecewise, continuous groundwater elevation grids depict hydraulic gradients that agree with independent SME knowledge of subsurface conditions, the grids are suitable for particle-tracking analyses to depict approximate rates and directions of groundwater flow and potential contaminant migration in near the 200 East Area facilities.

The simplified two-dimensional groundwater flow simulator that underlies TRIM is not a substitute for existing three-dimensional groundwater flow and contaminant transport models at the Hanford Site (e.g., the CPGWM and the Plateau to River Groundwater Transport Model). There are many simplifications in the underlying groundwater flow simulator developed for the purposes of this ECF. These simplifications include using a single layer representing only water table conditions, the regularization objective sought in TRIM of homogeneity without specific regard for the values or physical meaning of the resulting parameters, and the simplified representation of the lateral boundaries of the area of interest. Because of these and other simplifications and limitations, the MODFLOW-USG simulator underlying TRIM should not be used as an alternative to the existing three-dimensional groundwater flow and contaminant transport models (i.e., the CPGWM and Plateau to River Groundwater Transport Model) for mass-conserved simulations of contaminant transport.

## 3.2 Particle Tracking and Relative Detectability

The groundwater elevation map for the 200 East Area produced using TRIM depicts general patterns of hydraulic gradients and groundwater flow, identifying likely directions of contaminant migration if a release from a facility reaches the water table. Particle tracking provides a method of visualizing these directions and integrating the gradients to depict potential migration pathlines and enables a more thorough assessment of the suitability of monitoring well locations.

After the groundwater elevation grid was created using TRIM, the grid was used as the base for particle tracking. Particle tracking was performed using mod-PATH3DU, considering advective and dispersive transport mechanisms (Muffels et al., 2018, *User's Guide for mod-PATH3DU, A Groundwater Path and Travel-Time Simulator*). The parameters used to calculate particle pathlines assume migration of a conservative (i.e., nonreactive) dissolved contaminant. Calculated particle pathlines provide a visualization of how a hypothetical release from a facility reaching the water table would move and spread under conditions representative of 2018. Particle-tracking calculations that are specific to each facility and that assume both advective and dispersive transport mechanisms are used in this ECF to produce both particle pathlines and maps of relative detectability for comparison with the location of the final status monitoring wells.

### 3.2.1 Particle Tracking

Particle tracking considering both advection and dispersion was performed on the groundwater elevation grid to calculate the movement of a one-time release of a large number of particles representing an instantaneous release reaching the water table. To represent potential variations in migration pathways that may result due to dispersive processes, 20 particles were released from each release location, resulting in 20 pathlines originating from each location, each of which depicts the potential path of a dissolved contaminant particle released at the water table beneath a facility. The calculated particle pathlines provide a way to visualize how a hypothetical release to the water table from the facility would move and spread downgradient under flow conditions representative of 2018.

Calculated particle pathlines were further post-processed following the steps described in Chapter 6 to create maps of relative detectability for the purposes discussed below.

### 3.2.2 Relative Detectability

Counts of particles can be used as a simple surrogate for contaminant concentration to evaluate the relative efficacy of groundwater monitoring well locations. To show the relative migration potential of releases from each facility, the absolute particle counts for each facility were converted into a relative particle detectability index. This was done by counting the number of particles that pass through a pre-defined uniform particle calculation grid and then dividing the particle count in each grid cell by the maximum number of unique particles that crossed a single grid cell for that facility. The particle calculation grids used at each facility to develop the relative particle density maps are defined by 10 m by 10 m (33 ft by 33 ft) cells that are oriented parallel to the predominant groundwater flow direction under each facility. The calculation grids used to conduct relative detectability calculations for each facility and the corresponding contour (or color-scaled) maps are presented in the facility-specific sections in Chapter 7.

## 3.3 Evaluation of Vertical Migration Potential

Dissolved constituents that are released within the vadose zone (i.e., above the water table) and migrate downward, ultimately make their first impact to groundwater at the top of the aquifer (i.e., at the water table). Although the initial impact is at the water table, dissolved constituents that mix with actively moving groundwater over time have the potential to move vertically within the aquifer. When attempting to monitor and detect potential releases that have arrived at the water table, the possibility that constituents may migrate beneath the bottom of the screen interval of monitoring wells must be considered.

An analysis of the potential for the vertical migration of dissolved constituents is presented in ECF-200E-18-0066, *Groundwater Flow and Migration Calculations to Assess Monitoring Networks in the 200 East Area Dangerous Waste Management Units*. The analysis used an analytical calculation, the American Petroleum Institute (API) plume diving calculation (Nichols and Roth, 2006, "*Downward Solute Plume Migration: Assessment, Significance, and Implications for Characterization and Monitoring of "Diving Plumes"*) to estimate the likely rate of vertical migration of dissolved constituents downward under the influence of recharge at the water table. The calculations concluded that the plume depth fell within the intervals between the top of the water table and the bottom of the well screens for the existing final monitoring wells for most of the DWMUs in the 200 East Area, indicating that well depths are appropriate for detecting releases. The only DWMU that did not meet this condition was the 216-A-36B Crib. At this DWMU, the calculation demonstrated that there may be sufficient vertical migration due to accrual of recharge that it could result in the screened interval of downgradient monitoring wells being too shallow to effectively detect releases from the 216-A-36B Crib. This

determination relies upon the values for hydraulic conductivity and recharge used in the calculations. It was recommended that field tests be conducted within the downgradient monitoring wells for the 216-A-36B Crib to verify that the hydraulic conductivity value used in these calculations (derived from calibration of the CPGWM) is representative of the Rwie near the facility before committing resources to well deepening or replacement. The conditions assumed in in ECF-200E-18-0066 have not changed, so changes in the results of those calculations are not expected at this time. Therefore, these calculations have not been repeated herein but will be repeated if conditions change in the future.

# 4 Assumptions and Inputs

This chapter outlines the assumptions and inputs that underlie the calculations presented in this ECF.

## 4.1 Assumptions

Assumptions used for the groundwater flow analysis, groundwater elevation mapping, and particle tracking are discussed in the following sections.

### 4.1.1 Tikhonov Regularized Inverse Method of Water-Level Analysis

Water-level contour maps were constructed using a method that combines a simplified simulator of groundwater flow and Tikhonov regularization (used in both calibration and Pareto front analysis modes). The resulting groundwater elevation contour maps provide plausible interpretations of groundwater levels and hydraulic gradients between measured locations that match measured water levels and monitoring wells to a degree consistent with the tradeoff between that fit and parameter complexity. These interpretations achieve flow conservation by using the underlying groundwater flow simulator as the interpolation mechanism between measurement locations. The accuracy of the contours is influenced by several factors, including the following:

- Accuracy of the measured or recorded water levels
- Number, distribution, and location of monitoring wells
- Relationship between the vertical open intervals of the monitoring wells and those of any extraction and injection wells

These potential sources of error mean that the maps are interpreted as reasonable approximations that provide useful inference in interpreting likely directions and rates of groundwater movement, particularly in regions of low hydraulic gradients. The maps also help identify areas downgradient of the 200 East Area facilities that would likely be impacted by a potential release reaching the underlying water table. Based on SME knowledge and understanding of the groundwater system in the 200 East Area, these estimates are assumed to be representative of observed conditions.

### 4.1.2 Particle Tracking

Particle tracking based on groundwater-level mapping for the 200 East Area facilities relies on outputs (i.e., grids of mapped groundwater elevations) computed using TRIM. As a result, the assumptions and limitations that underlie the preparation of the maps are implicit in any subsequent particle tracking.

Particle tracking that considers advection and dispersion relies upon the assumption that the values of the dispersion coefficients in the two principal directions (longitudinal and transverse) are representative of physical processes that act to disperse dissolved constituents in groundwater at the scale of the calculations.

Because the time required for any release from a waste facility to traverse the vadose zone is not addressed in these calculations, the conditions assumed for the particle release year (in this ECF, for the year 2018) are assumed to represent conditions for the year that contamination from hypothetical releases reaches the water table (i.e., not the year of the release from the facility).

## 4.2 Input Data

This section summarizes the general input requirements for the calculations described in this ECF.

### 4.2.1 Water-Level Mapping Input

Appendix A of this ECF provides tables of the annual average measured groundwater levels for 2018, which are the inputs used for water-level mapping.

#### *4.2.1.1 Migration Parameters for Particle Tracking*

Only a small number of parameters is required for the migration calculations performed using the groundwater-level maps and particle-tracking methods. The mobile porosity and hydraulic conductivity values were defined specific to each HSU as presented in CP-47631, *Model Package Report: Central Plateau Groundwater Model, Version 8.4.5*. Table 4-1 lists the values for each HSU. Dispersivity values are assumed constant throughout the entire region and are listed in Table 4-1.

**Table 4-1. Aquifer Transport Parameter Values**

| Property | | Value | Comments |
|---|---|---|---|
| Hydraulic conductivity | Hanford formation | 15,000 m/d (49,213 ft/d) | CP-47631 |
| | CCU | 18,200 m/d (59,711 ft/d) | CP-47631 |
| | Rwie | 35.6 m/d (117 ft/d) | CP-47631 |
| Effective porosity | Hanford formation and CCU | 0.25 | CP-47631 |
| | Rwie | 0.08 | CP-47631 |
| Longitudinal dispersivity | | 3.5 m (11.5 ft) | Introduced for stability of the transport calculations using recommendation from the MT3DMS manual (Zheng and Wang, 1999) |
| Transverse dispersivity | | 0.7 m (2.3 ft) | 20% of longitudinal (DOE/RL-2008-56) |

References:

CP-47631, *Model Package Report: Central Plateau Groundwater Model, Version 8.4.5*.

DOE/RL-2008-56, *200 West Area Pre-Conceptual Design for Final Extraction/Injection Well Network: Modeling Analyses*.

Zheng and Wang, 1999, *MT3DMS: A Modular Three-Dimensional Multispecies Transport Model for Simulation of Advection, Dispersion, and Chemical Reactions of Contaminants in Groundwater Systems; Documentation and User's Guide*.

MT3DMS = Modular Transport, Three-Dimensional, Multi-Species Model

CCU = Cold Creek unit

Rwie = Ringold Formation member of Wooded Island – unit E

The primary purpose of the calculations presented in this ECF is to estimate directions of potential contaminant migration in order to assess the efficacy of each facility-specific monitoring well network. Appropriate values for dispersivity in transport calculations are generally recognized to be scale-dependent. For purposes of these calculations, the simulations of transport in the saturated zone assume values for dispersivity in two of the possible three directions: longitudinal (3.5 m [11.5 ft]) and transverse (0.7 m [2.3 ft]). These values are on the lower end of values identified as typical of field-scale sites by, among others, Gelhar et al., 1992, "A Critical Review of Data on Field-Scale Dispersion in Aquifers"; and Xu and Eckstein, 1995, "Use of Weighted Least-Squares Method in Evaluation of the Relationship Between Dispersivity and Field Scale." The range of values listed below for longitudinal dispersion are based on a typical migration distance from the potential source to the monitoring network

of about 200 m (656 ft) and the recommendations of Gelhar et al., 1992; and Xu and Eckstein, 1995, as incorporated in the U.S. Environmental Protection Agency's online calculator (EPA, 2016, "Estimated Longitudinal Dispersivity"):

- 0.37 m (1.2 ft) (lower limit) (Gelhar et al., 1992)
- 1100 m (3,609 ft) (upper limit) (Gelhar et al., 1992)
- 6.21 m (20.4 ft) (Xu and Eckstein, 1995)
- 20 m (66 ft) (1/10$^{th}$ of migration distance; rule of thumb)

The values for longitudinal dispersivity used in the calculations presented in this ECF (3.5 m [11.5 ft]) are at the lower end. Dispersivity values appropriate for the calculations presented in this ECF are considered to be on the lower end primarily because the dominant historical mechanism leading to contamination spread at the Central Plateau (hydraulic transients from wastewater disposal) has diminished over time. Although the historical Central Plateau groundwater plumes are on the order of hundreds of meters in length or width, the distance and scale relevant to specifying dispersion lengths for this ECF are the typical distances from potential release locations to downgradient monitoring wells, which is substantially less than the scale of the historical plumes.

The assumption of a lower-end value for longitudinal dispersivity has two implications for evaluating the efficacy of a monitoring network for detecting a release: (1) lower-end values result in relatively narrower plumes than using higher-end values, and (2) the lower values result in relatively higher detectability for monitoring wells that are located directly in the path of a release. Given the objective of verifying the suitability of the spatial distribution of final network monitoring wells, emphasis was placed on producing results that do not overestimate the likely width of groundwater impacts resulting from a hypothetical release.

### 4.2.2 Particle Starting Locations

The particle release locations for the calculations include the plausible area over which a potential release might occur from each facility. For the tank farms, particle starting locations were specified around the perimeter of each SST. For other facilities, the particle release locations were specified to be spaced approximately 50 m (164 ft) between release points, either along the facility perimeter or throughout the footprint of a pre-defined release location.

Twenty particles were released from each particle release location to provide sufficient density of particles in space and time as required for the calculations. The particles were tracked using random seed values as the basis for calculating dispersion. The starting locations for the releases simulated from each facility are described in the facility-specific sections in Chapter 7.

This page intentionally left blank

# 5 Software Applications, Descriptions, Installation and Checkout, and Statements of Validity

Software used to perform the calculations for this ECF was in accordance with PRC-PRO-IRM-309, *Controlled Software Management*.

## 5.1 Approved Software

The software used for this ECF was approved and complies with PRC-PRO-IRM-309. The software is managed under the following documents, consistent with PRC-PRO-IRM-309:

- CHPRC-00257, *MODFLOW and Related Codes Functional Requirements Document*
- CHPRC-00258, *MODFLOW and Related Codes Software Management Plan*
- CHPRC-00259, *MODFLOW and Related Codes Software Test Plan*
- CHPRC-00260, *MODFLOW and Related Codes Requirements Traceability Matrix*
- CHPRC-00261, *MODFLOW and Related Codes Acceptance Test Report*

PRC-PRO-IRM-309 distinguishes between safety software and support software based upon whether the software calculates reportable results or provides run support, visualization, or similar functions. Section 5.2 provides brief descriptions of the software.

## 5.2 Software Description

A controlled calculation software, MODFLOW-USG (Panday et al., 2013), was used for the calculations that support this ECF.

- **Software title:** MODFLOW-USG solves transient groundwater flow equations using the control-volume, finite-difference discretization technique.
- **Software version:** USG-Transport, Version 1.0.0
- **Hanford Information Systems Inventory identification number:** 2517
- Workstation type and property number (from which software is run): S.S. Papadopulos & Associates, Inc., FE563.

## 5.3 Support Software

The following software programs are classified as support software.

- **PEST:** Estimates parameter values that minimize the objective functions to calibrate models using inverse theory (Doherty, 2016).
- **Groundwater Vistas:** Provided graphical tools used for model quality assurance and model input/output review (Rumbaugh and Rumbaugh, 2017).
- **ArcGIS®:** Visualization and post-processing tool for assessing simulated plume distributions, identifying extraction/injection well coordinates, and mapping auxiliary data (Mitchell, 1999, *The ESRI Guide to GIS Analysis, Volume 1: Geographic Patterns & Relationships*).

---

ArcGIS® is a registered trademark of the Environmental Systems Research Institute, Inc., Redlands, California.

- **Surfer®:** Data interpolation for visualization, model implementation, and quality assurance.
- **mod-PATH3DU:** Particle-tracking code for calculating the three-dimensional flow pathlines and travel times of solute particles.
- **Python™:** The calculation and visualization of particle counts used Python, an interpreted, object-oriented programming language, with scripts executed using the Anaconda® freeware. Python Version 2.7.11 is distributed with Anaconda 4.1.1 (64-bit).
- **AlgoMesh:** A mesh-generating software used for creating unstructured triangular and Voronoi grids for MODFLOW-USG (AlgoMesh Version 1.2.0.37827, 64-bit [HydroAlgorithmics, 2016]).

## 5.4 Software Installation and Checkout

Safety software is checked out in accordance with procedures specified in PRC-PRO-IRM-309. Executables are obtained from the CH2M HILL Plateau Remediation Company software owner, who maintains the configuration-managed copies in MKS Integrity®. Installation tests identified in CHPRC-00259 are performed on the software and successful installation is confirmed. Software installation and checkout forms are required and must be approved for installations used to perform model runs. Approved users are registered in the Hanford Information Systems Inventory for safety software.

### 5.4.1 Statement of Valid Software Application

The software identified above was used consistent with intended uses, as identified in CHPRC-00257, and is a valid use of this software for this application. The software was used within its limitations, as identified in CHPRC-00257.

---

Surfer® is a registered trademark of Golden Software, LLC, Golden, Colorado.
Python™ is a trademark of Python Software Foundation, Beaverton, Oregon.
Anaconda® is a registered trademark of Anaconda, Inc., Austin, Texas.
MKS Integrity® is a registered trademark of MKS, Inc., Needham, Massachusetts.

# 6 Calculations

This chapter describes the calculations performed to examine all 200 East Area facilities. The steps identified in this chapter were used to develop the necessary input files, perform calculations, and post-process the outputs to produce the results presented in this ECF.

## 6.1 Water-Level Analysis

Groundwater elevation maps presented in this ECF and used in all subsequent particle-tracking calculations were produced using a two-step process:

1. **Data compilation**: Input data were compiled from retrieved database sources. Outliers were flagged by constructing trend plots of the measured data and were excluded from calculations. Average groundwater elevations were then calculated for 2018 based on the filtered monthly measurements and used to define the targets for the calibration process.

2. **Calibration**: The hydraulic conductivity field for the simplified two-dimensional groundwater flow simulator was inherited from the TRIM analysis completed for and described in ECF-200E-18-0085. The boundary conditions described in Chapter 3 were then used as parameters for PEST in estimation mode to approximate average measured groundwater levels for 2018. Targets corresponding to the north and southeast of the model were assigned higher weights during the calibration process so the overall average measured gradient across the 200 East Area is respected.

   Table 6-1 lists the calibration targets and their associated weights. During the calibration process, wells that repeatedly registered high residuals were flagged and compared to adjacent measurements. Based on understandings of any nearby stresses, surrounding geology, and inferred flow directions (i.e., upgradient versus downgradient), these wells and/or surrounding wells were assigned lower weights due to lower confidence in measurements.

**Table 6-1. Calibration Targets for 2018**

| Well Name | Average Measured Water Level (m NAVD88) | Grid Interpolated Water Level (m NAVD88) | Residual (Estimated Error) (m NAVD88) | Calibration Weight |
|---|---|---|---|---|
| 299-E17-18 | 121.657 | 121.673 | -0.016 | 10 |
| 299-E17-21 | 121.688 | 121.694 | -0.006 | 10 |
| 299-E17-22 | 121.682 | 121.678 | 0.004 | 10 |
| 299-E17-23 | 121.668 | 121.678 | -0.010 | 10 |
| 299-E17-25 | 121.688 | 121.682 | 0.006 | 10 |
| 299-E18-2 | 121.742 | 121.737 | 0.005 | 10 |
| 299-E23-1 | 121.670 | 121.688 | -0.018 | 10 |
| 299-E24-16* | 121.703 | 121.678 | 0.025 | 2 |
| 299-E24-18 | 121.668 | 121.681 | -0.013 | 10 |
| 299-E24-21 | 121.678 | 121.682 | -0.004 | 10 |
| 299-E24-22 | 121.678 | 121.680 | -0.002 | 10 |
| 299-E24-24 | 121.679 | 121.688 | -0.008 | 10 |

**Table 6-1. Calibration Targets for 2018**

| Well Name | Average Measured Water Level (m NAVD88) | Grid Interpolated Water Level (m NAVD88) | Residual (Estimated Error) (m NAVD88) | Calibration Weight |
|---|---|---|---|---|
| 299-E24-25* | 121.662 | 121.686 | -0.024 | 2 |
| 299-E24-33 | 121.685 | 121.680 | 0.005 | 10 |
| 299-E25-19 | 121.687 | 121.671 | 0.016 | 10 |
| 299-E25-24* | 121.688 | 121.666 | 0.023 | 2 |
| 299-E25-25* | 121.688 | 121.668 | 0.020 | 2 |
| 299-E25-34 | 121.680 | 121.676 | 0.004 | 10 |
| 299-E25-35 | 121.683 | 121.674 | 0.009 | 10 |
| 299-E25-93 | 121.676 | 121.677 | -0.001 | 10 |
| 299-E26-10 | 121.712 | 121.708 | 0.004 | 10 |
| 299-E26-13 | 121.689 | 121.682 | 0.007 | 10 |
| 299-E26-14 | 121.788 | 121.786 | 0.002 | 10 |
| 299-E26-15 | 121.706 | 121.718 | -0.012 | 10 |
| 299-E26-4 | 121.684 | 121.680 | 0.004 | 10 |
| 299-E26-79 | 121.727 | 121.727 | 0.000 | 10 |
| 299-E27-12 | 121.683 | 121.685 | -0.002 | 10 |
| 299-E27-14 | 121.681 | 121.684 | -0.003 | 10 |
| 299-E27-15 | 121.682 | 121.686 | -0.004 | 10 |
| 299-E27-17 | 121.687 | 121.691 | -0.004 | 10 |
| 299-E27-18 | 121.699 | 121.692 | 0.008 | 10 |
| 299-E27-21 | 121.672 | 121.683 | -0.011 | 10 |
| 299-E27-22* | 121.708 | 121.686 | 0.022 | 2 |
| 299-E27-23 | 121.677 | 121.684 | -0.007 | 10 |
| 299-E27-7 | 121.682 | 121.686 | -0.003 | 10 |
| 299-E27-8 | 121.690 | 121.690 | 0.000 | 10 |
| 299-E27-9 | 121.691 | 121.689 | 0.002 | 10 |
| 299-E28-1 | 121.682 | 121.692 | -0.010 | 10 |
| 299-E28-17 | 121.691 | 121.694 | -0.003 | 10 |
| 299-E28-18 | 121.705 | 121.697 | 0.008 | 10 |
| 299-E28-27 | 121.696 | 121.694 | 0.002 | 10 |
| 299-E29-54* | 121.672 | 121.694 | -0.022 | 2 |
| 299-E32-5 | 121.705 | 121.707 | -0.002 | 10 |
| 299-E32-6 | 121.708 | 121.709 | -0.001 | 10 |

**Table 6-1. Calibration Targets for 2018**

| Well Name | Average Measured Water Level (m NAVD88) | Grid Interpolated Water Level (m NAVD88) | Residual (Estimated Error) (m NAVD88) | Calibration Weight |
|---|---|---|---|---|
| 299-E32-8 | 121.715 | 121.712 | 0.003 | 10 |
| 299-E33-14 | 121.694 | 121.693 | 0.001 | 10 |
| 299-E33-267 | 121.692 | 121.694 | -0.002 | 10 |
| 299-E33-28 | 121.698 | 121.696 | 0.002 | 10 |
| 299-E33-31 | 121.690 | 121.694 | -0.004 | 10 |
| 299-E33-32 | 121.689 | 121.694 | -0.005 | 10 |
| 299-E33-339 | 121.690 | 121.693 | -0.003 | 10 |
| 299-E33-34 | 121.706 | 121.704 | 0.002 | 20 |
| 299-E33-342 | 121.690 | 121.694 | -0.004 | 10 |
| 299-E33-37 | 121.693 | 121.692 | 0.001 | 10 |
| 299-E33-38 | 121.697 | 121.694 | 0.003 | 10 |
| 299-E33-41 | 121.686 | 121.693 | -0.007 | 10 |
| 299-E33-42 | 121.692 | 121.694 | -0.001 | 10 |
| 299-E33-44 | 121.699 | 121.694 | 0.006 | 10 |
| 299-E34-10 | 121.704 | 121.692 | 0.012 | 10 |
| 299-E34-9 | 121.694 | 121.693 | 0.002 | 10 |
| 699-37-43 | 121.645 | 121.643 | 0.002 | 20 |
| 699-37-47a | 121.665 | 121.661 | 0.004 | 10 |
| 699-49-55a | 121.733 | 121.724 | 0.009 | 20 |
| 699-49-57a | 121.723 | 121.733 | -0.010 | 20 |

*Well assigned a low weight for PEST calibration.

NAVD88 = *North American Vertical Datum of 1988*

Table 6-1 also lists the final residuals obtained for the calibration targets. A residual, or estimated error, value for each measured point was calculated as the difference between the measured value and the value interpolated by the calculation. The target residual, which would indicate acceptable calibration, is <0.03 m (0.01 ft). Figure 6-1 shows the cumulative frequency plot of the absolute residuals obtained from the calibration. A total of 95% of the residuals are within 0.03 m (0.01 ft) of average measured groundwater levels for 2018. Thus, the calibration of this interpolation is deemed acceptable, and the results are usable for the purposes of this evaluation. Figure 6-2 provides a scatterplot comparing the calculated groundwater elevations with the measured groundwater elevations for 2018 (as obtained at the conclusion of the regularized inversion steps).

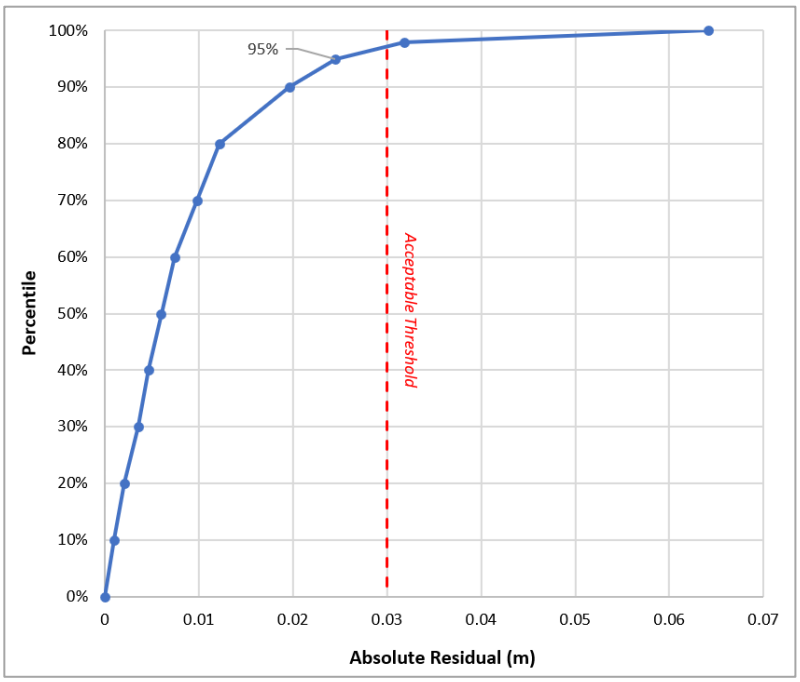


**Figure 6-1. Cumulative Relative Frequency of Absolute Residuals for 2018**

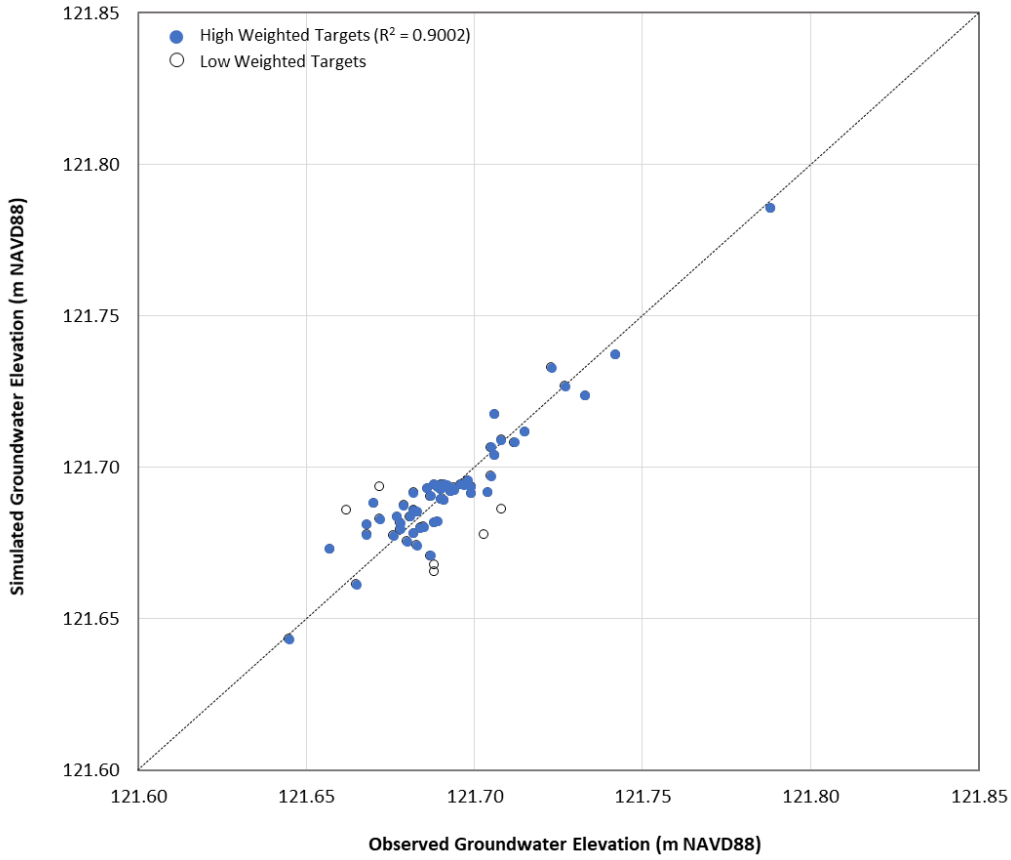


**Figure 6-2. Comparison of Observed Versus Simulated Groundwater Elevations**

## 6.2 Particle Tracking

Following the calibration process, groundwater elevations calculated throughout the domain of the simplified groundwater flow simulator were imported into the Groundwater Vistas graphical user interface and then exported as a regular grid using the Surfer software grid format for use as input for the particle-tracking calculations.

For the particle-tracking calculations presented in this ECF, an input file representing particle starting locations (release points) was prepared in an ArcGIS shapefile format. Particle starting locations were generated using one of the following approaches:

- **Tank farms:** Release points were located around the perimeter of each SST.
- **LLBG WMAs:** Release points were located along the centerline of Green Islands trenches.
- **Ditches, ponds, and trenches:** Release points were located along the centerline or on an equally spaced grid within the facility footprint.

The ArcGIS shapefile was then used as input to the mod-PATH3DU program. The following steps were then implemented:

1. A mod-PATH3DU particle-tracking input file that included the prescribed dispersion parameters was generated to simulate both advection and dispersion.
2. To simulate dispersion in particle tracking, the random-walk particle-tracking option implemented within mod-PATH3DU was used. As described in the software documentation (CHPRC-00261), for consistency, this random-walk module reads and uses the same dispersion inputs as the Hanford Site version of the transport simulator MT3DMS (Modular Transport, Three-Dimensional, Multi-Species Model).
3. Two American Standard Code for Information Interchange (ASCII) files representing the aquifer sediment mobile porosity and hydraulic conductivity distributions were generated based on the HSU zones shown in Figure 3-2 and the values from Table 4-1.
4. A maximum tracking time was set for each facility that allowed the majority of the particles released to migrate beyond the locations of the facility's monitoring wells during the calculations.
5. Particles were released and tracked from each particle starting location as follows:
   - Twenty particles were released from each starting location to provide the high density of particles in space and time required for the calculations.
   - mod-PATH3DU was executed to perform the particle-tracking calculations and produce a binary pathline output file containing the pathline for each tracked particle. Particles were tracked from each starting location using a different random seed value for the dispersion calculations.
6. A post-processing program (writep3doutput.exe) was executed to convert the mod-PATH3DU binary pathline output file into both an ArcGIS shapefile format and an ASCII text file format, both of which list particle locations and travel time.

The resulting particle tracks were superimposed upon figures that showed monitoring well locations to determine whether the monitoring locations are in the migration pathway of the simulated releases from the facilities.

## 6.3 Relative Detectability

Relative detectabilities were calculated to create maps that illustrate potential impacts of releases downgradient of each facility. The following steps were used to create this output.

1. An ArcGIS shapefile grid large enough to envelop all pathlines generated during particle tracking was defined. This subgrid was composed of 10 m by 10 m (33 ft by 33 ft) cells.

2. For each mapped event, the ArcGIS "Join" tool was used to intersect the pathlines with the regular subgrid and determine the count of unique pathlines intersecting each subgrid cell. The relative detectability within a subgrid cell for a given release scenario is calculated as follows:

$$RD = \frac{1}{MNP}\sum_{1}^{n} P_i N_i \qquad \textbf{(Equation 1)}$$

where:

| | | |
|---|---|---|
| $RD$ | = | relative detectability (ranging from zero to one) |
| $MNP$ | = | maximum number of particles that traversed any subgrid cell in all scenarios |
| $P_i$ | = | ascribed weight or probability of subscenario $i$ |
| $N_i$ | = | number of particles that traversed the calculation subgrid cell during subscenario $i$ |
| $n$ | = | total number of subscenarios within the simulated scenario |

Since only one scenario was being simulated for each facility, with 20 particles released from each starting location, Equation 1 is reduced to the following:

$$RD = \frac{N}{MNP}$$

This grid of relative detectability indices was converted to an ASCII grid format and imported into ArcGIS, after which bilinear interpolation was used to develop the relative detectability maps presented in facility-specific sections in Chapter 7.

The relative detectability maps illustrate two main features: (1) the relative likelihood of constituents impacting the water table migrating through different areas the aquifer downgradient of the DWMU, and (2) the relative suitability of each existing or proposed monitoring well location for detecting releases from the DWMU (i.e., in comparison to other existing or proposed monitoring well locations).
The relative detectability calculations and maps do not provide an absolute quantitative metric against which an existing or proposed monitoring well location can be compared or measured (e.g., a relative detectability limit above which wells should be placed when new wells are proposed) for several reasons. First, there are many aspects of potential future releases that cannot be known with certainty (e.g., timing, volume, rate, mass, and precise location of the release). As a consequence, an absolute metric, which would depend on these and other unknowable quantities, cannot reasonably be determined. Second, the overarching goal for each final monitoring well network is to have a distribution of wells that spans the expected range of detectability for each DWMU, rather than locating wells preferentially in the highest detectability areas only. As a result, during network evaluation and well placement in the design of the final well networks, areas of high relative detectability were identified and targeted. Locations at the fringes of detectability were also identified and monitored due to uncertainties in flow and migration directions and the timing of any future releases. In this re-evaluation, the analysis emphasized development of well networks that will continue to provide collective coverage of the general area of detectability in acknowledgement of these goals and uncertainties.

# 7 Results

This chapter presents outputs from the described calculations. Results of the calculations include the following:

- The 200 East Area water-level mapping results for 2018
- A map of 200 East Area calculated particle paths for the flow conditions determined for 2018 considering advective and dispersive migration
- Maps of calculated particle pathlines for each of the facilities for the flow conditions determined for 2018 considering advective and dispersive migration
- Maps of relative detectability downgradient of each facility based on the flow conditions determined for 2018

Figure 7-1 shows the groundwater elevation contours throughout the 200 East Area that were prepared using the methods and inputs described in this ECF. The figure shows general patterns of groundwater elevations and hydraulic gradients for conditions represented for 2018. Figure 7-2 shows the particle pathlines that were calculated at each facility. By showing the pathlines combined on the scale of the entire 200 East Area, Figure 7-2 shows patterns of groundwater flow and migration, as well as general patterns of spreading that might accompany contaminant migration for the groundwater flow conditions representative of 2018. The results for each 200 East Area facility are included in this chapter.

## 7.1 216-A-29 Ditch Input and Results

Section 4.2 describes the general input for the calculations. for the 216-A-29 Ditch. The following discussion provides additional information on the particle starting locations and calculational grid used. The results developed from the calculations specific to the 216-A-29 Ditch are also presented.

Located in the eastern part of the 200 East Area, the 216-A-29 Ditch is an unlined ditch placed into service in November 1955 to convey wastewater from the PUREX Plant chemical sewer to 216-B-3 Pond (Section 3.8 in DOE/RL-2016-66, *Hanford Site RCRA Groundwater Monitoring Report for 2016*). The 216-A-29 Ditch was removed from service in 1991 (Section 3.8 in DOE/RL-2016-66).

The 216-A-29 Ditch final status monitoring network (Figure 7-3) was determined in SGW-60592, *Engineering Evaluation Report for the 216-A-29 Ditch Groundwater Monitoring*, and consists of 4 upgradient wells (299-E25-34, 299-E25-43, 299-E25-47, and 299-E26-13) and 11 downgradient wells (existing wells 299-E25-35, 299-E25-238, 299-E25-239, and 299-E26-80; and proposed wells 216-A-29_PW-1, 216-A-29_PW-2, 216-A-29_PW-3, 216-A-29_PW-4, 216-A-29_PW-5, 216-A-29_PW-6, and 216-A-37-1_PW-3) (proposed as a shared network well for the 216-A-37-1 Crib).

### 7.1.1 Release Locations and Relative Detectability Grid for the 216-A-29 Ditch

The starting locations for the particle-tracking calculations represent the area over which a potential release from a given facility would impact the underlying water table. The particle releases were located at plausible release sites throughout the facility. Twenty particles were released from each release location specified along the centerline of the unit (Figure 7-4) and were tracked to provide the density of particles in space and time required for the calculations.

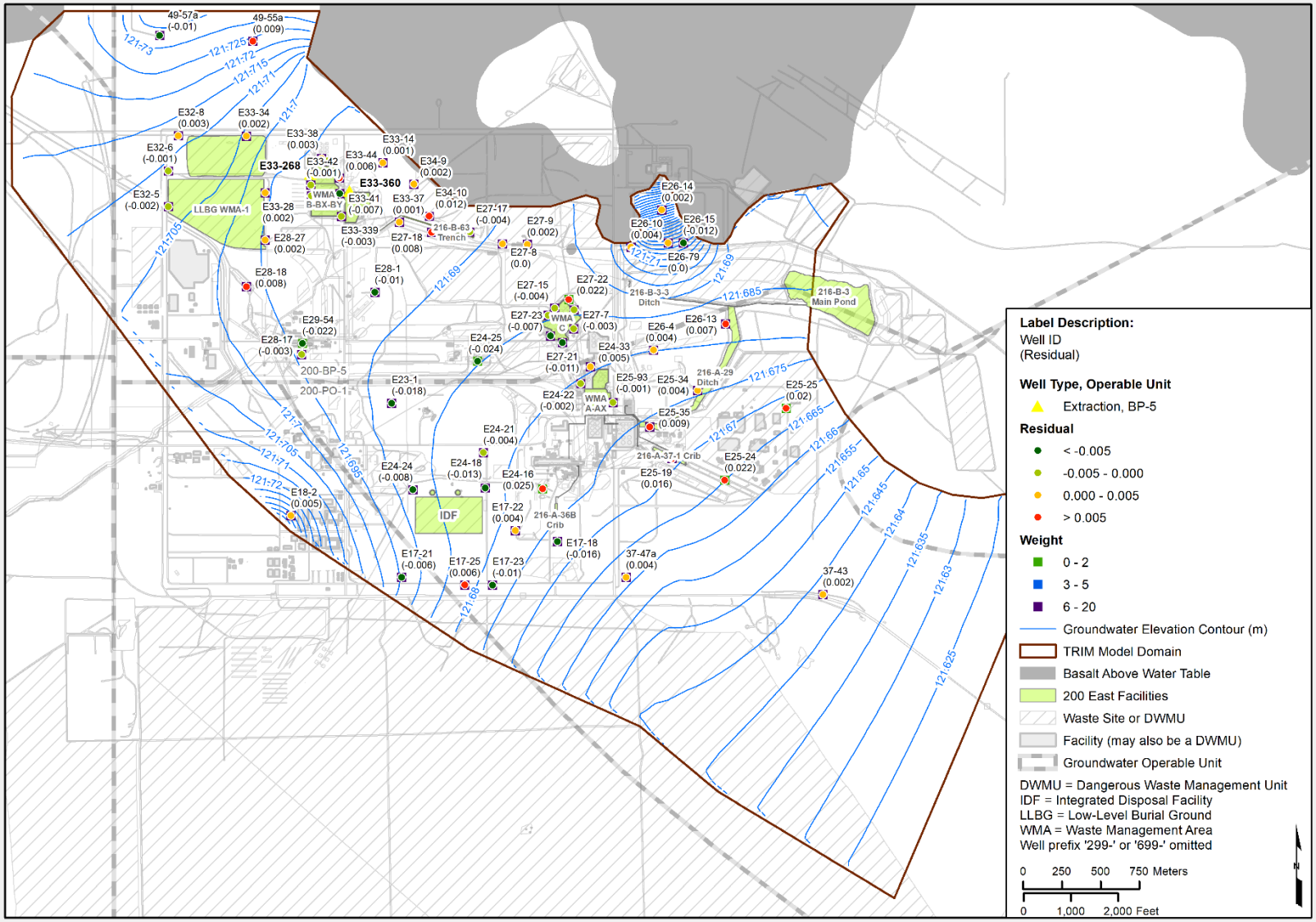


Figure 7-1. Mapped Groundwater Elevations and Calibration Residuals, 2018

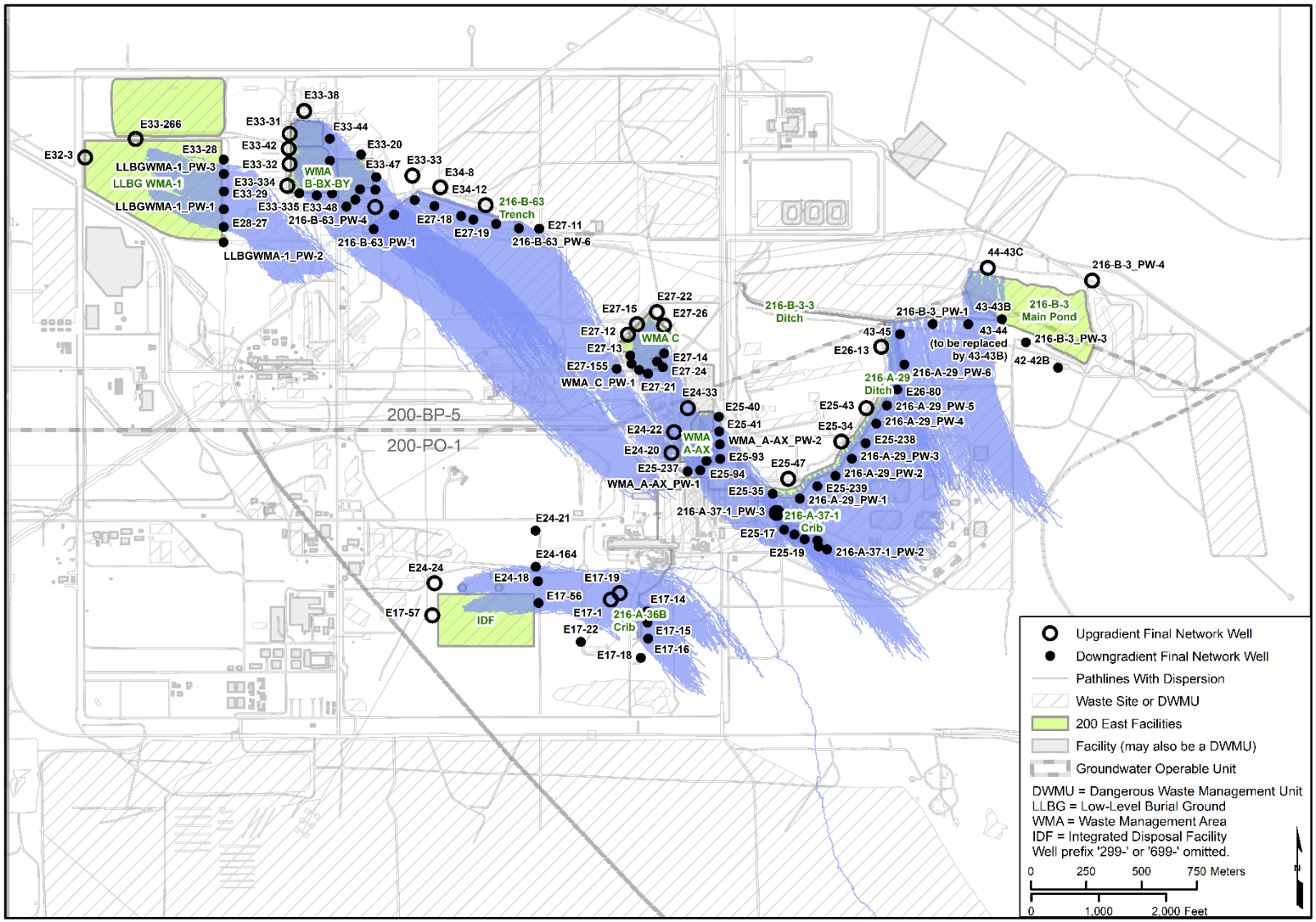


**Figure 7-2. Estimated Particle Pathlines, Advection, and Dispersion – 200 East Area, 2018**

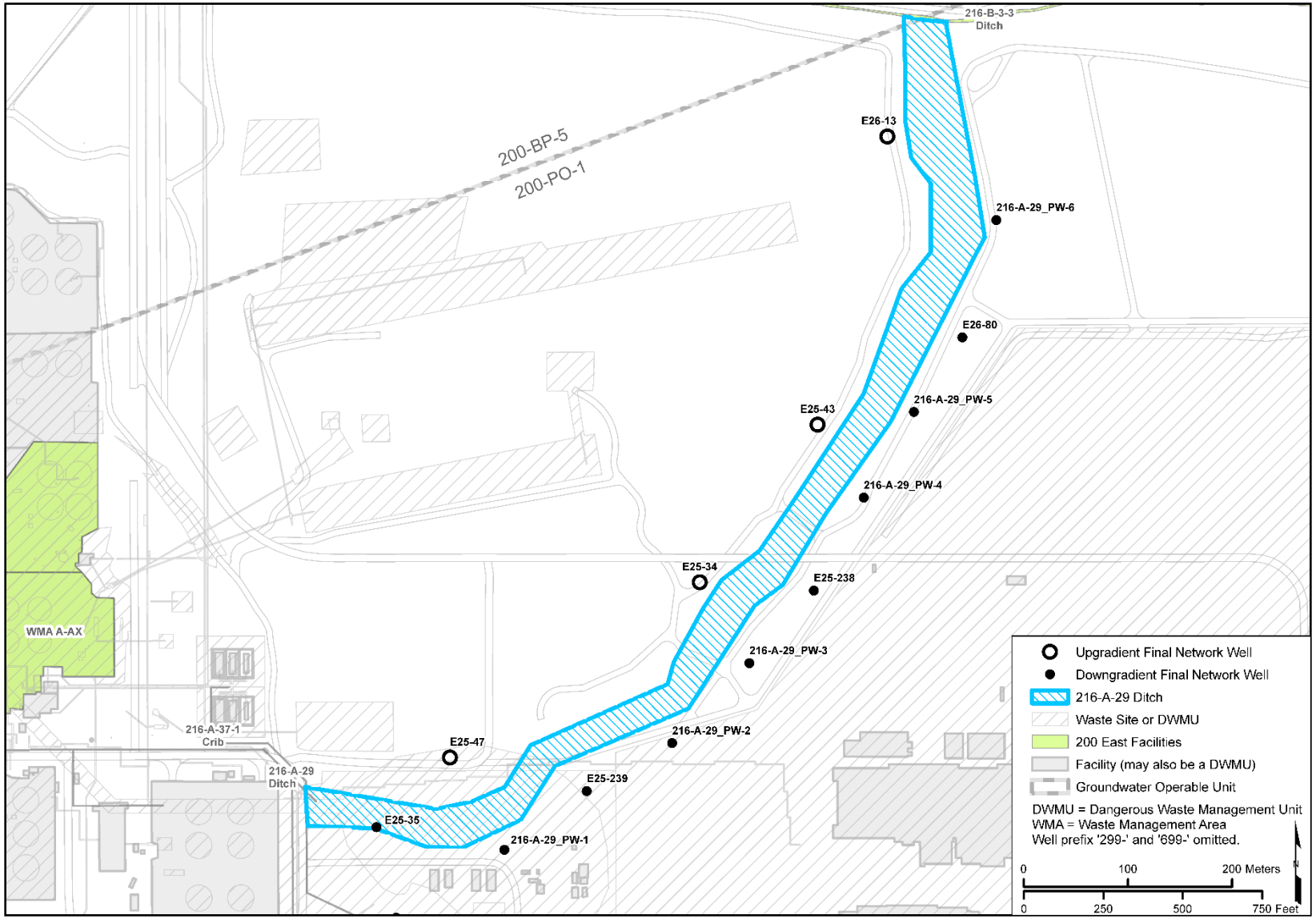


**Figure 7-3. Final Status Monitoring Network for the 216-A-29 Ditch**

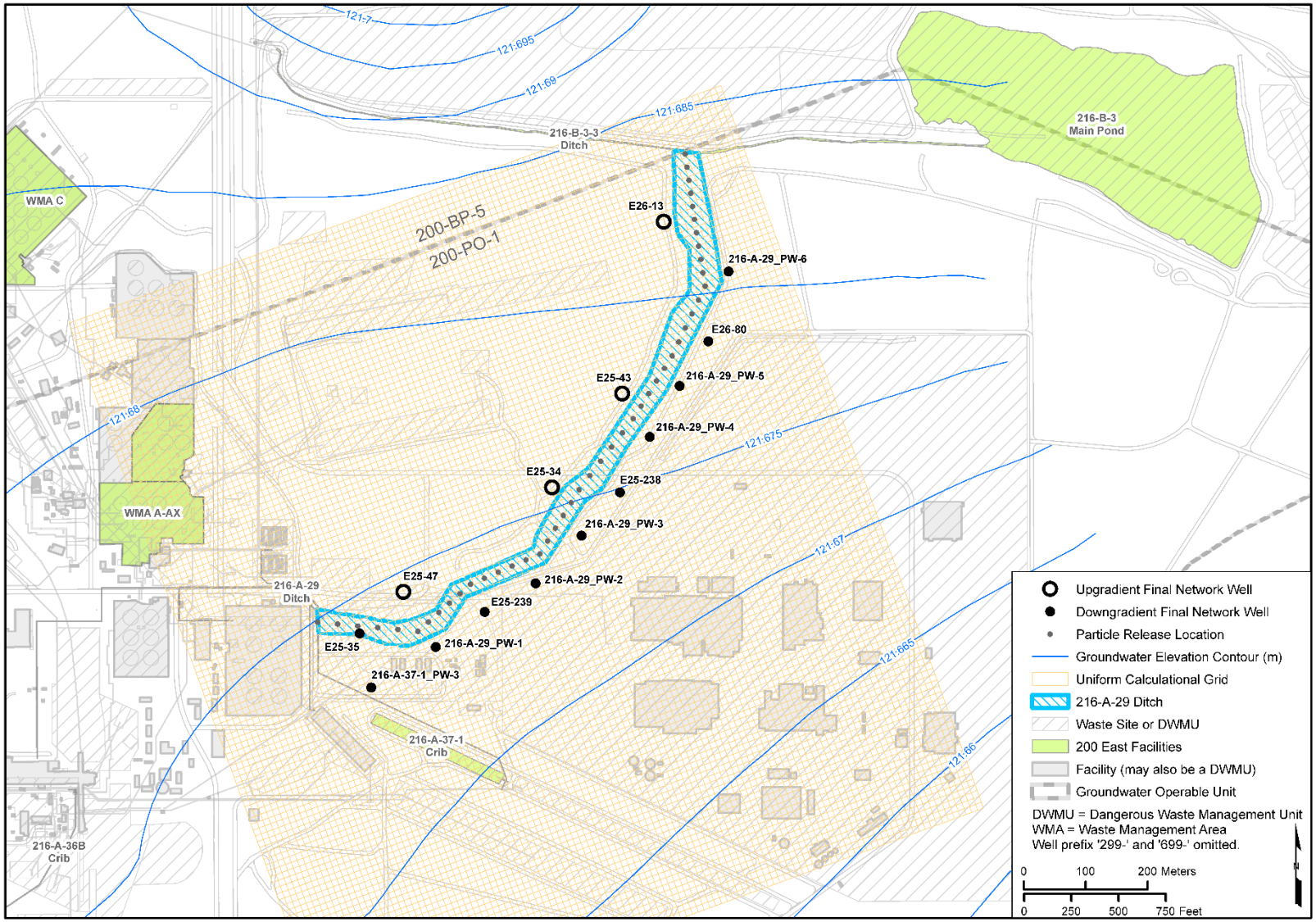


**Figure 7-4. Release Locations and Calculational Grid for the 216-A-29 Ditch**

A contour map of relative detectability is generated by counting the number of particles that pass through a pre-defined uniform calculational grid (Figure 7-4). The grid used to develop the relative detectability map is defined by 10 m by 10 m (33 ft by 33 ft) cells and is oriented to be parallel to the predominant groundwater flow direction at the 216-A-29 Ditch.

### 7.1.2 Results for the 216-A-29 Ditch

The groundwater elevation contours shown in Figure 7-1 form the basis for the facility-specific calculations performed in this ECF. The groundwater elevations near the 216-A-29 Ditch for 2018 are shown in Figure 7-5, and the outputs of the particle tracking and relative detectability calculations are discussed in the following sections.

#### *7.1.2.1 Particle Tracking*

After the groundwater elevation contour maps and underlying piecewise continuous elevation grids were prepared using TRIM, particle tracking was implemented using both advection and dispersion. The particle pathlines that were produced depict the patterns of spreading that might accompany contaminant migration near the unit for the flow conditions in 2018. Figure 7-5 shows the particle pathlines developed based on the groundwater elevations prepared throughout the 200 East Area using TRIM. The resulting maps were prepared based on the release of 20 particles from each starting location to provide the high density of particles in space and time required for these detailed facility-specific calculations. Figure 7-5 shows the particle pathlines calculated after 380 days of travel, by which time most of the particles would have arrived at or passed by the final status groundwater monitoring wells. Figure 7-5 depicts an instantaneous release to the water table from the release locations in the 216-A-29 Ditch to illustrate the adequacy of the well network for monitoring the entire facility.

#### *7.1.2.2 Relative Detectability Map*

To compare the relative density of the particles that pass by each monitoring well location, a relative detectability index was calculated at a subgrid level (described in Section 6.3), and a corresponding contour map was generated. Figure 7-6 shows the relative detectability map developed based on the instantaneous release of a large number of particles at the facility after 380 days of calculated travel, by which time all particles would have arrived at or passed by the final status groundwater monitoring wells. Figure 7-6 shows areas of relatively higher and lower potential impact from a release at the facility that reaches the water table for conditions represented for 2018.

The goal of well placement is for well locations to span the range of detectable areas downgradient of the 216-A-29 Ditch. The relative detectability map shows that under the evaluated range of conditions, the final status well network continues to meet this goal.

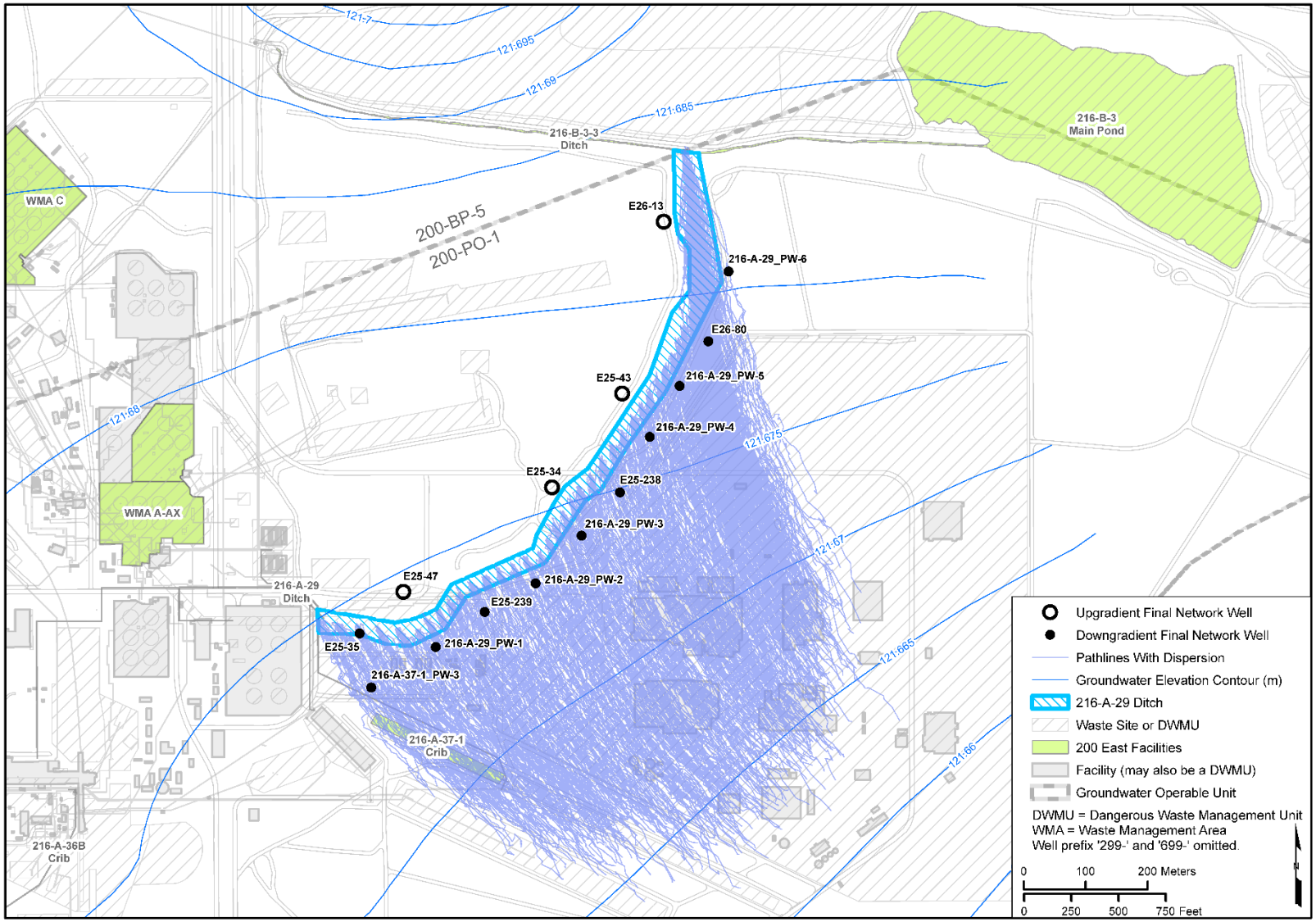


**Figure 7-5. Groundwater Elevations and Particle Pathlines for the 216-A-29 Ditch, 2018**

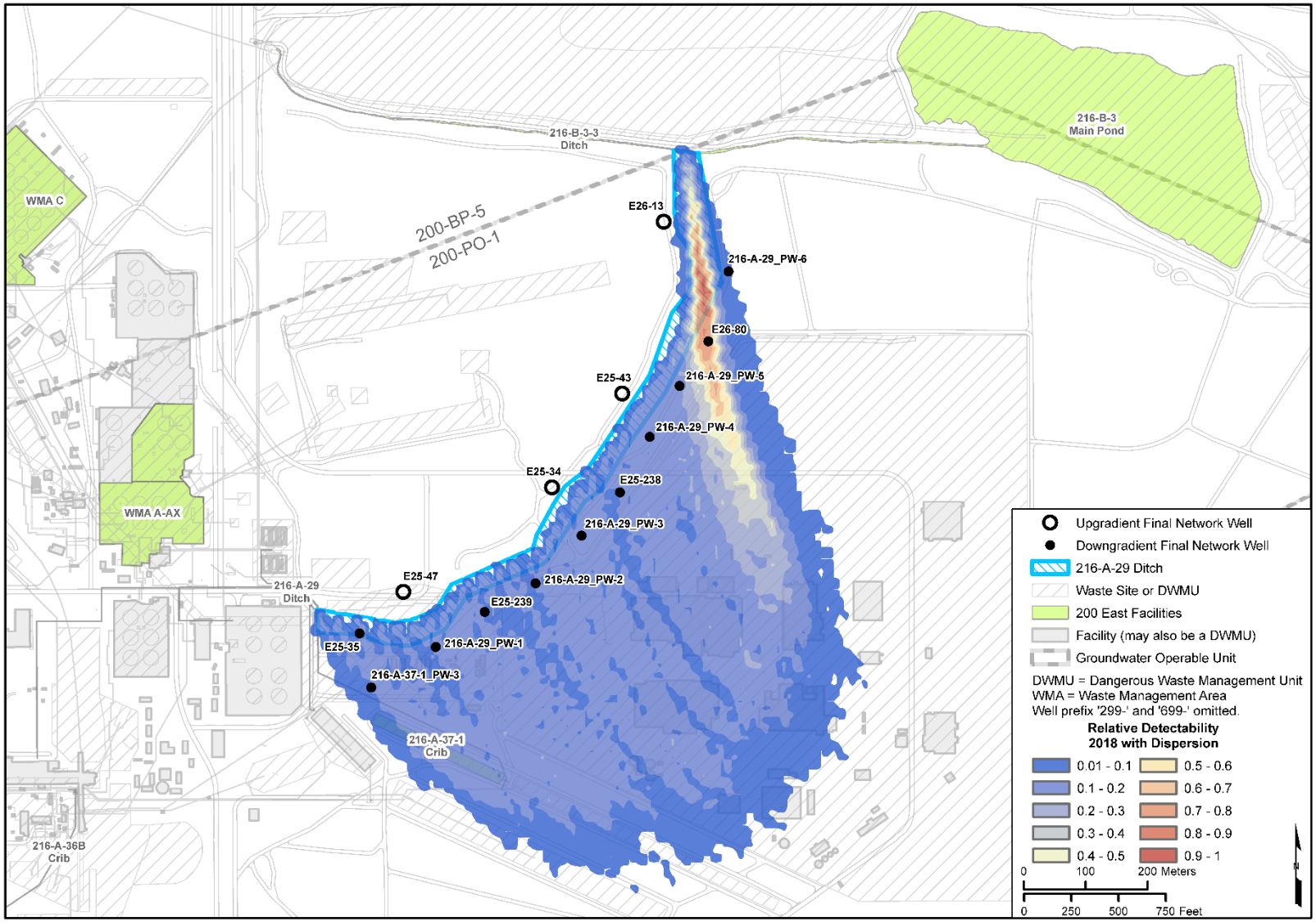


**Figure 7-6. Relative Detectability Map for the 216-A-29 Ditch, 2018**

## 7.2 216-A-36B Crib Input and Results

Section 4.2 describes the general input for the calculations for the 216-A-36B Crib. The following discussion provides additional information on the particle starting locations and calculational grid used. The results developed from the calculations specific to the 216-A-36B Crib are also presented.

Located in the southeastern part of the 200 East Area, the 216-A-36B Crib is a nonoperating treatment, storage, and disposal unit. The crib is approximately 150 m (490 ft) long, 2.3 to 3.4 m (7.5 to 11.2 ft) wide at its base, and 7 m (23 ft) deep (Section 2.4 in DOE/RL-2016-66). The 216-A-36B Crib was originally part of the 216-A-36 Crib that was used to percolate ammonia scrubber waste effluent from PUREX Plant operations to the soil column. The crib received PUREX effluent starting in September 1965 (DOE/RL-2010-93, *Interim Status Groundwater Monitoring Plan for the 216-A-36B PUREX Plant Crib*). In March 1966, a grout barrier was installed to isolate the northern portion of the crib, separating the crib into 216-A-36A (the northern section) and 216-A-36B (the southern section) (DOE/RL-2010-93).

The 216-A-36B Crib final status monitoring network (Figure 7-7) was determined in SGW-60595, *Engineering Evaluation Report for the 216-A-36B Crib Groundwater Monitoring*, and consists of two upgradient wells (existing wells 299-E17-1 and 299-E17-19) and four downgradient wells (existing wells 299-E17-14, 299-E17-15, 299-E17-16, and 299-E17-18).

### 7.2.1 Release Locations and Relative Detectability Grid for the 216-A-36B Crib

The starting locations for the particle-tracking calculations represent the area over which a potential release from a given facility would impact the underlying water table. The particle releases were located at plausible release sites throughout the facility. Twenty particles were released from each release location specified along the centerline of the unit (Figure 7-8) and tracked to provide the density of particles in space and time required for the calculations.

A contour map of relative detectability was generated by counting the number of particles that pass through a pre-defined uniform calculational grid (Figure 7-8). The grid used to develop the relative detectability maps is defined by 10 m by 10 m (33 ft by 33 ft) cells and is oriented to be parallel to the predominant groundwater flow direction at the 216-A-36B Crib.

### 7.2.2 Results for the 216-A-36B Crib

The groundwater elevation contours shown in Figure 7-2 form the basis for the facility-specific calculations performed in this ECF. The elevations near the 216-A-36B Crib for 2018 are shown in Figure 7-9, and the outputs of the particle tracking and relative detectability calculations are discussed in the following sections.

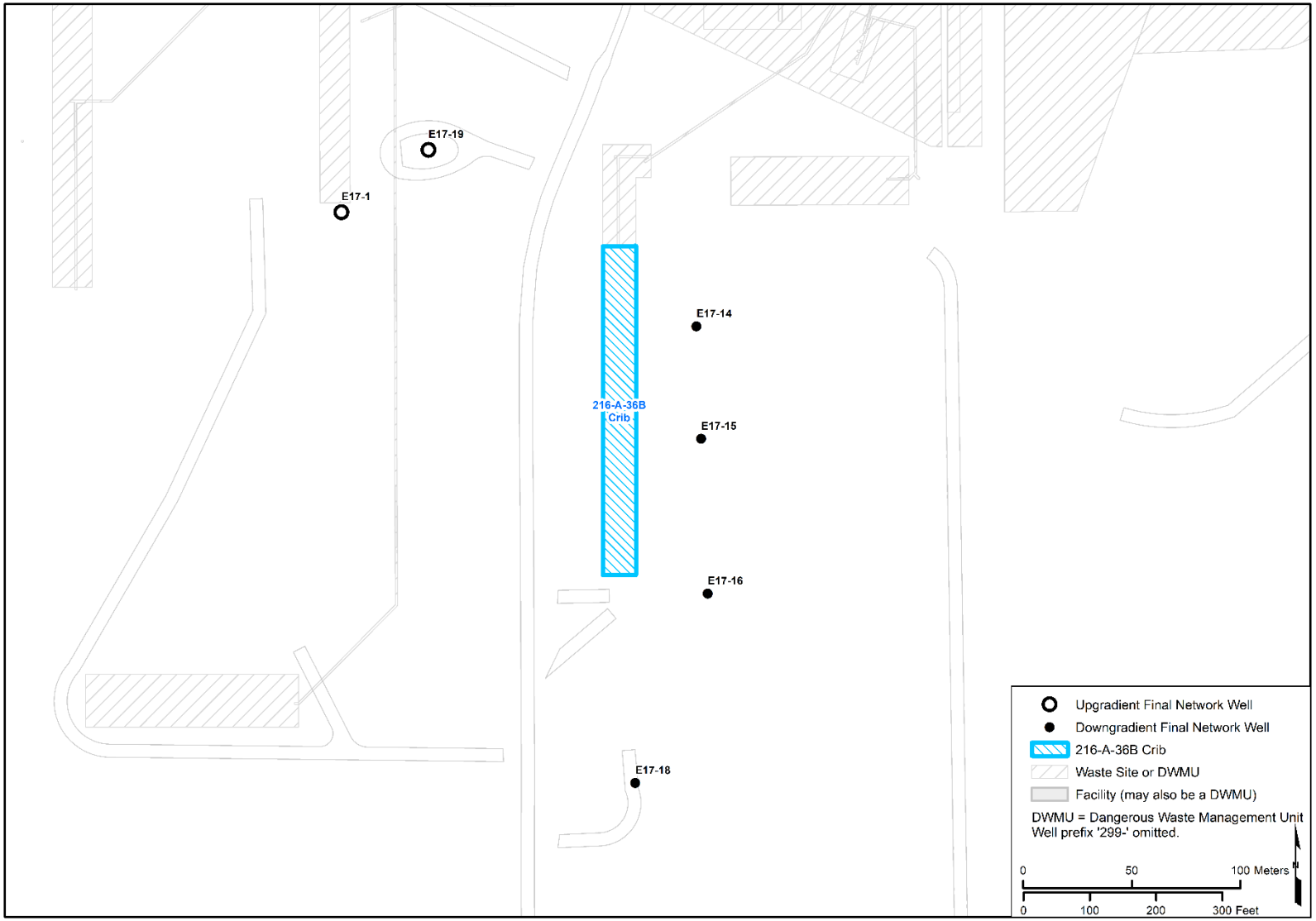


**Figure 7-7. Final Status Monitoring Network for the 216-A-36B Crib**

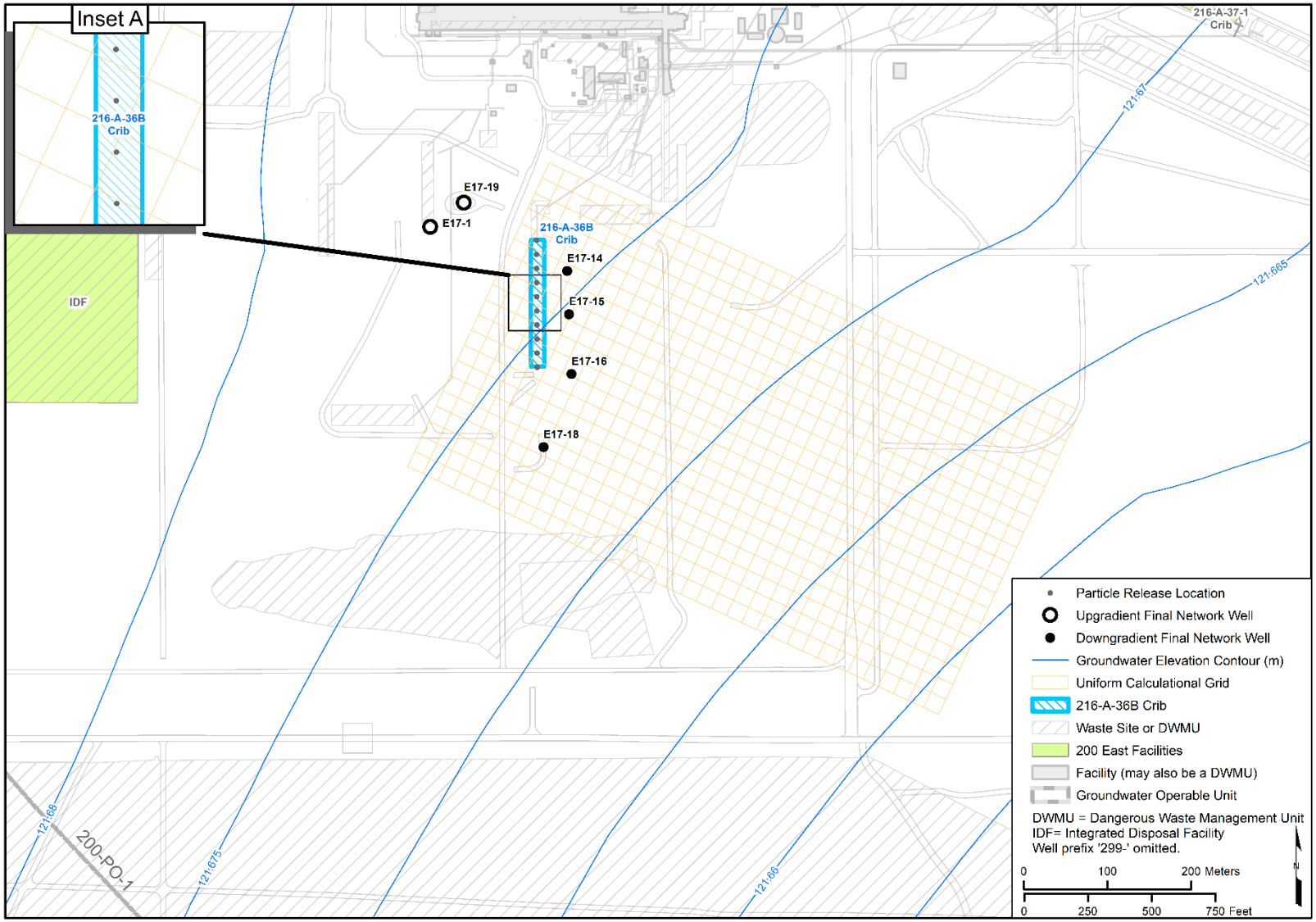


**Figure 7-8. Release Locations and Calculational Grid for the 216-A-36B Crib**

#### *7.2.2.1 Particle Tracking*

After the groundwater elevation contour maps and underlying piecewise continuous elevation grids were prepared using TRIM, particle tracking was implemented using both advection and dispersion. The particle pathlines that were produced depict the patterns of spreading that might accompany the contaminant migration near the unit for the flow conditions in 2018. Figure 7-9 shows the particle pathlines developed based on the groundwater elevations prepared throughout the 200 East Area using TRIM. The resulting maps were prepared based on the release of 20 particles from each starting location to provide the high density of particles in space and time required for the detailed facility-specific calculations. Figure 7-9 shows the particle pathlines calculated after 100,000 days of travel, by which time most of the particles would have arrived at or passed by the final status groundwater monitoring wells. Figure 7-9 depicts an instantaneous release to the water table from the release locations in the 216-A-36B Crib to illustrate the adequacy of the well network for monitoring the entire facility.

#### *7.2.2.2 Relative Detectability Map*

To compare the relative density of the particles that pass by each monitoring well location, a relative detectability index was calculated at a subgrid level (described in Section 6.3), and a corresponding contour map was generated. Figure 7-10 shows the relative detectability map developed based on the instantaneous release of a large number of particles at the facility after 100,000 days of calculated travel, by which time all particles would have arrived at or passed by the final status groundwater monitoring wells. Figure 7-10 depicts areas of relatively higher and lower potential impact from a release at the facility that reaches the water table for conditions represented in 2018.

The goal of well placement is for well locations to span the range of detectable areas downgradient of the 216-A-36B Crib. The relative detectability map shows that under the evaluated range of conditions, the final status well network continues to meet this goal.

## 7.3 216-A-37-1 Crib Input and Results

Section 4.2 describes the general input for the calculations for the 216-A-37-1 Crib. The following discussion describes the particle starting locations and calculational grid used. The results developed from the calculations specific to the 216-A-37-1 Crib are also presented.

The 216-A-37-1 Crib, located in the eastern part of the 200 East Area, is a nonoperating treatment, storage, and disposal unit. The crib is approximately 213 m (699 ft) long and 5.2 m (17.1 ft) deep (Section 2.5 in DOE/RL-2016-66). Figure 2-2 in DOE/RL-2010-92, *Interim Status Groundwater Monitoring Plan for the 216-A-37-1 PUREX Plant Crib*, shows that the crib is 3 m (10 ft) wide at its base. During its operation, the 216-A-37-1 Crib was used to percolate condensate from the 242A evaporator process to the soil column (DOE/RL-2010-92).

The 216-A-37-1 Crib final status monitoring network (Figure 7-11) was determined in SGW-60593, *Engineering Evaluation Report for the 216-A-37-1 Crib Groundwater Monitoring*, and consists of one upgradient well (proposed well 216-A-37-1_PW-3) and six downgradient wells (existing wells 299-E25-17, 299-E25-19, 299-E25-20, and 299-E25-95; and proposed wells 216-A-37-1_PW-1 and 216-A-37-1_PW-2).

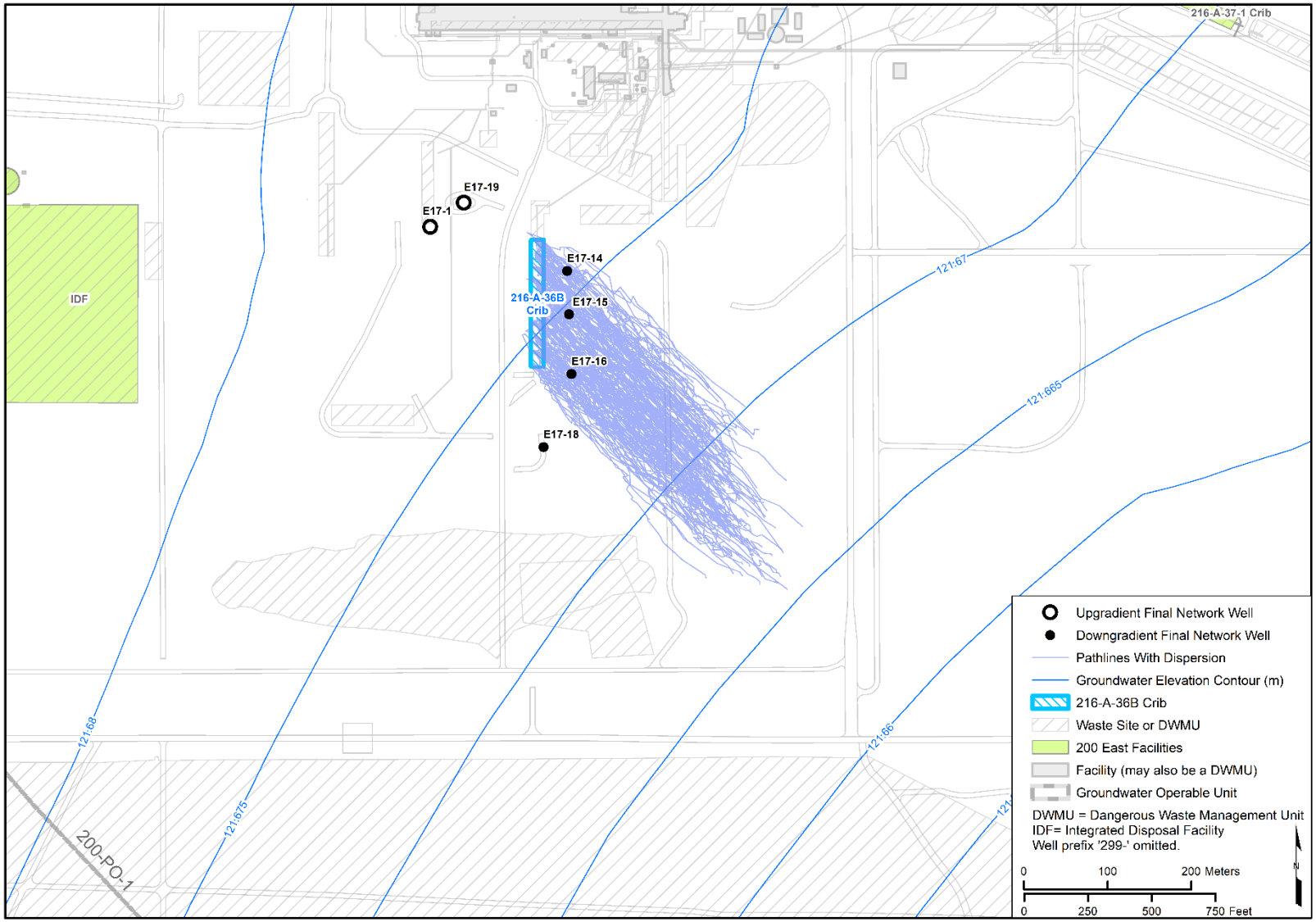


**Figure 7-9. Groundwater Elevations and Particle Pathlines for the 216-A-36B Crib, 2018**

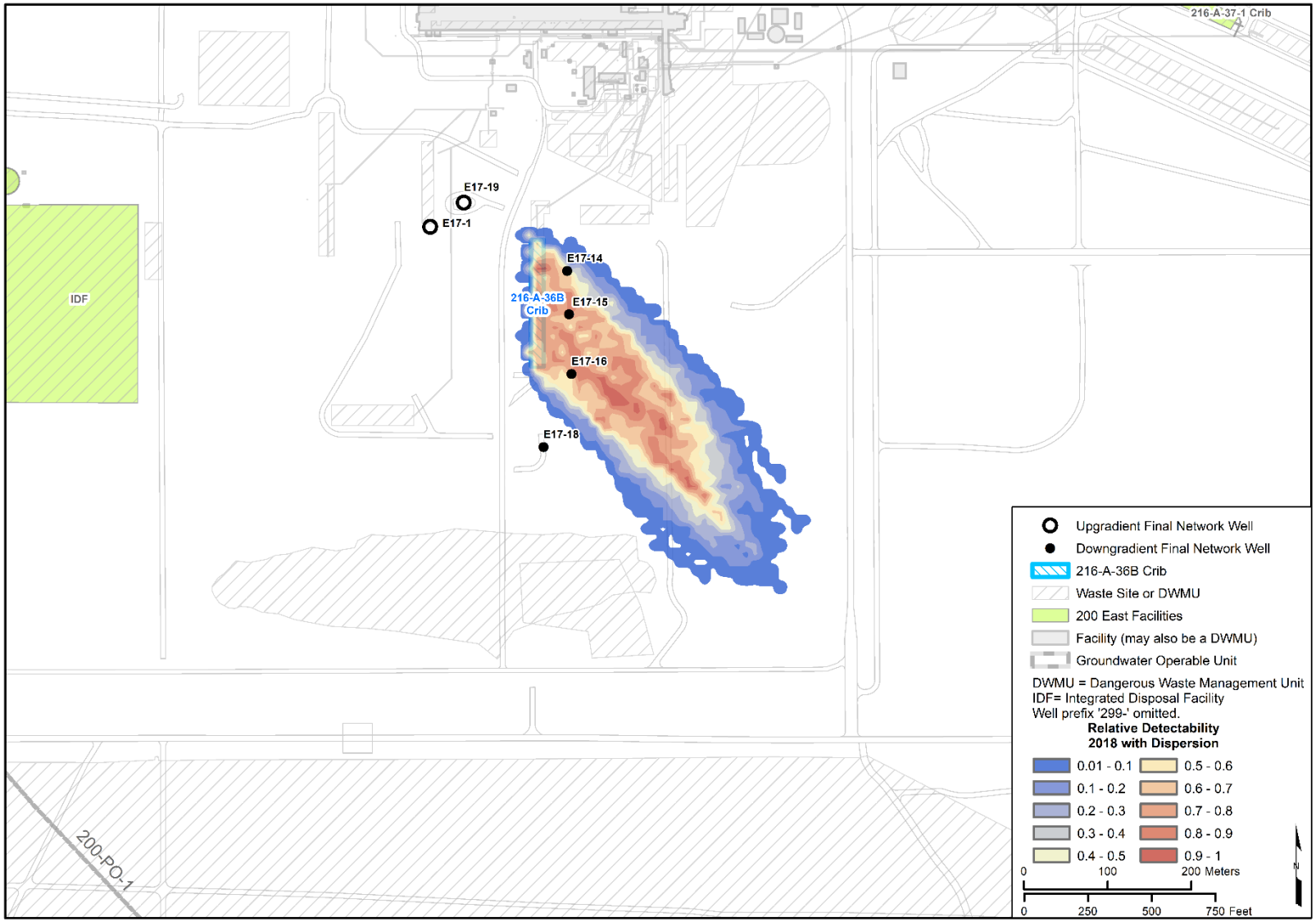


**Figure 7-10. Relative Detectability Map for the 216-A-36B Crib, 2018**

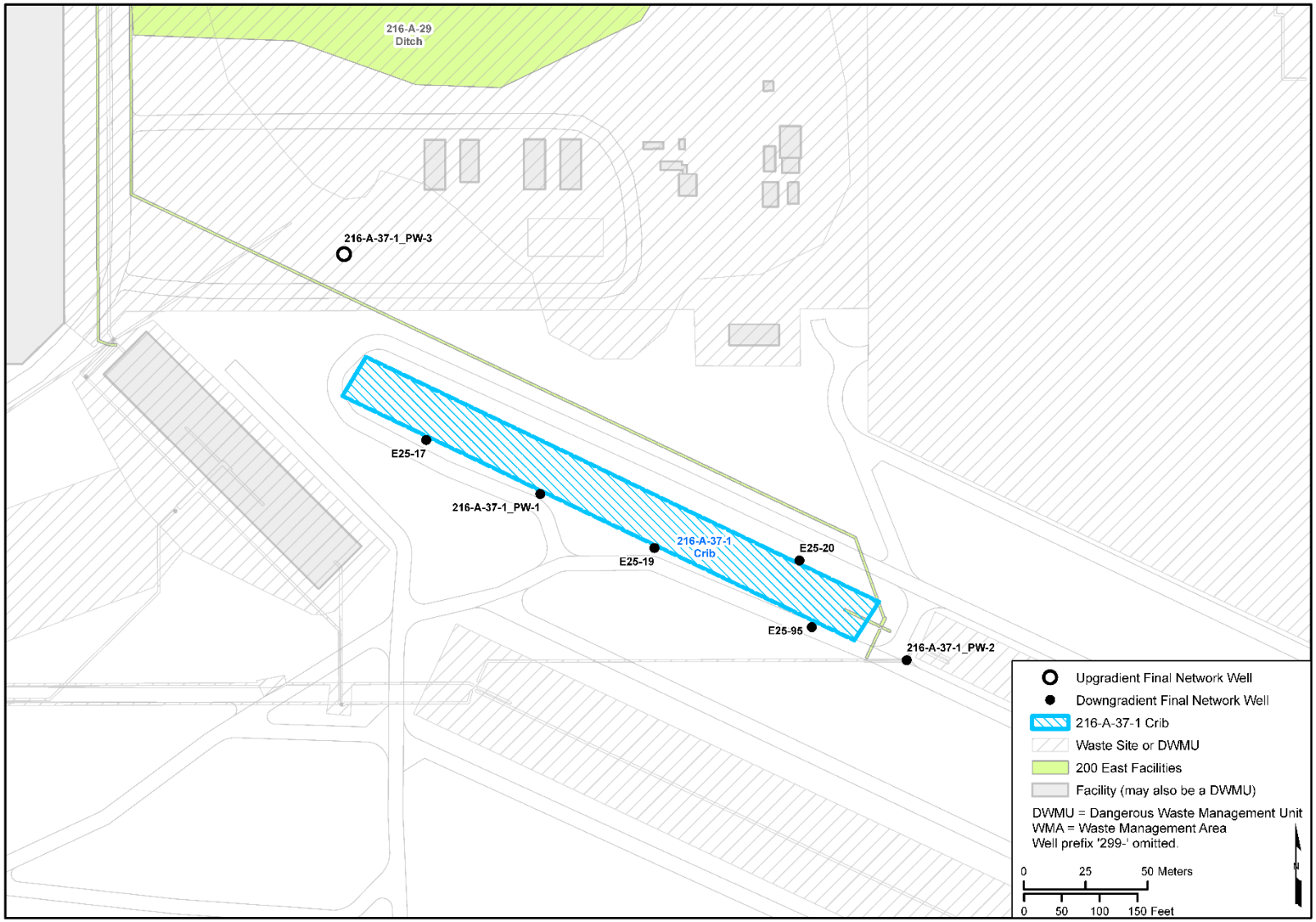


**Figure 7-11. Final Status Monitoring Network for the 216-A-37-1 Crib**

### 7.3.1 Release Locations and Relative Detectability Grid for the 216-A-37-1 Crib

The starting locations for the particle-tracking calculations represent the area over which a potential release from a given facility would impact the underlying water table. The particle releases were located at plausible release sites throughout the facility. Twenty particles were released from each release location specified along the centerline of the unit (Figure 7-12) and tracked to provide the density of particles in space and time required for the calculations.

A contour map of relative detectability was generated by counting the number of particles that pass through a pre-defined uniform calculational grid (Figure 7-12). The grid used to develop the relative detectability maps is defined by 10 m by 10 m (33 ft by 33 ft) cells and is oriented to be parallel to the predominant groundwater flow direction at the 216-A-37-1 Crib.

### 7.3.2 Results for the 216-A-37-1 Crib

The groundwater elevation contours shown in Figure 7-1 form the basis for the facility-specific calculations performed in this ECF. The elevations near the 216-A-37-1 Crib for 2018 are shown in Figure 7-13, and the outputs of the particle tracking and relative detectability calculations are discussed in the following sections.

#### *7.3.2.1 Particle Tracking*

After the groundwater elevation contour maps and underlying piecewise continuous elevation grids were prepared using TRIM, particle tracking was implemented using both advection and dispersion. The particle pathlines that were produced depict the patterns of spreading that might accompany the contaminants migration near the unit for the flow conditions in 2018. Figure 7-13 shows the particle pathlines developed based on the groundwater elevations prepared throughout the 200 East Area using TRIM. The resulting maps were prepared based on the release of 20 particles from each starting location to provide the high density of particles in space and time required for these detailed facility-specific calculations. Figure 7-13 shows the particle pathlines calculated after 425 days of travel, by which time most of the particles would have arrived at or passed by the final status groundwater monitoring wells. Figure 7-13 depicts an instantaneous release to the water table from the release locations in the 216-A-37-1 Crib to illustrate the adequacy of the well network for monitoring the entire facility.

#### *7.3.2.2 Relative Detectability Map*

To compare the relative density of the particles that pass by each monitoring well location, a relative detectability index was calculated at a subgrid level (described in Section 6.3), and a corresponding contour map was generated. Figure 7-14 shows the relative detectability map developed based on the instantaneous release of a large number of particles at the facility after 425 days of calculated travel, by which time all particles would have arrived at or passed by the final status groundwater monitoring wells. Figure 7-14 depicts areas of relatively higher and lower potential impact from a release at the facility that reaches the water table for conditions represented in 2018.

The goal of well placement is for well locations to span the range of detectable areas downgradient of the 216-A-371 Crib. The relative detectability map shows that under the evaluated range of conditions, the final status well network continues to meet this goal.

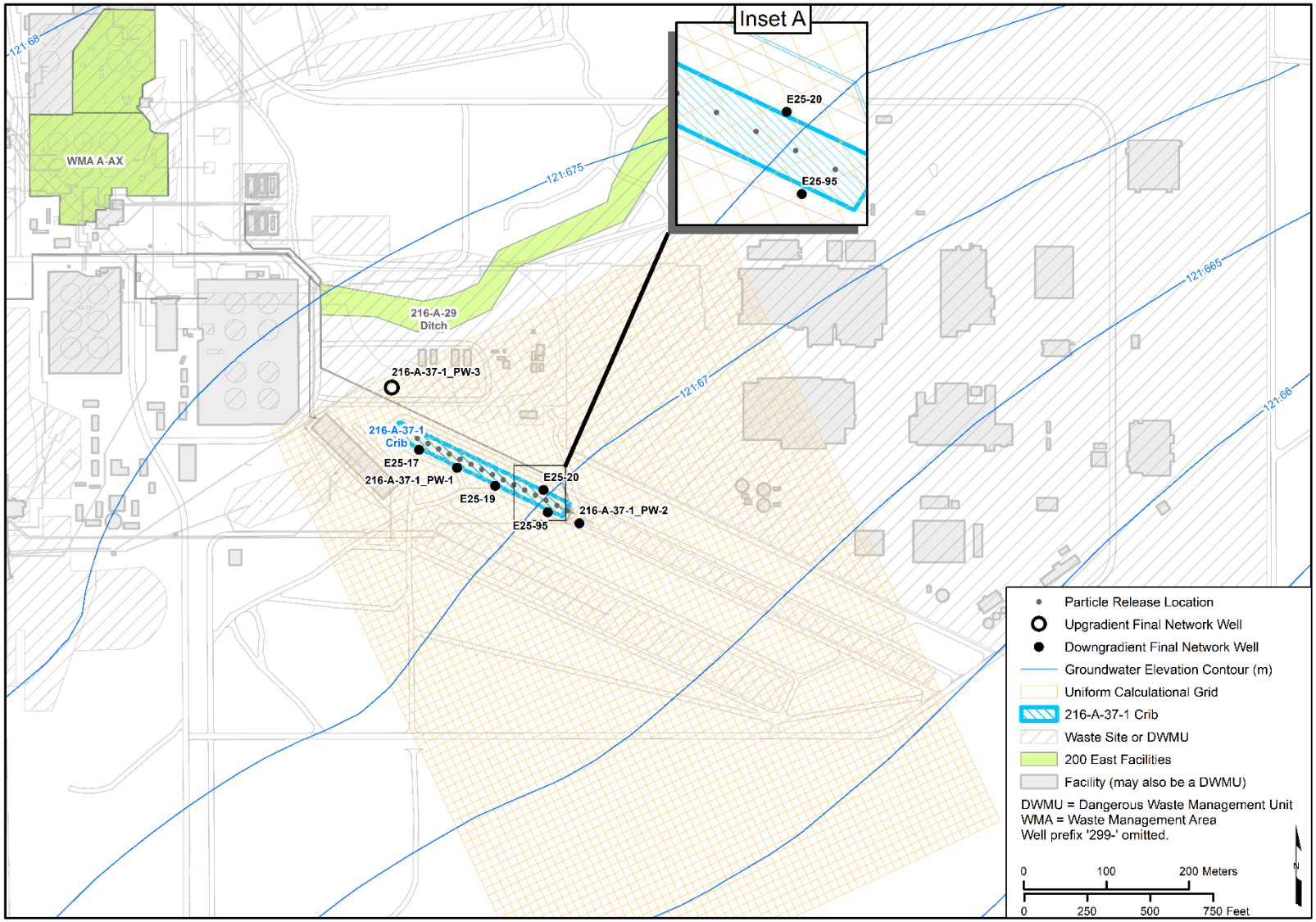


**Figure 7-12. Release Locations and Calculational Grid for the 216-A-37-1 Crib**

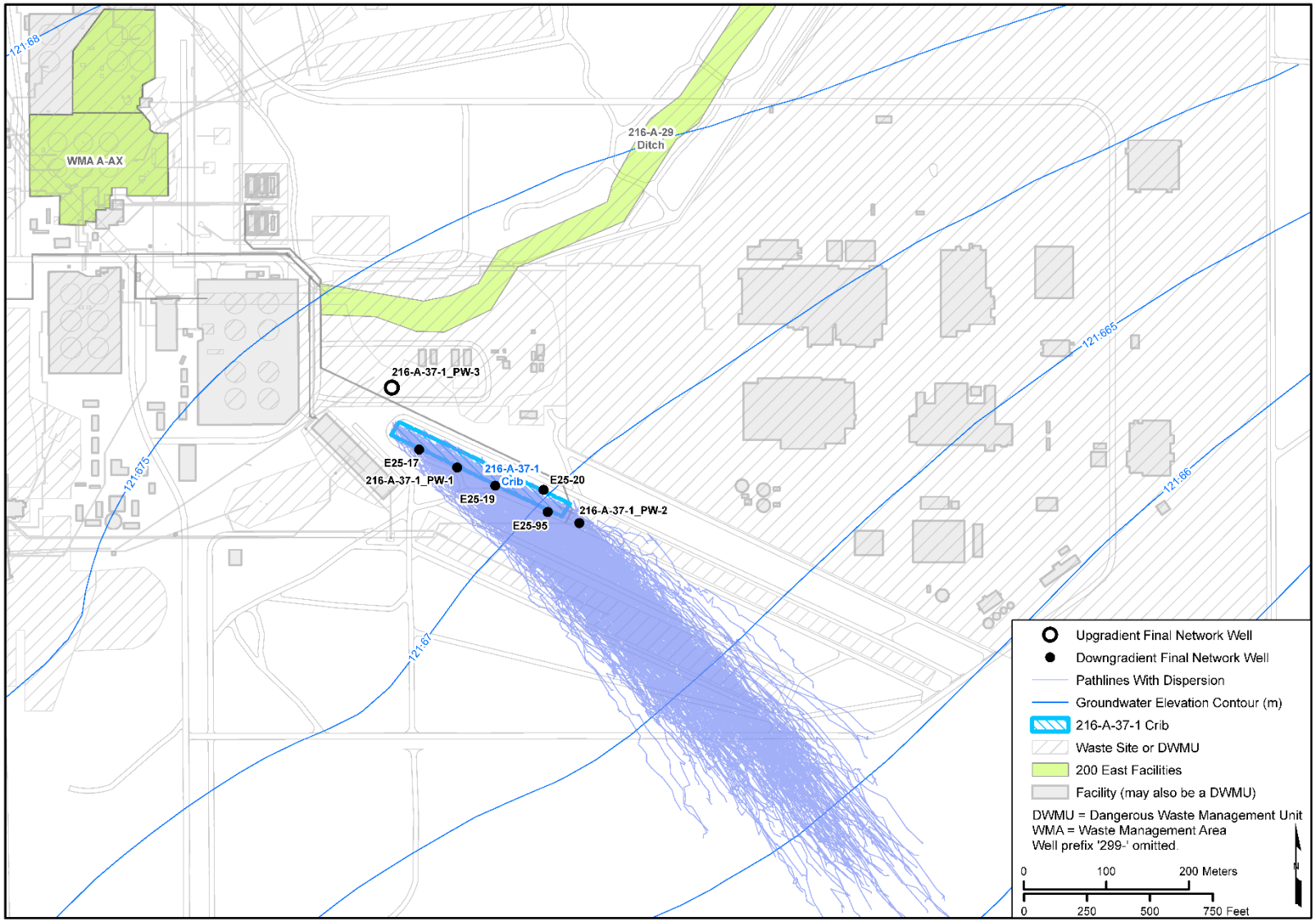


**Figure 7-13. Groundwater Elevations and Particle Pathlines for the 216-A-37-1 Crib, 2018**

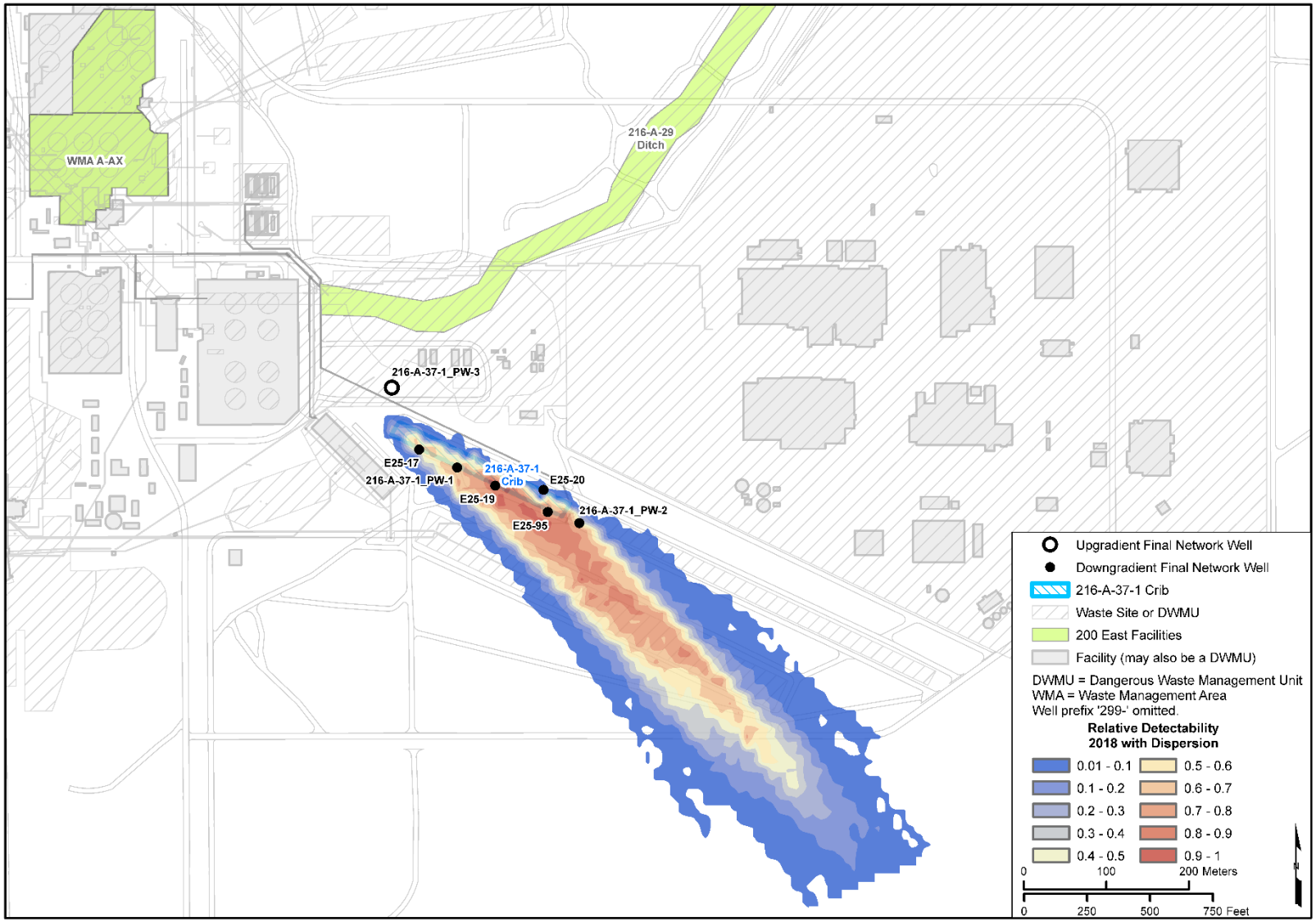


**Figure 7-14. Relative Detectability Map for the 216-A-37-1 Crib, 2018**

## 7.4 216-B-3 Main Pond Input and Results

Section 4.2 describes the general input for the calculations. for the 216-B-3 Main Pond DWMU. The following discussion describes the particle starting locations and calculational grid used. The results developed from the calculations specific to the 216-B-3 Main Pond DWMU are also presented.

The 216-B-3 Main Pond DWMU comprises the 216-B-3 Main Pond (hereinafter referred to as the Main Pond) and the 216-B-3-3 Ditch. The Main Pond and the 216-B-3-3 Ditch are collectively referred to as "216-B-3 Pond" hereinafter. For groundwater monitoring of the DWMU, only the Main Pond and the eastern portion of the 216-B-3-3 Ditch (from its juncture with the 216-A-29 Ditch to where the 216-B-3-3 Ditch enters the Main Pond) are included (Chapter 1 in DOE/RL-2008-59, *Interim Status Groundwater Monitoring Plan for the 216-B-3 Pond*). For the analysis discussed here, the facility-specific representation of 216-B-3 Pond excludes the western portion of the 216-B-3-3 Ditch.

The 216-B-3 Pond is located in the eastern part of the 200 East Area. The pond is an unlined surface impoundment that historically received wastewater (e.g., steam condensate and chemical sewer) discharges from B Plant and then later from the PUREX Plant. During operations, the Main Pond covered about 14.2 ha (35 ac) with a depth up to 6.1 m (20 ft). (Section 1.1.1 in PNNL-15479, *Groundwater Monitoring Plan for the Hanford Site 216-B-3 Pond RCRA Facility*).

The 216-B-3 Pond final status monitoring network (Figure 7-15) was determined in SGW-60591, *Engineering Evaluation Report for the 216-B-3 Main Pond Groundwater Monitoring*, and consists of two upgradient wells (existing well 699-44-43C and proposed well 216-B-3_PW-4) and six downgradient wells (existing wells 699-42-42B, 699-43-43B, and 699-43-45 and proposed wells 216-B-3_PW-1, 216-B-3_PW-2, and 216-B-3_PW-3).

### 7.4.1 Release Locations and Relative Detectability Grid for the 216-B-3 Pond

To prepare a relative detectability map, a distribution of facility-specific starting locations is required. The starting locations for the particle-tracking calculations represent the area over which a potential release from a given facility would impact the underlying water table. Particles were not released in the eastern portion of the 216-B-3 Pond complex (i.e., eastern extent of the Main Pond) due to the hydrogeologic conditions encountered in that area. As described in Section 2.2 of PNNL-15479, the lithologic and hydrologic data collected from drilling and groundwater monitoring indicate that the uppermost aquifer beneath the 216-B-3 Pond complex occurs in confined and unconfined conditions, depending upon location. The uppermost aquifer is unconfined to the west, southwest, and north of the Main Pond and becomes progressively more confined to the east and southeast. The boundary between confined and unconfined conditions is not exactly known and may be gradational. The Ringold Formation member of Wooded Island – unit A (Rwia) comprises the bulk of the uppermost aquifer in the Main Pond area (with some Hanford formation in the far west). The Ringold lower mud unit forms a confining horizon and potential perching layer to the east. The saturated hydraulic conductivity of the Ringold lower mud is very low compared to the Rwia and Hanford formation. As a consequence, the potential for migration within the Ringold lower mud is anticipated to be vastly less than within the Rwia and Hanford formation, and the Ringold lower mud may isolate portions of the aquifer from contamination resulting from surface releases.

The particle releases were located at plausible release sites throughout the western extent of the Main Pond and the adjoining ditch (Figure 7-16). Twenty particles were released and tracked from each release location to provide the density of particles in space and time required for the calculations.

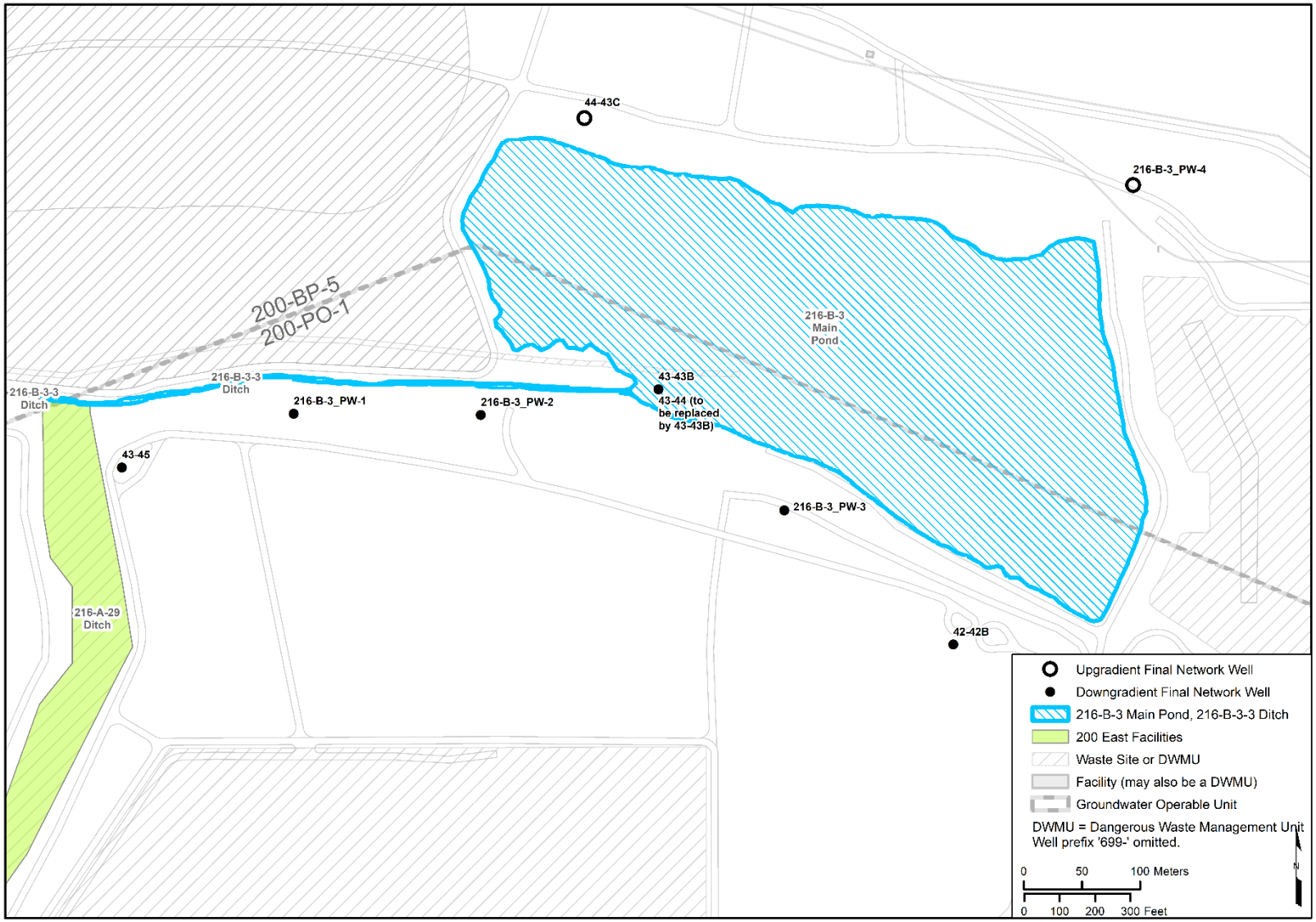


**Figure 7-15. Final Status Monitoring Network for the 216-B-3 Pond**

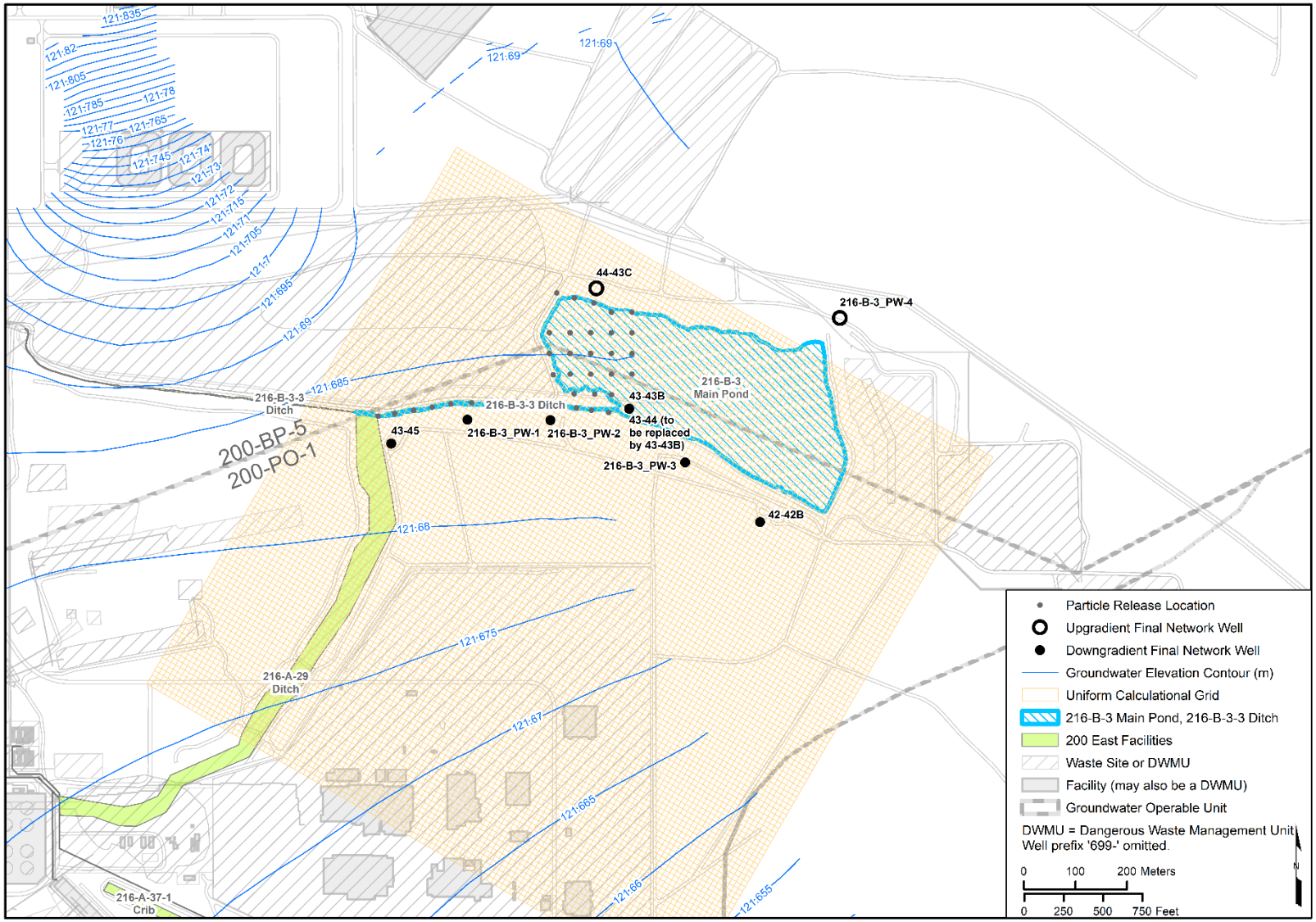


**Figure 7-16. Release Locations and Calculational Grid for the 216-B-3 Pond**

A contour map of relative detectability was generated by counting the number of particles that pass through a pre-defined uniform calculational grid (Figure 7-16). The grid used to develop the relative detectability maps is defined by 10 m by 10 m (33 ft by 33 ft) cells and is oriented to be parallel to the predominant groundwater flow direction at 216-B-3 Pond.

### 7.4.2 Results for the 216-B-3 Pond

The groundwater elevation contours shown in Figure 7-1 form the basis for the facility-specific calculations performed in this ECF. The elevations near 216-B-3 Pond for 2018 are shown in Figure 7-17, and the outputs of the particle tracking and relative detectability calculations are discussed in the following sections.

#### *7.4.2.1 Particle Tracking*

After the groundwater elevation contour maps and underlying piecewise continuous elevation grids were prepared using TRIM, particle tracking was implemented using both advection and dispersion. The particle pathlines that were produced depict the patterns of spreading that might accompany the contaminant migration near the unit for the flow conditions in 2018. Figure 7-17 shows the particle pathlines developed based on the groundwater elevations prepared throughout the 200 East Area using TRIM. The resulting maps were prepared based on the release of 20 particles from each starting location to provide the high density of particles in space and time required for these detailed facility-specific calculations. Figure 7-17 shows the particle pathlines calculated after 500 days of travel, by which time most of the particles would have arrived at or passed by the final status groundwater monitoring wells. Figure 7-17 depicts an instantaneous release to the water table from the release locations in the 216-B-3 Pond to illustrate the adequacy of the well network for monitoring the entire facility.

#### *7.4.2.2 Relative Detectability Map*

To compare the relative density of the particles that pass by each monitoring well location, a relative detectability index was calculated at a subgrid level (described in Section 6.3), and a corresponding contour map was generated. Figure 7-18 shows the relative detectability map developed based on the instantaneous release of a large number of particles at the facility after 500 days of calculated travel, by which time all particles would have arrived at or passed by the final status groundwater monitoring wells. Figure 7-18 depicts areas of relatively higher and lower potential impact from a release at the facility that reaches the water table for conditions represented for 2018.

The goal of well placement is for well locations to span the range of detectable areas downgradient of 216-B-3 Pond. The relative detectability map shows that under the evaluated range of conditions, the final status well network continues to meet this goal.

## 7.5 216-B-63 Trench Input and Results

Section 4.2 describes the general input for the calculations for the 216-B-63 Trench. The following discussion describes the particle starting locations and calculational grid used. The results developed from the calculations specific to the 216-B-63 Trench are also presented.

The 216-B-63 Trench, located in the north-central part of the 200 East Area, was used as an emergency percolation trench for chemical sewer wastes from B Plant. Discharges to the 216-B-63 Trench ceased in 1992 (Section 2.7 in DOE/RL-2016-66).

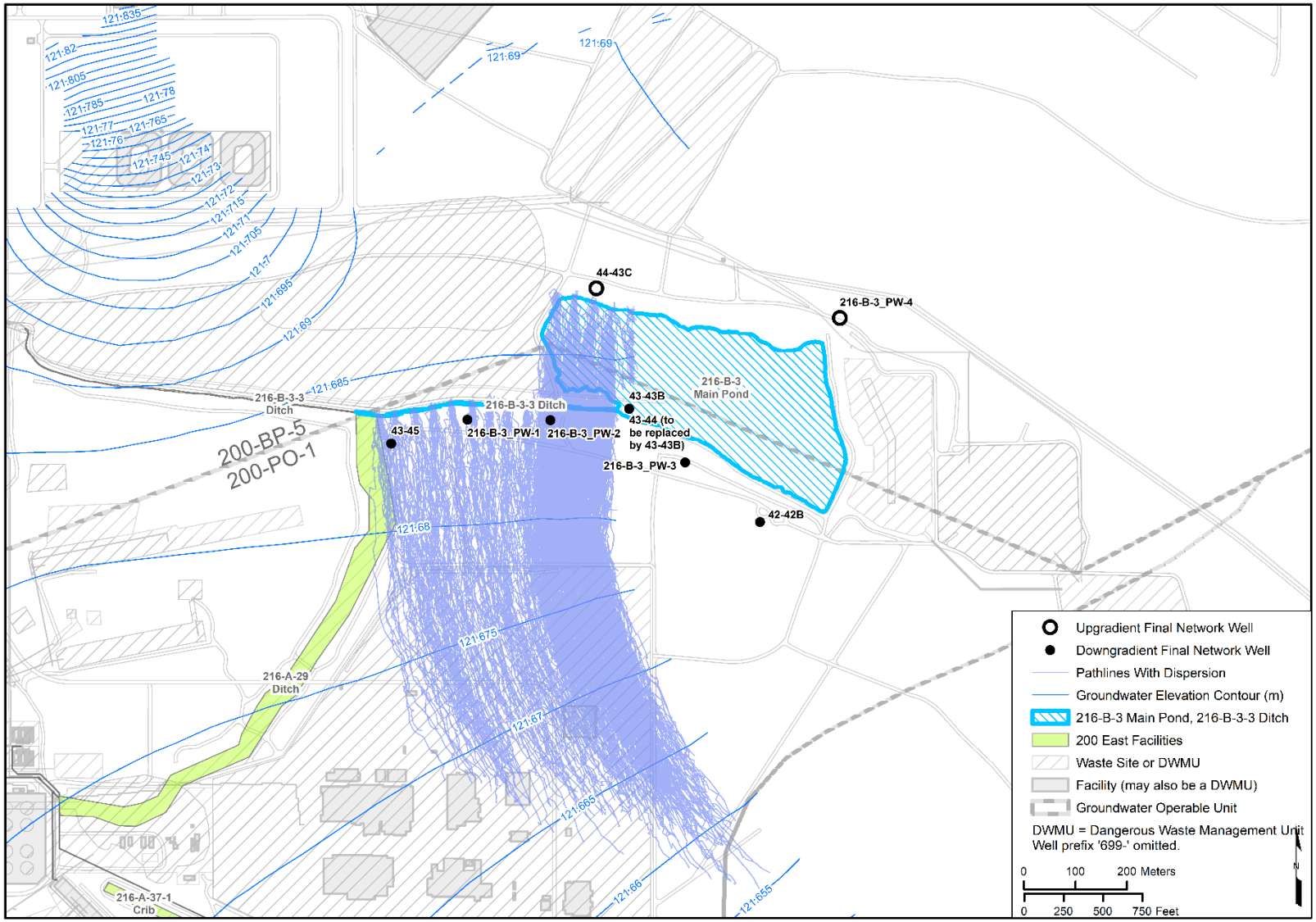


**Figure 7-17. Groundwater Elevations and Particle Pathlines for the 216-B-3 Pond, 2018**

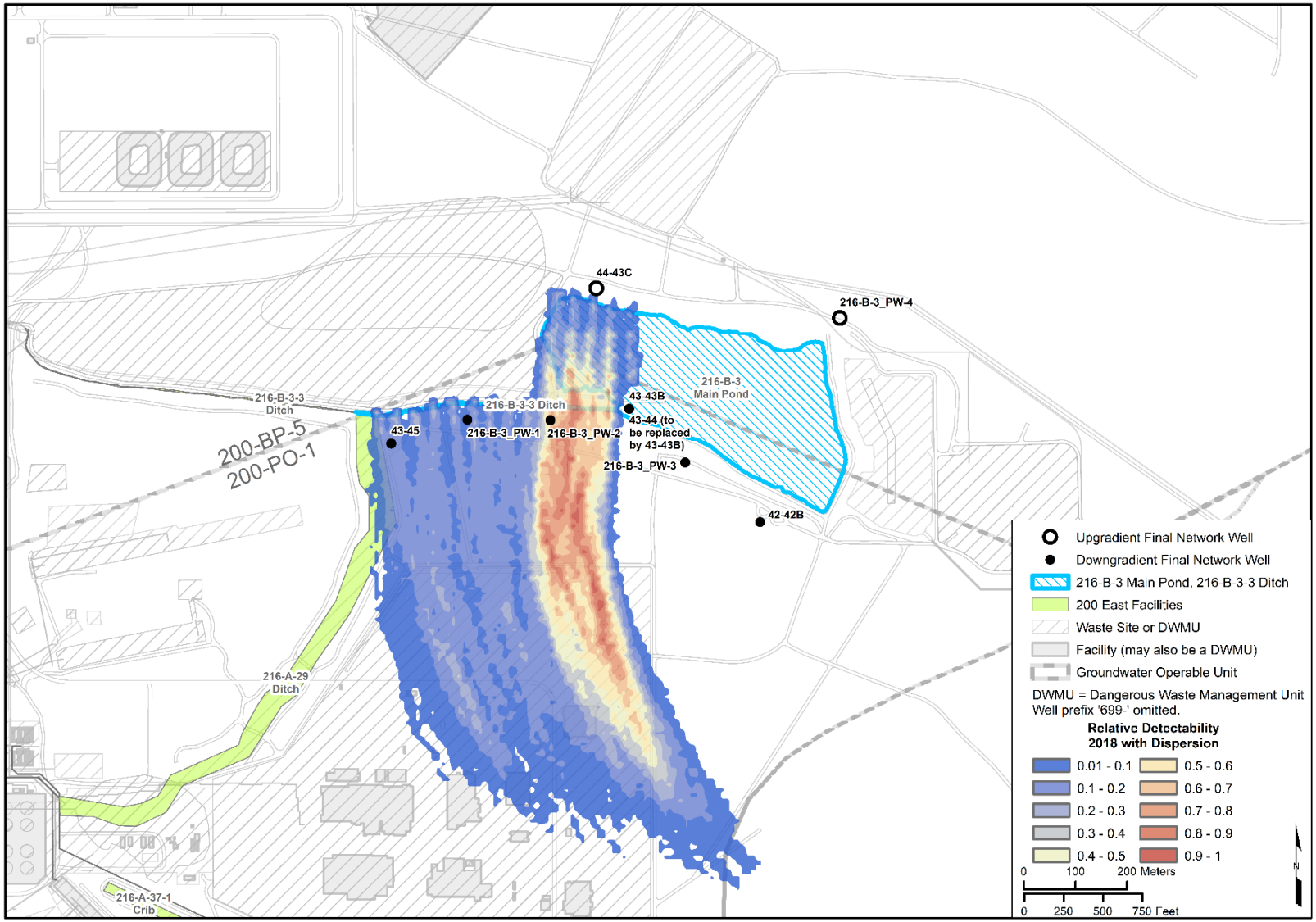


**Figure 7-18. Relative Detectability Map for the 216-B-3 Pond, 2018**

The 216-B-63 Trench final status monitoring network (Figure 7-19) was determined in SGW-60594, *Engineering Evaluation Report for the 216-B-63 Trench Groundwater Monitoring*, and consists of four upgradient wells (existing wells 299-E33-33, 299-E34-8, and 299-E34-12; and proposed well 216-B-63_PW-4) and nine downgradient wells (existing wells 299-E27-11, 299-E27-16, 299-E27-18, 299-E27-19, and 299-E33-37; and proposed wells 216-B-63_PW-1, 216-B-63_PW-2, 216-B-63_PW-5, and 216-B-63_PW-6).

### 7.5.1 Release Locations and Relative Detectability Grid for the 216-B-63 Trench

The starting locations for the particle-tracking calculations represent the area over which a potential release from a given facility would impact the underlying water table. The particle releases were located at plausible release sites throughout the facility. Twenty particles were released from each release location specified along the centerline of the unit (Figure 7-20) and tracked to provide the density of particles in space and time required for the calculations.

A contour map of relative detectability is generated by counting the number of particles that pass through a pre-defined uniform calculational grid (Figure 7-20). The grid used to develop the relative detectability maps is defined by 10 m by 10 m (33 ft by 33 ft) cells and is oriented to be parallel to the predominant groundwater flow direction at the 216-B-63 Trench.

### 7.5.2 Results for the 216-B-63 Trench

The groundwater elevation contours shown in Figure 7-1 form the basis for the facility-specific calculations performed in this ECF. The elevations near the 216-B-63 Trench for CY 2018 are shown in Figure 7-21, and the outputs of the particle tracking and relative detectability calculations are discussed in the following sections.

#### *7.5.2.1 Particle Tracking*

After the groundwater elevation contour maps and underlying piecewise continuous elevation grids were prepared using TRIM, particle tracking was implemented using both advection and dispersion. The particle pathlines that were produced depict the patterns of spreading that might accompany the contaminant migration near the unit for the flow conditions in 2018. Figure 7-21 shows the particle pathlines developed based on the groundwater elevations prepared throughout the 200 East Area using TRIM. The resulting maps were prepared based on the release of 20 particles from each starting location to provide the high density of particles in space and time required for these detailed facility-specific calculations. Figure 7-21 shows the particle pathlines calculated after 800 days of travel, by which time most of the particles would have arrived at or passed by the final status groundwater monitoring wells. Figure 7-21 depicts an instantaneous release to the water table from the release locations in the 216-B-63 Trench to illustrate the adequacy of the well network for monitoring the entire facility.

#### *7.5.2.2 Relative Detectability Map*

To compare the relative density of the particles that pass by each monitoring well location, a relative detectability index was calculated at a subgrid level (described in Section 6.3) and a corresponding contour map was generated. Figure 7-22 shows the relative detectability map developed based on the instantaneous release of a large number of particles at the facility after 800 days of calculated travel, by which time all particles would have arrived at or passed by the final status groundwater monitoring wells. Figure 7-22 depicts areas of relatively higher and lower potential impact from a release at the facility that reaches the water table for conditions represented by 2018.

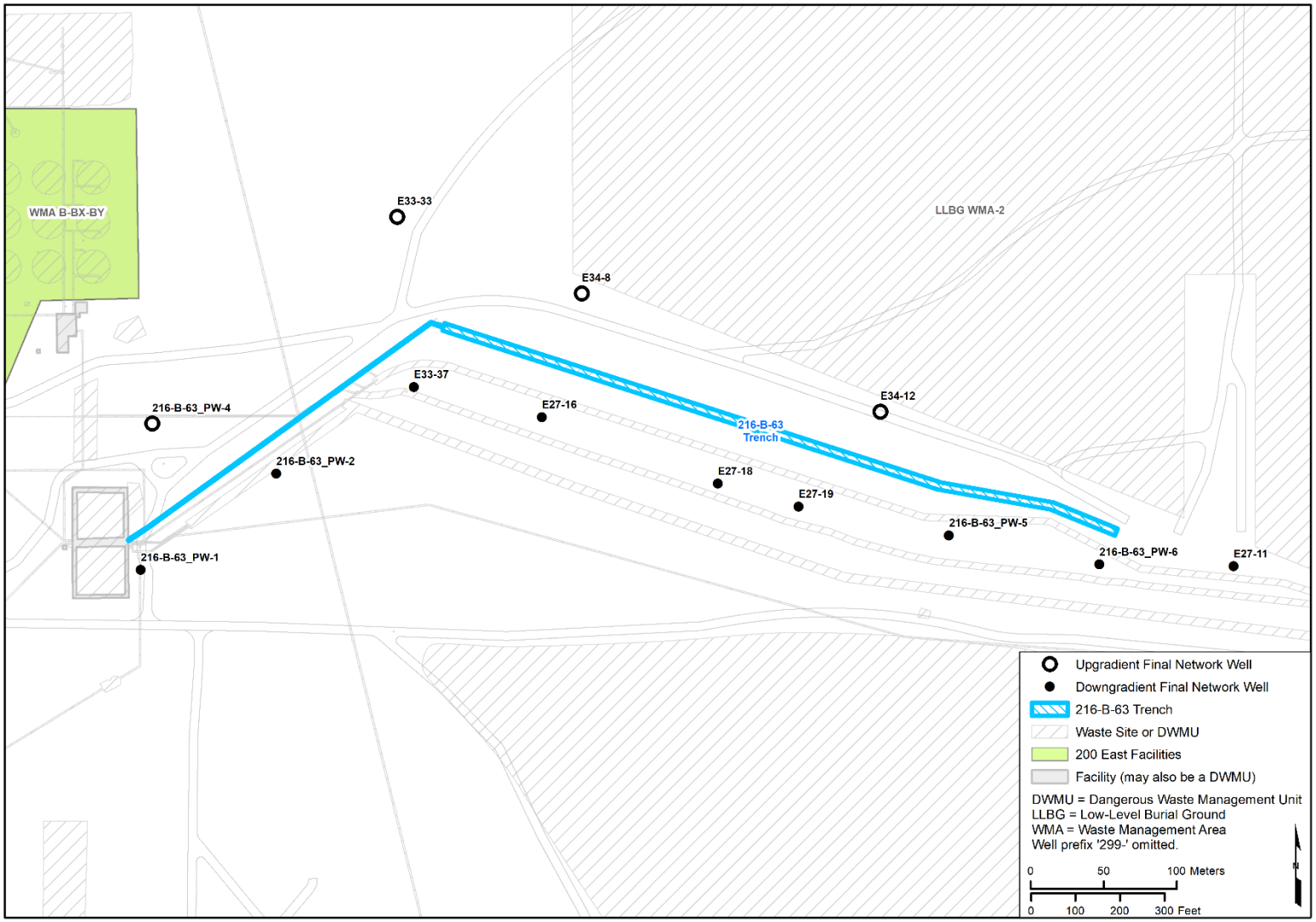


**Figure 7-19. Final Status Monitoring Network for the 216-B-63 Trench**

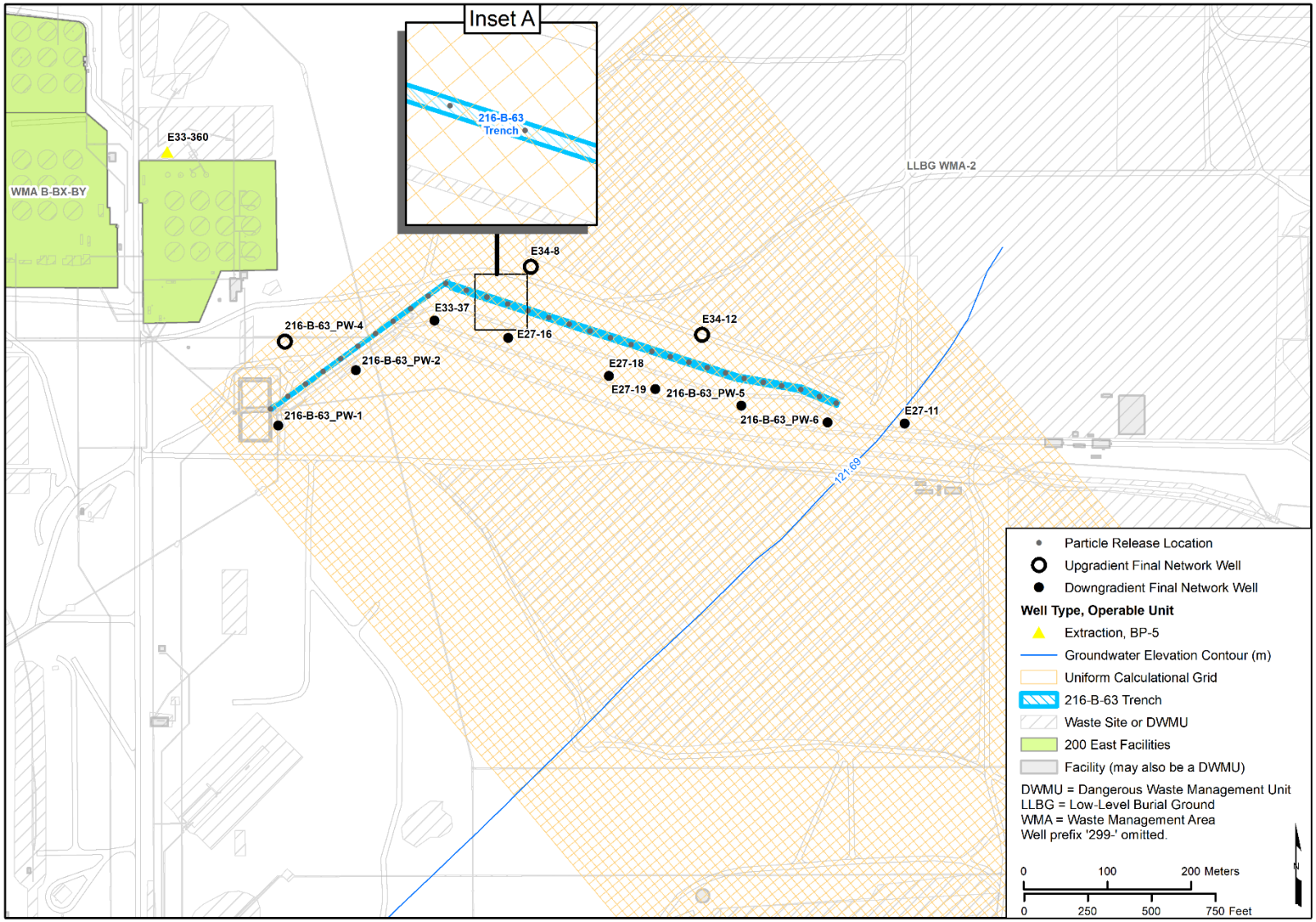


**Figure 7-20. Release Locations and Calculational Grid for the 216-B-63 Trench**

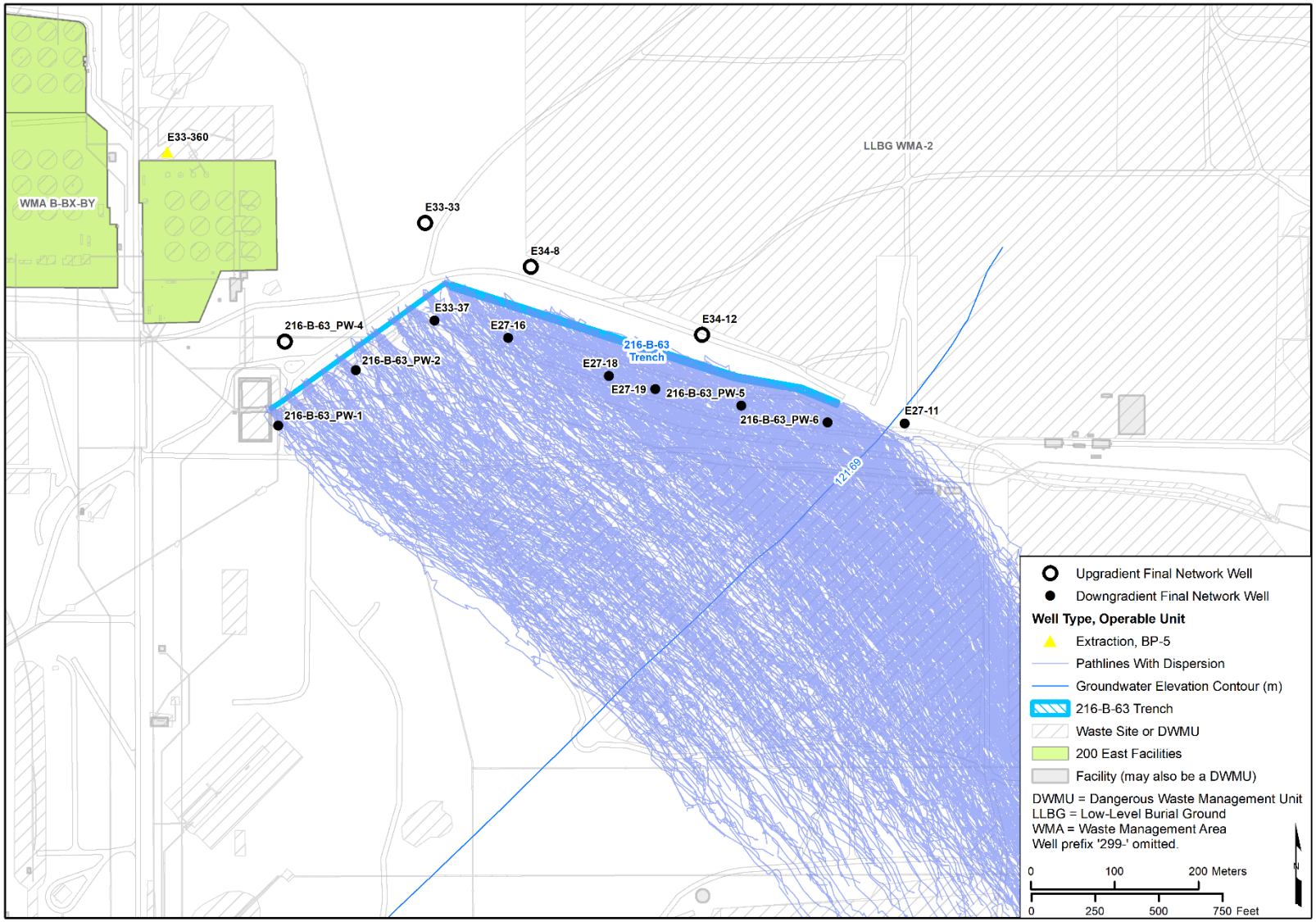


**Figure 7-21. Groundwater Elevations and Particle Pathlines for the 216-B-63 Trench, 2018**

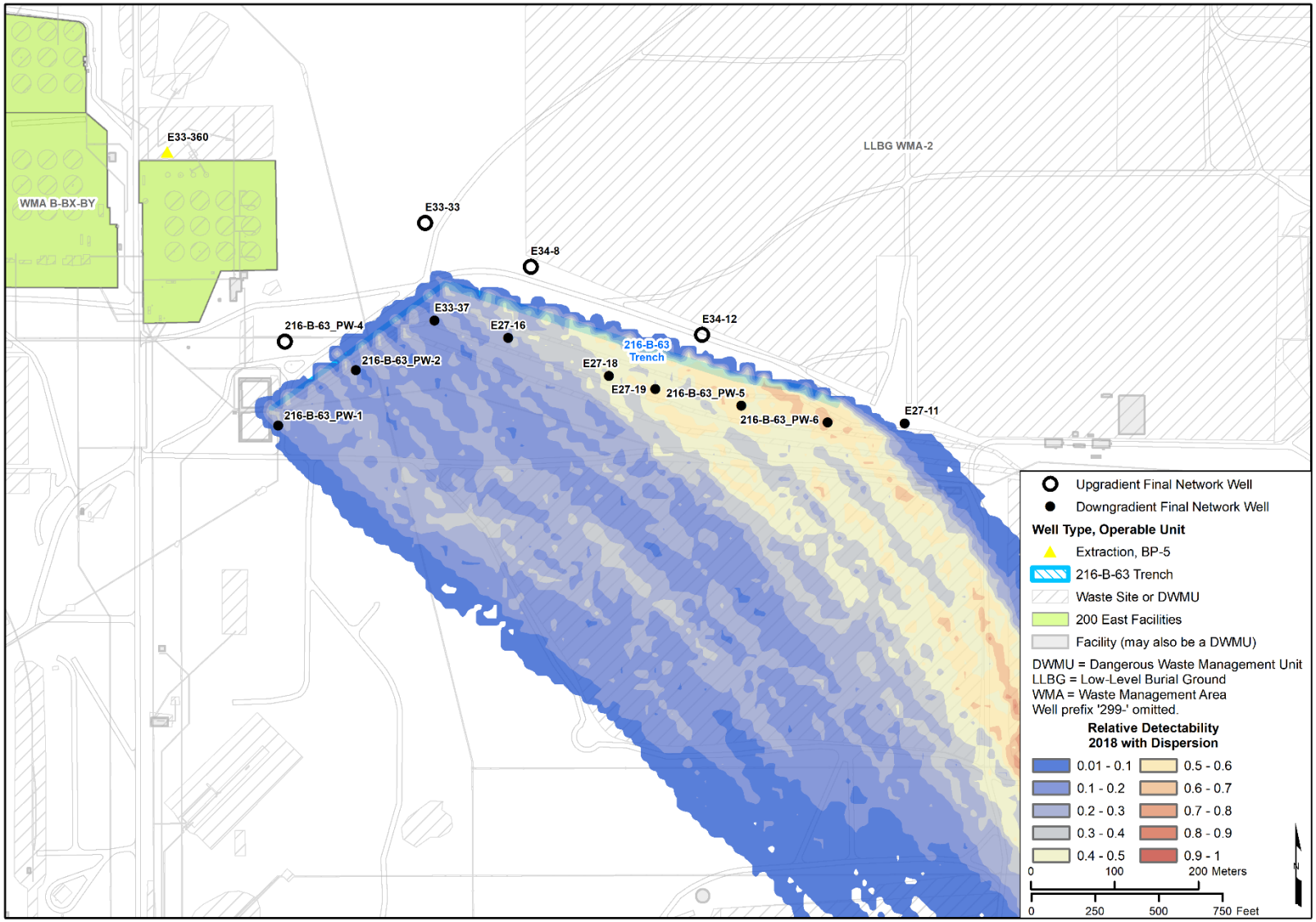


**Figure 7-22. Relative Detectability Map for the 216-B-63 Trench, 2018**

The goal of well placement is for well locations to span the range of detectable areas downgradient of the 216-B-63 Trench. The relative detectability map shows that under the evaluated range of conditions, the final status well network continues to meet this goal.

## 7.6 Integrated Disposal Facility Input and Results

Section 4.2 describes the general input for the calculations for IDF. The following discussion describes the particle starting locations and calculational grid used. The results developed from the calculations specific to IDF are also presented.

The IDF is double-lined landfill consisting of two disposal areas called cells, although the facility can be expanded as needed to a total capacity of six cells. Construction of the first two IDF cells was completed in April 2006 (Section 1.1 in DOE/RL-2012-57, *Annual Summary of the Integrated Disposal Facility Performance Assessment 2012*). The cells were designed to accept mixed low-level waste, possibly including treated low-level/low-activity waste, that will have gone through the vitrification process at the Hanford Site Waste Treatment Plant.

The IDF is approximately 457 m (1,500 ft) wide by 233 m (765 ft) long by 12.8 m (42 ft) deep for the "first expansion," with a capacity of nearly 165,000 $m^3$ (215,000 $yd^3$) (Section 1.1 in DOE/RL-2012-57). The design includes two leachate collection systems, which are compliant with the *Resource Conservation and Recovery Act of 1976* (RCRA) and are designed to catch liquid that may seep through the waste. Once liquid reaches this liner, it is removed and taken to a facility where the liquid is treated, the contaminants removed, and the liquid then safely returned to the soil. Because the IDF is designed to allow for future expansion, construction of additional liners in the future will connect to the previously constructed liner. The disposal landfill cover will be designed and located to satisfy the dangerous waste disposal requirements once a decision is made to construct the final cover over the landfill.

The IDF final status monitoring network (Figure 7-23) was determined in SGW-62007, *Engineering Evaluation Report for the Integrated Disposal Facility Groundwater Monitoring*, and consists of two upgradient wells (existing well 299-E24-24 and proposed well IDF_PW-4 [299-E17-57]) and five downgradient wells (existing wells 299-E17-22, 299-E24-18, and 299-E24-21; and proposed wells IDF_PW-1 [299-E17-56], and IDF_PW-3 [299-E24-164]). The proposed wells were scheduled to be drilled in 2019 and well identifications were assigned prior to drilling.

### 7.6.1 Release Locations and Relative Detectability Grid for the Integrated Disposal Facility

The starting locations for the particle-tracking calculations represent the area over which a potential release from a given facility would impact the underlying water table. The particle releases were located at plausible release sites throughout the facility. Twenty particles were released from each release location specified along the centerline of the unit (Figure 7-24) and tracked to provide the density of particles in space and time required for the calculations.

A contour map of relative detectability is generated by counting the number of particles that pass through a pre-defined uniform calculational grid (Figure 7-24). The grid used to develop the relative detectability maps is defined by 10 m by 10 m (33 ft by 33 ft) cells and is oriented to be parallel to the predominant groundwater flow direction at the IDF.

### 7.6.2 Results for the Integrated Disposal Facility

The groundwater elevation contours shown in Figure 7-1 form the basis for the facility-specific calculations performed in this ECF. The elevations near IDF for 2018 are shown in Figure 7-25, and the outputs of the particle tracking and relative detectability calculations are discussed in the following sections.

#### *7.6.2.1 Particle Tracking*

After the groundwater elevation contour maps and underlying piecewise continuous elevation grids were prepared using TRIM, particle tracking was implemented using both advection and dispersion.
The particle pathlines that were produced depict the patterns of spreading that might accompany the contaminant migration near the unit ditch for the flow conditions for CY 2018. Figure 7-25 shows the particle pathlines developed based on the groundwater elevations prepared throughout the 200 East Area using TRIM. The resulting maps were prepared based on the release of 20 particles from each starting location to provide the high density of particles in space and time required for these detailed facility-specific calculations. Figure 7-25 shows the particle pathlines calculated after 73,000 days of travel, by which time it was determined that most of the particles would have arrived at or passed by the final status groundwater monitoring wells. Figure 7-25 depicts an instantaneous release to the water table from the release locations in the IDF to illustrate the adequacy of the well network for monitoring the entire facility.

#### *7.6.2.2 Relative Detectability Map*

To compare the relative density of the particles that pass by each monitoring well location, a relative detectability index was calculated at a subgrid level(described in Section 6.3) and a corresponding contour map was generated. Figure 7-26 shows the relative detectability map developed based on the instantaneous release of a large number of particles at the facility after 73,000 days of calculated travel, by which time it was determined that all particles would have arrived at or passed by the final status groundwater monitoring wells. The map depicts areas of relatively higher and lower potential impact from a release at the facility that reaches the water table, for conditions represented by CY 2018.

The goal of well placement is for the well locations to span the range of detectable areas downgradient of the IDF. The relative detectability map shows that under the evaluated range of conditions, the final status well network continues to meet this goal.

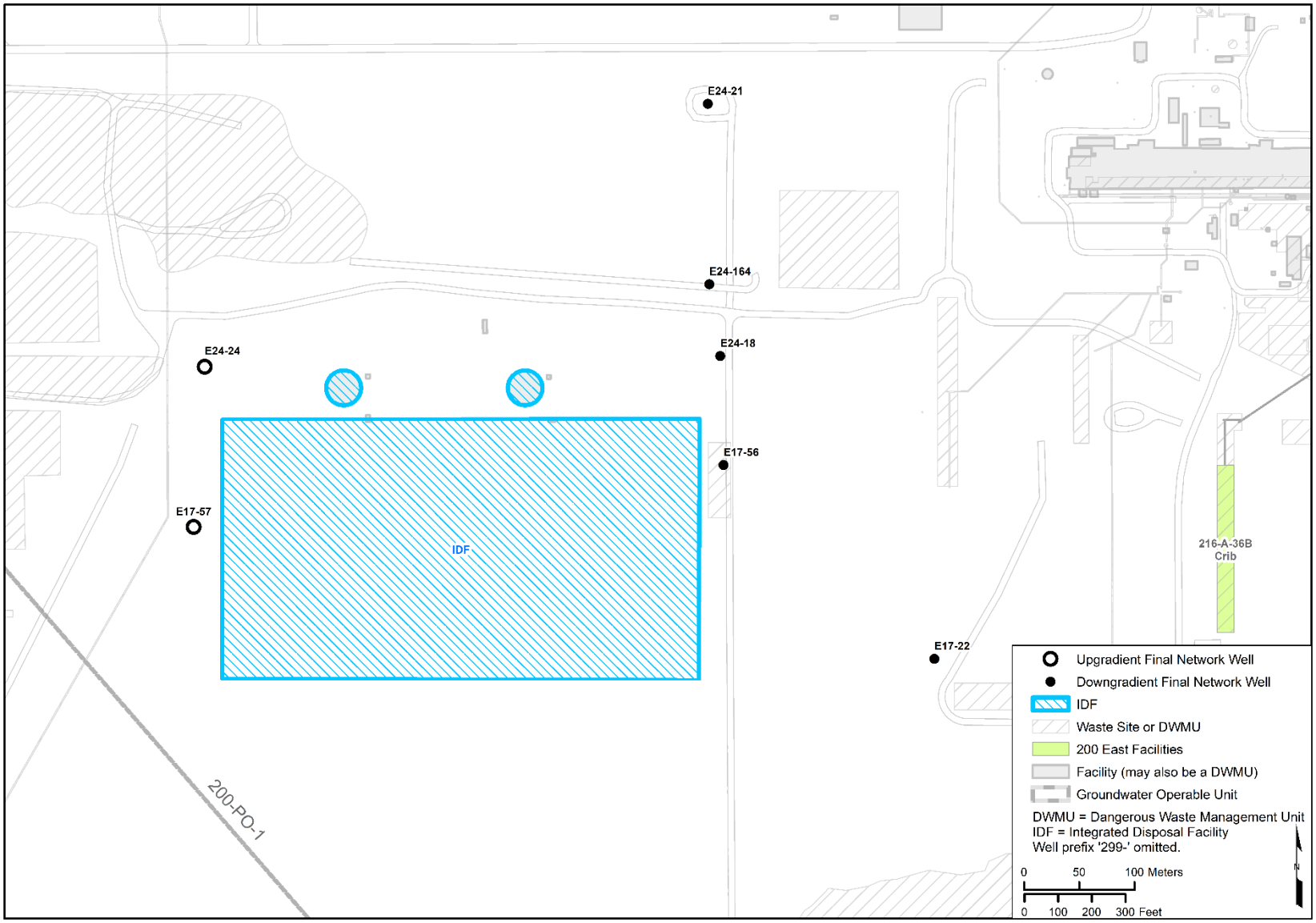


**Figure 7-23. Final Status Monitoring Network for the IDF**

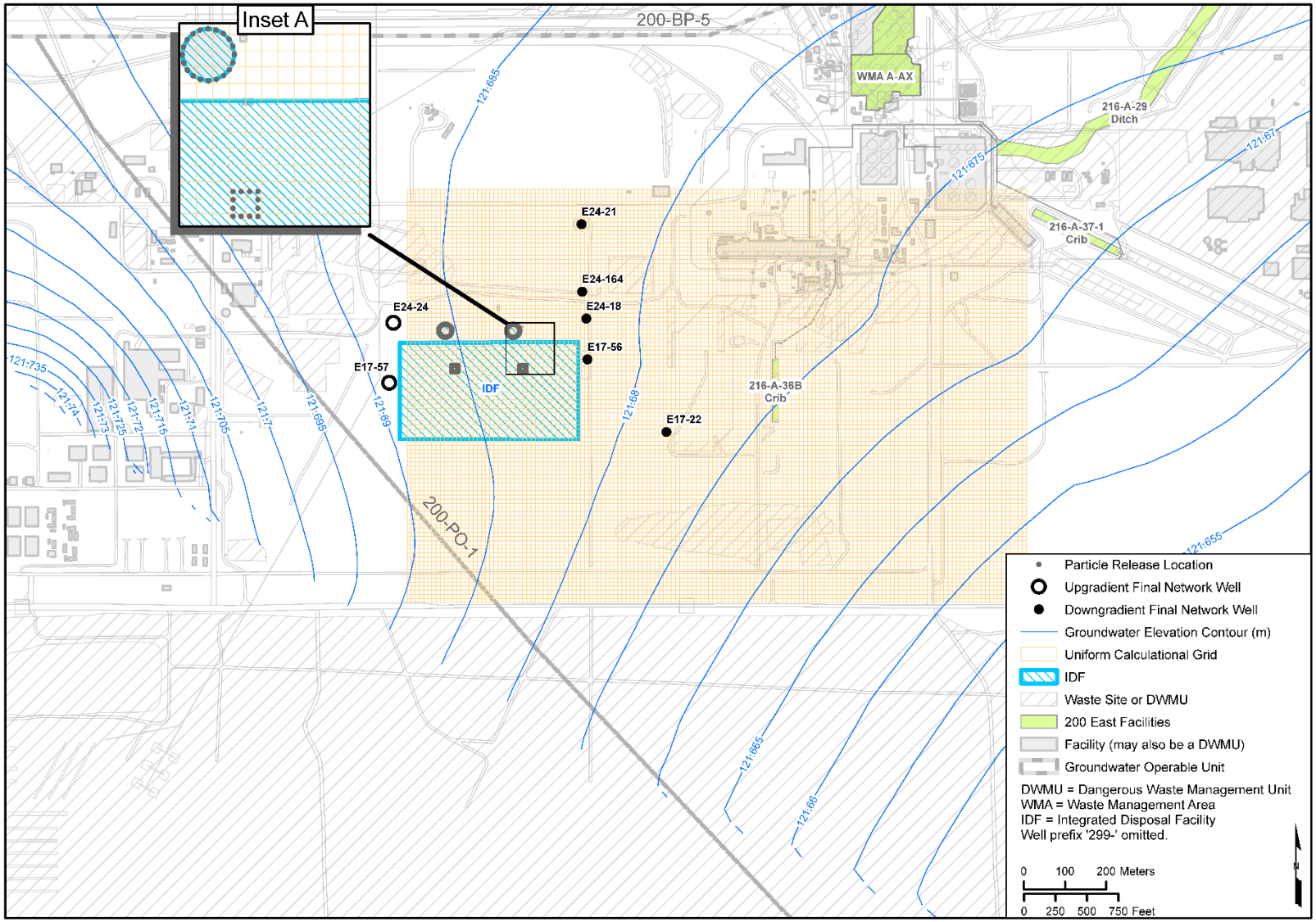


**Figure 7-24. Release Locations and Calculational Grid for the IDF**

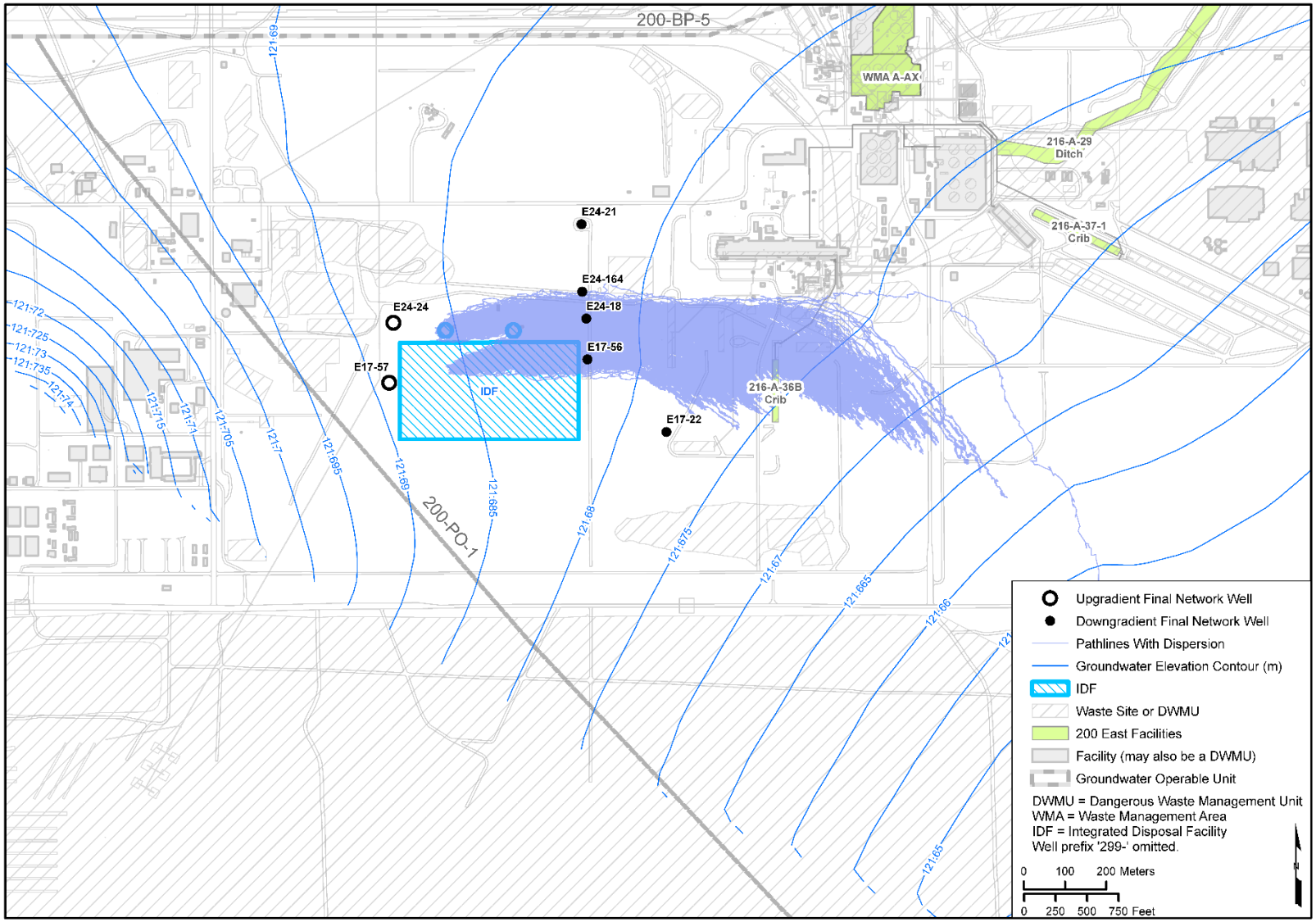


**Figure 7-25. Groundwater Elevations and Particle Pathlines for the IDF, 2018**

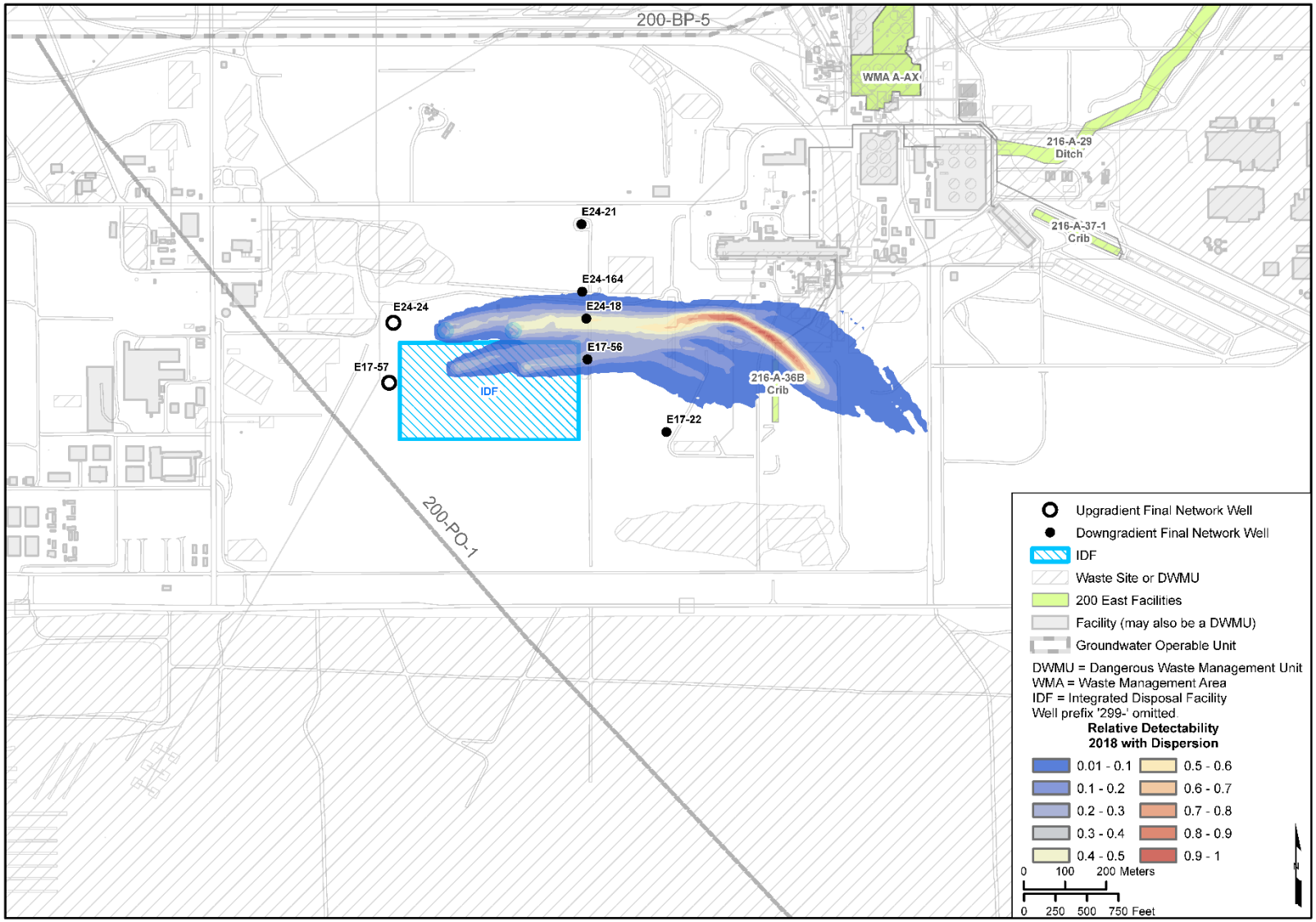


**Figure 7-26. Relative Detectability Map for the IDF, 2018**

## 7.7 Low-Level Burial Ground Waste Management Area-1 Input and Results

The general input to the calculations is described in Section 4.2. This section gives a more detailed description of the particle starting locations and calculational grid used. The results developed from the calculations specific to LLBG WMA-1 are also presented.

LLBG WMA-1, located in the northwest corner of the 200 East Area, is an inactive treatment, storage, and disposal unit that is regulated as a landfill (Figure 7-27). It contains the 218-E-10 Burial Ground, consisting of 14 unlined and covered trenches that operated between 1955 and 2000.

In general, the LLBG consists of trenches where low-level radioactive is buried. However, there are discrete areas within the LLBG, referred to as "Green Islands," where regulated mixed waste (waste with both a radioactive and dangerous waste component regulated by WAC 173-303, "Dangerous Waste Regulations") was disposed in unlined trenches after the advent of RCRA and, therefore, subject to regulation under RCRA. The LLBG closure units (Green Islands) refer to the discrete portions of the LLBG that contain mixed waste subject to WAC 173-303 requirements. The Green Islands do not include the entire trench, but only the portion of the trench where the regulated waste is buried (DOE, 2016, "Proposal to Address Mixed Waste Containers in the Low-Level Burial Grounds Operating Group").

The LLBG WMA-1 final status monitoring network (Figure 7-27) was determined in SGW-60590, *Engineering Evaluation Report for Low-Level Burial Grounds Waste Management Area-1 Green Islands Groundwater Monitoring*, and consists of two upgradient wells (existing wells 299-E32-3 and 299-E33-266) and six downgradient wells (existing wells 299-E28-27, 299-E33-28, and 299-E33-29; and proposed wells LLBGWMA-1_PW-1, LLBGWMA-1_PW-2, and LLBGWMA-1_PW-3).

### 7.7.1 Release Locations and Relative Detectability Grid for Low-Level Burial Ground Waste Management Area-1

The starting locations for the particle-tracking calculations represent the area over which a potential release from a given facility would impact the underlying water table. The particle releases were located at plausible release sites throughout the facility. Twenty particles were released from each release location specified along the centerline of the unit (Figure 7-28) and tracked to provide the density of particles in space and time required for the calculations.

A contour map of relative detectability is generated by counting the number of particles that pass through a pre-defined uniform calculational grid (Figure 7-28). The grid used to develop the relative detectability maps is defined by 10 m by 10 m (33 ft by 33 ft) cells and is oriented to be parallel to the predominant groundwater flow direction at the LLBG WMA-1.

### 7.7.2 Results for Low-Level Burial Ground Waste Management Area-1

The groundwater elevation contours shown in Figure 7-1 form the basis for the facility-specific calculations performed in this ECF. The elevations near LLBG WMA-1 for 2018 are shown in Figure 7-29, and the outputs of the particle tracking and relative detectability calculations are discussed in the following sections.

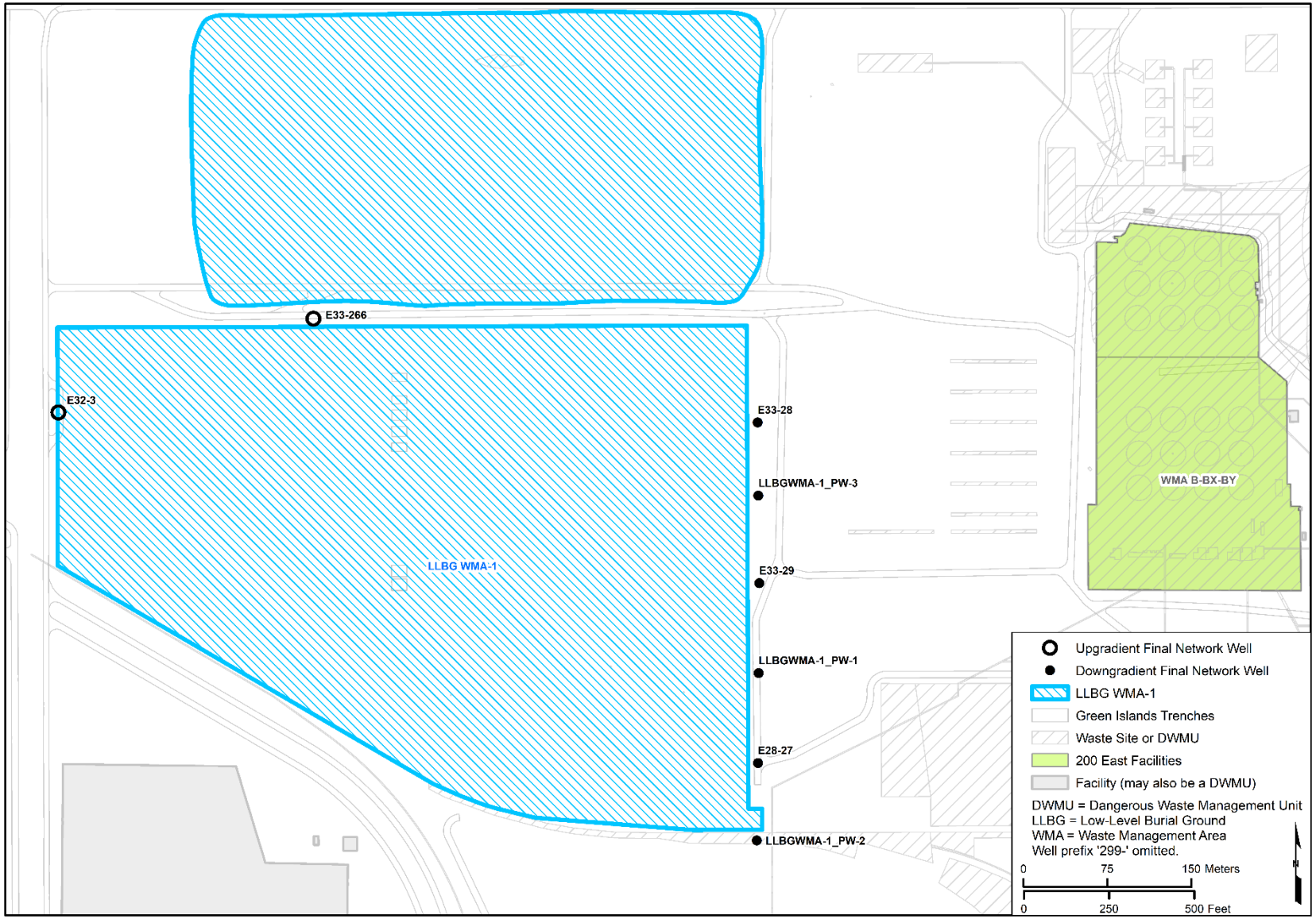


**Figure 7-27. Final Status Monitoring Network for LLBG WMA-1**

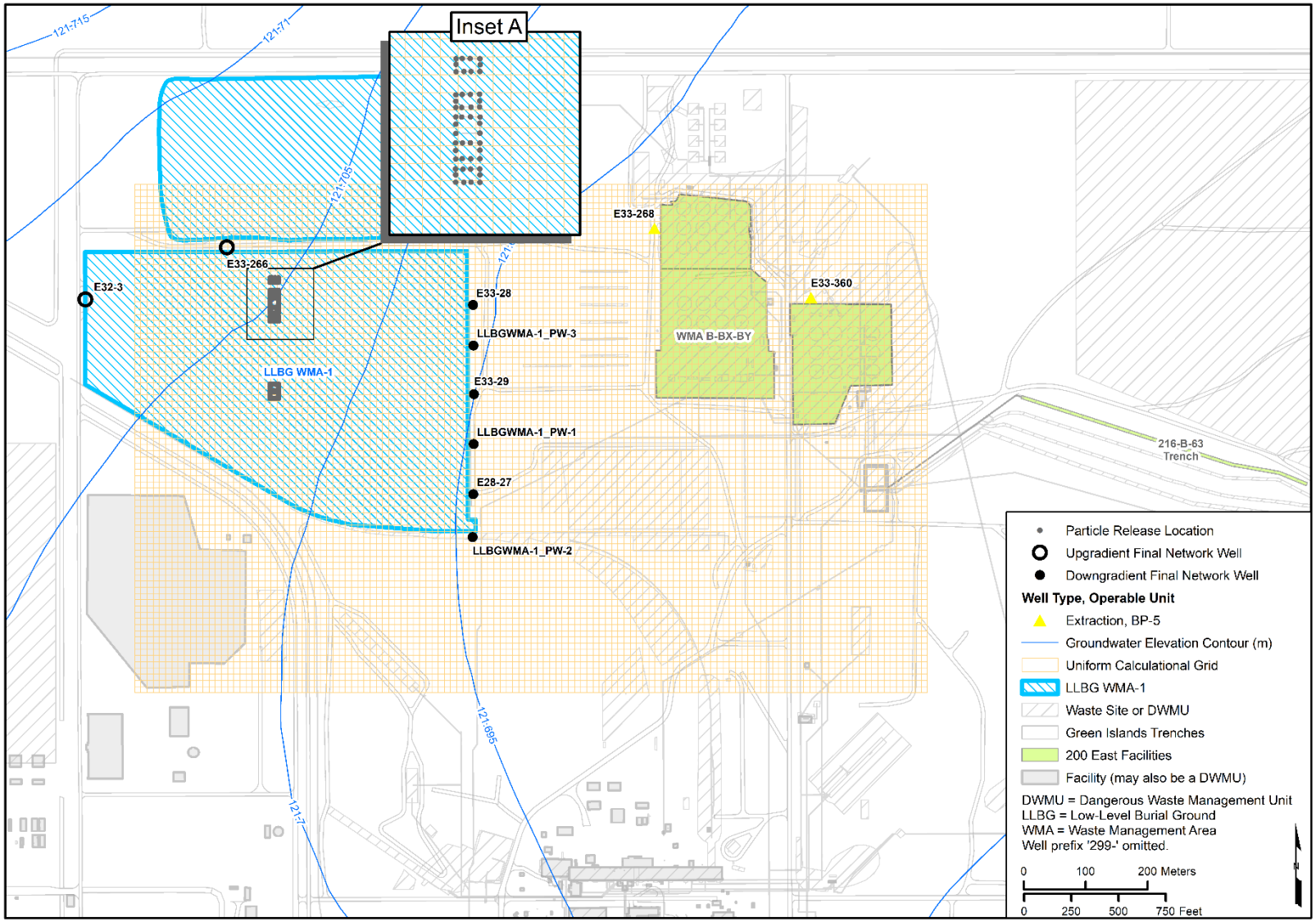


**Figure 7-28. Release Locations and Calculational Grid for LLBG WMA-1**

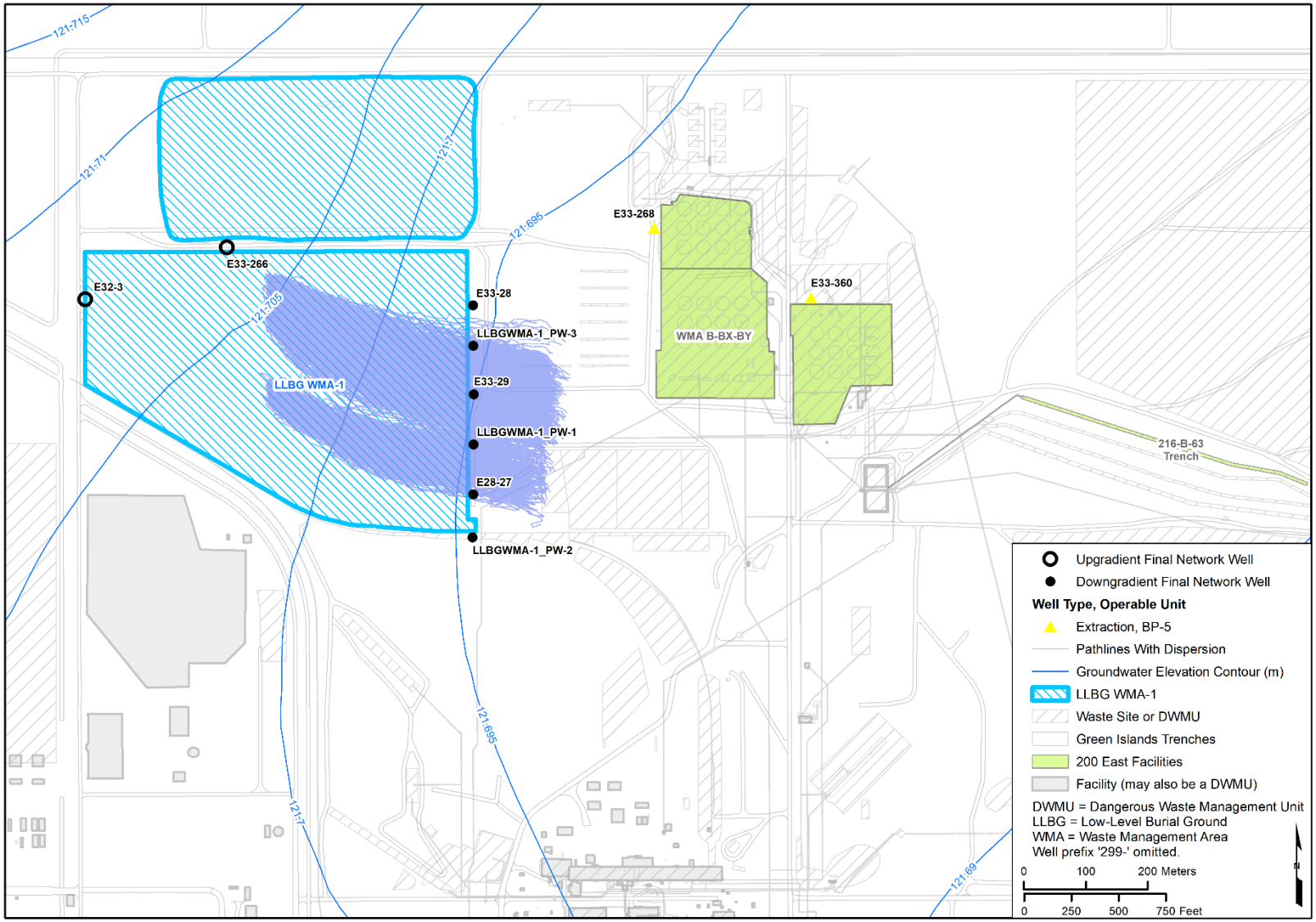


**Figure 7-29. Groundwater Elevations and Particle Pathlines for LLBG WMA-1, 2018**

#### *7.7.2.1 Particle Tracking*

After the groundwater elevation contour maps and underlying piecewise continuous elevation grids were prepared using TRIM, particle tracking was implemented using both advection and dispersion. The particle pathlines that were produced depict the patterns of spreading that might accompany the contaminant migration near the unit for the flow conditions in 2018. Figure 7-29 shows the particle pathlines developed based on the groundwater elevations prepared throughout the 200 East Area using TRIM. The resulting maps were prepared based on the release of 20 particles from each starting location to provide the high density of particles in space and time required for these detailed facility-specific calculations. Figure 7-29 shows the particle pathlines calculated after 100 days of travel, by which time most of the particles would have arrived at or passed by the final status groundwater monitoring wells. Figure 7-29 depicts an instantaneous release to the water table from the release locations in the LLBG WMA-1 to illustrate the adequacy of the well network for monitoring the entire facility.

#### *7.7.2.2 Relative Detectability Map*

To compare the relative density of the particles that pass by each monitoring well location, a relative detectability index was calculated at a subgrid level (described in Section 6.3) and a corresponding contour map was generated. Figure 7-30 shows the relative detectability map developed based on the instantaneous release of a large number of particles at the facility after 100 days of calculated travel, by which time all particles would have arrived at or passed by the final status groundwater monitoring wells. Figure 7-30 depicts areas of relatively higher and lower potential impact from a release at the facility that reaches the water table for conditions represented by 2018.

The goal of well placement is for well locations to span the range of detectable areas downgradient of the LLBG WMA-1. The relative detectability map shows that under the evaluated range of conditions, the final status well network continues to meet this goal.

## 7.8 Single-Shell Tank Waste Management Area A-AX Input and Results

Section 4.2 provides the general input to the calculations for SST WMA A-AX. The following discussion describes the particle starting locations and calculational grid used. The results developed from the calculations specific to SST WMA A-AX are also presented.

The SST WMA A-AX, centrally located in the 200 East Area, contains 10 SSTs, 5 french drains, and various other liquid-handling structures. This equipment was used to manage tank waste from PUREX Plant and B Plant between 1956 and 1980 (Chapter 1 in DOE/RL-2015-49, *Interim-Status Groundwater Quality Assessment Plan for the Single-Shell Tank Waste Management Area A-AX*).

The SST WMA A-AX final status monitoring network (Figure 7-31) was determined in SGW-60586, *Engineering Evaluation Report for Single-Shell Tank Waste Management Area A-AX Groundwater Monitoring*, and consists of three upgradient wells (existing wells 299-E24-20, 299-E24-22, and 299-E24-33) and seven downgradient wells (existing wells 299-E25-40, 299-E25-41, 299-E25-93, 299-E25-94, and 299-E25-237; and proposed wells WMA_A-AX_PW-1 and WMA_A-AX_PW-2).

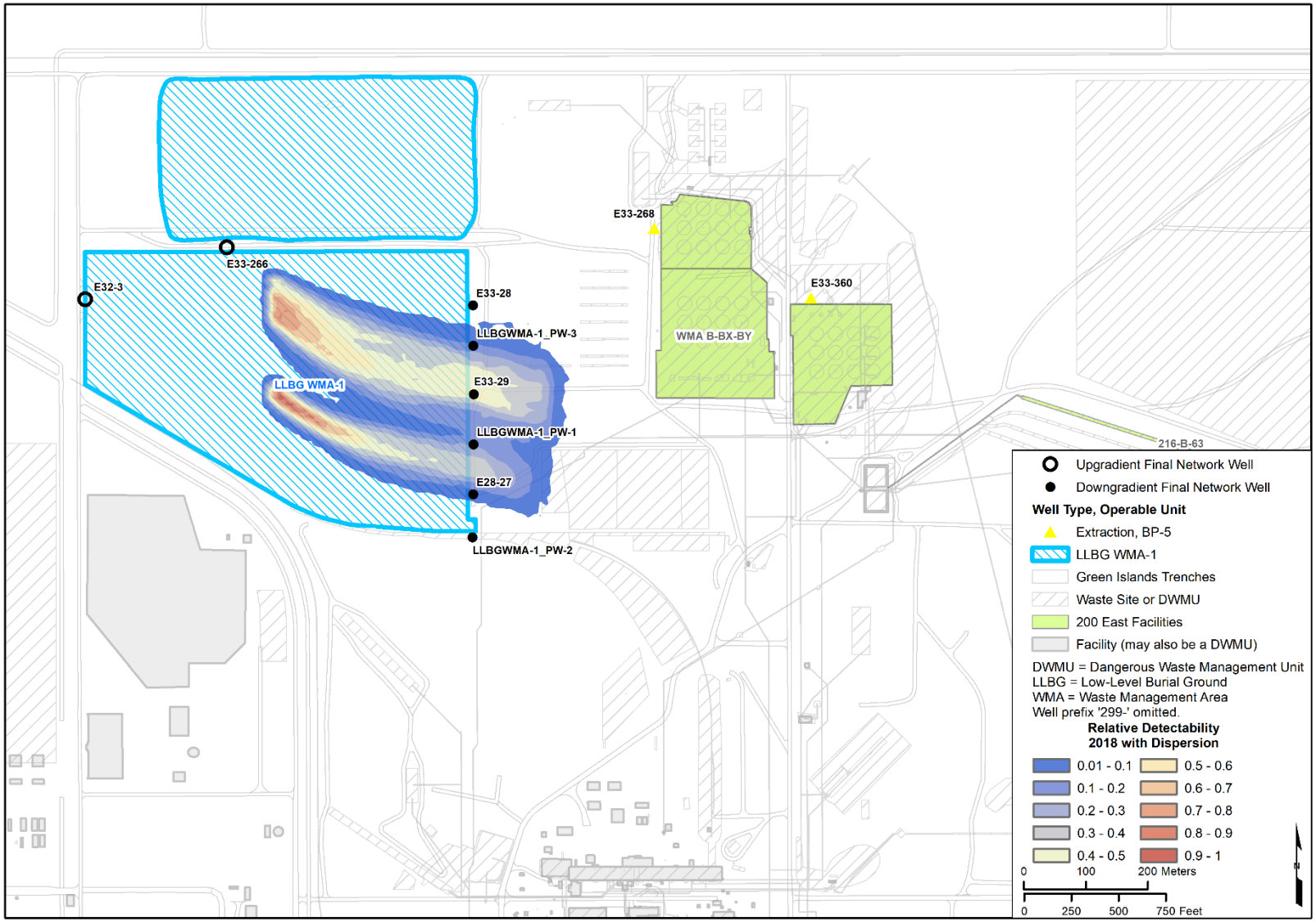


**Figure 7-30. Relative Detectability Map for LLBG WMA-1, 2018**

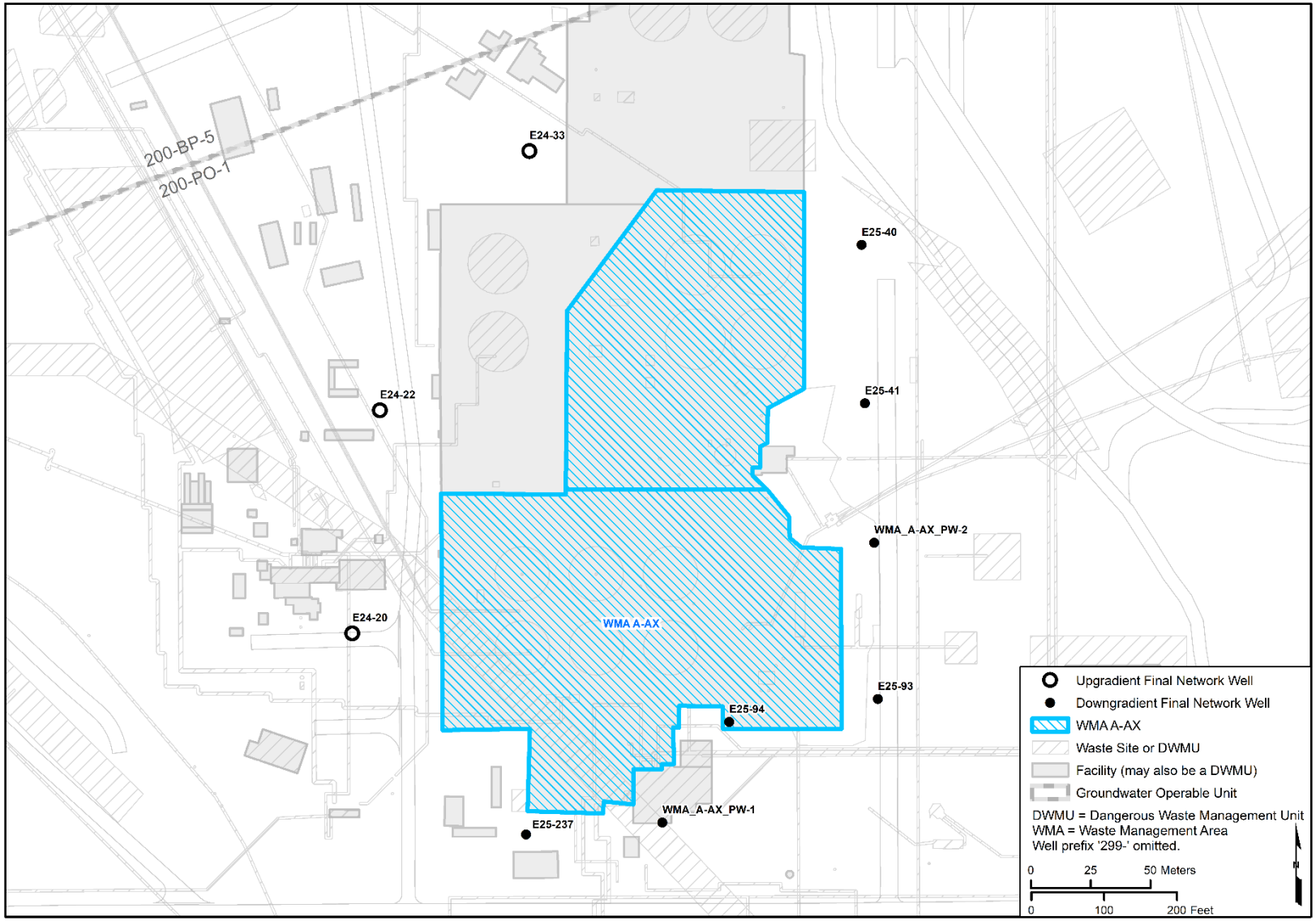


**Figure 7-31. Final Status Monitoring Network for SST WMA A-AX**

### 7.8.1 Release Locations and Relative Detectability Grid for Single-Shell Tank Waste Management Area A-AX

The starting locations for the particle-tracking calculations represent the area over which a potential release from a given facility would impact the underlying water table. The particle releases were located at plausible release sites throughout the facility. Twenty particles were released from each release location specified along the centerline of the unit (Figure 7-32) and tracked to provide the density of particles in space and time required for the calculations.

A contour map of relative detectability is generated by counting the number of particles that pass through a pre-defined uniform calculational grid (Figure 7-32). The grid used to develop the relative detectability maps is defined by 10 m by 10 m (33 ft by 33 ft) cells and is oriented to be parallel to the predominant groundwater flow direction at SST WMA A-AX.

### 7.8.2 Results for the Single-Shell Tank Waste Management Area A-AX

The groundwater elevation contours shown in Figure 7-1 form the basis for the facility-specific calculations performed in this ECF. The elevations near SST WMA A-AX for 2018 are shown in Figure 7-33 and in the following sections.

#### *7.8.2.1 Particle Tracking*

After the groundwater elevation contour maps and underlying piecewise continuous elevation grids were prepared using TRIM, particle tracking was implemented using both advection and dispersion. The particle pathlines that were produced depict the patterns of spreading that might accompany the contaminant migration near the unit for the flow conditions in 2018. Figure 7-33 shows the particle pathlines developed based on the groundwater elevations prepared throughout the 200 East Area using TRIM. The resulting maps were prepared based on the release of 20 particles from each starting location to provide the high density of particles in space and time required for these detailed facility-specific calculations. Figure 7-33 shows the particle pathlines calculated after 500 days of travel, by which time most of the particles would have arrived at or passed by the final status groundwater monitoring wells. Figure 7-33 depicts an instantaneous release to the water table from the release locations in SST WMA A-AX to illustrate the adequacy of the well network for monitoring the entire facility.

#### *7.8.2.2 Relative Detectability Map*

To compare the relative density of the particles that pass by each monitoring well location, a relative detectability index was calculated at a subgrid level (described in Section 6.3) and a corresponding contour map was generated. Figure 7-34 shows the relative detectability map developed based on the instantaneous release of a large number of particles at the facility after 500 days of calculated travel, by which time all particles would have arrived at or passed by the final status groundwater monitoring wells. Figure 7-34 depicts areas of relatively higher and lower potential impact from a release at the facility that reaches the water table for conditions represented by 2018.

The goal of well placement is for well locations to span the range of detectable areas downgradient of SST WMA A-AX. The relative detectability map shows that under the evaluated range of conditions, the final status well network continues to meet this goal.

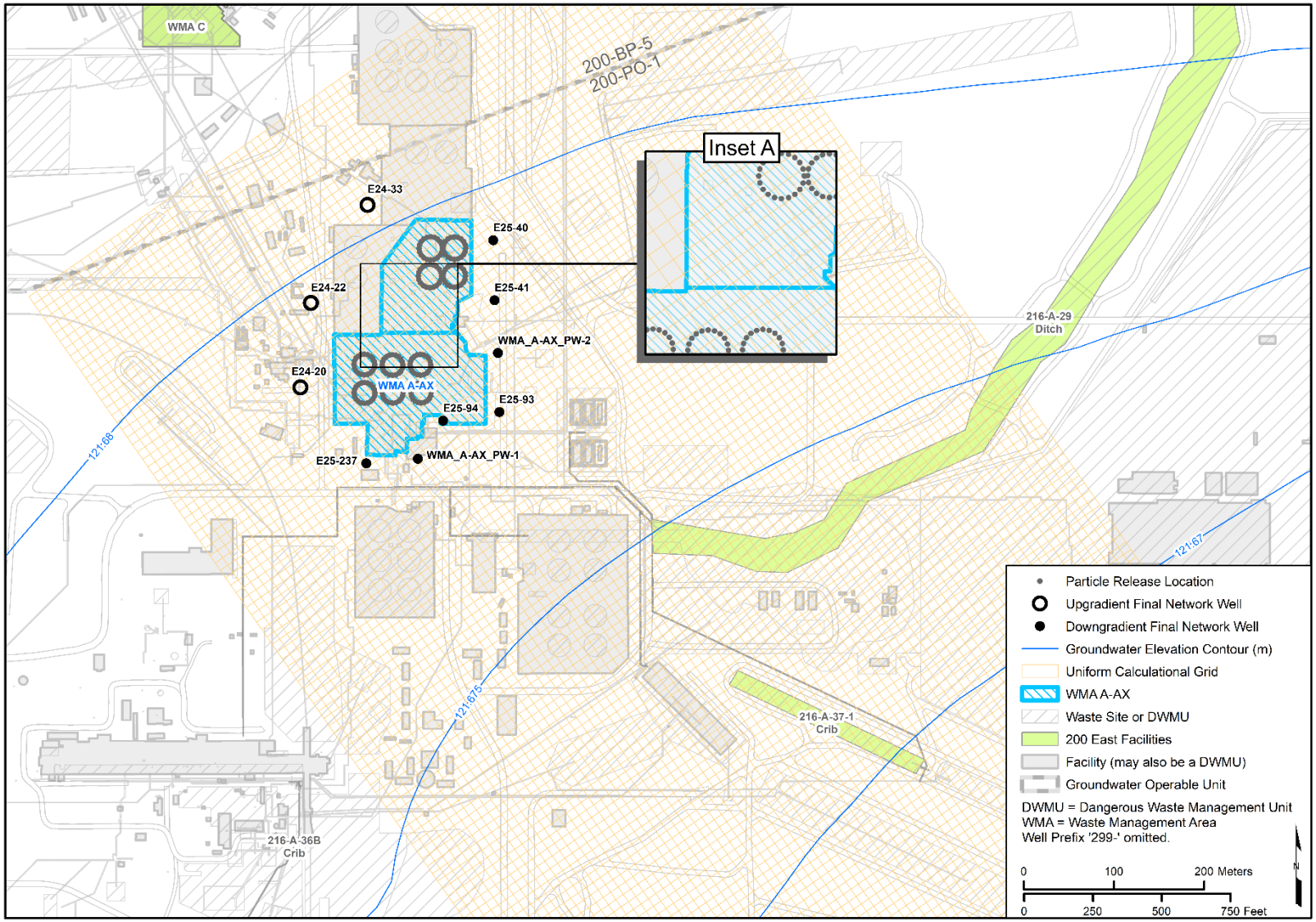


**Figure 7-32. Release Locations and Calculational Grid for SST WMA A-AX**

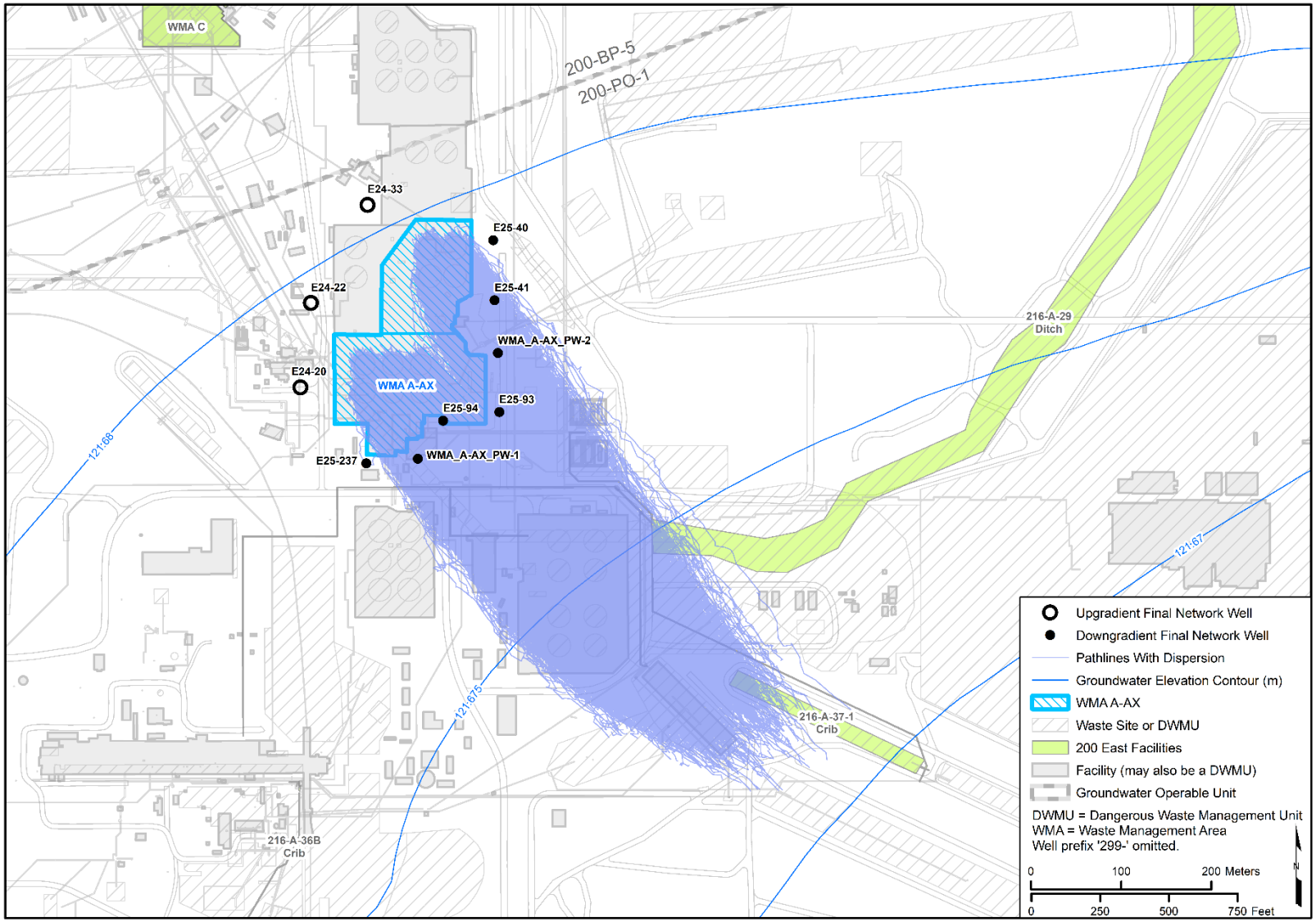


**Figure 7-33. Groundwater Elevations and Particle Pathlines for SST WMA A-AX, 2018**

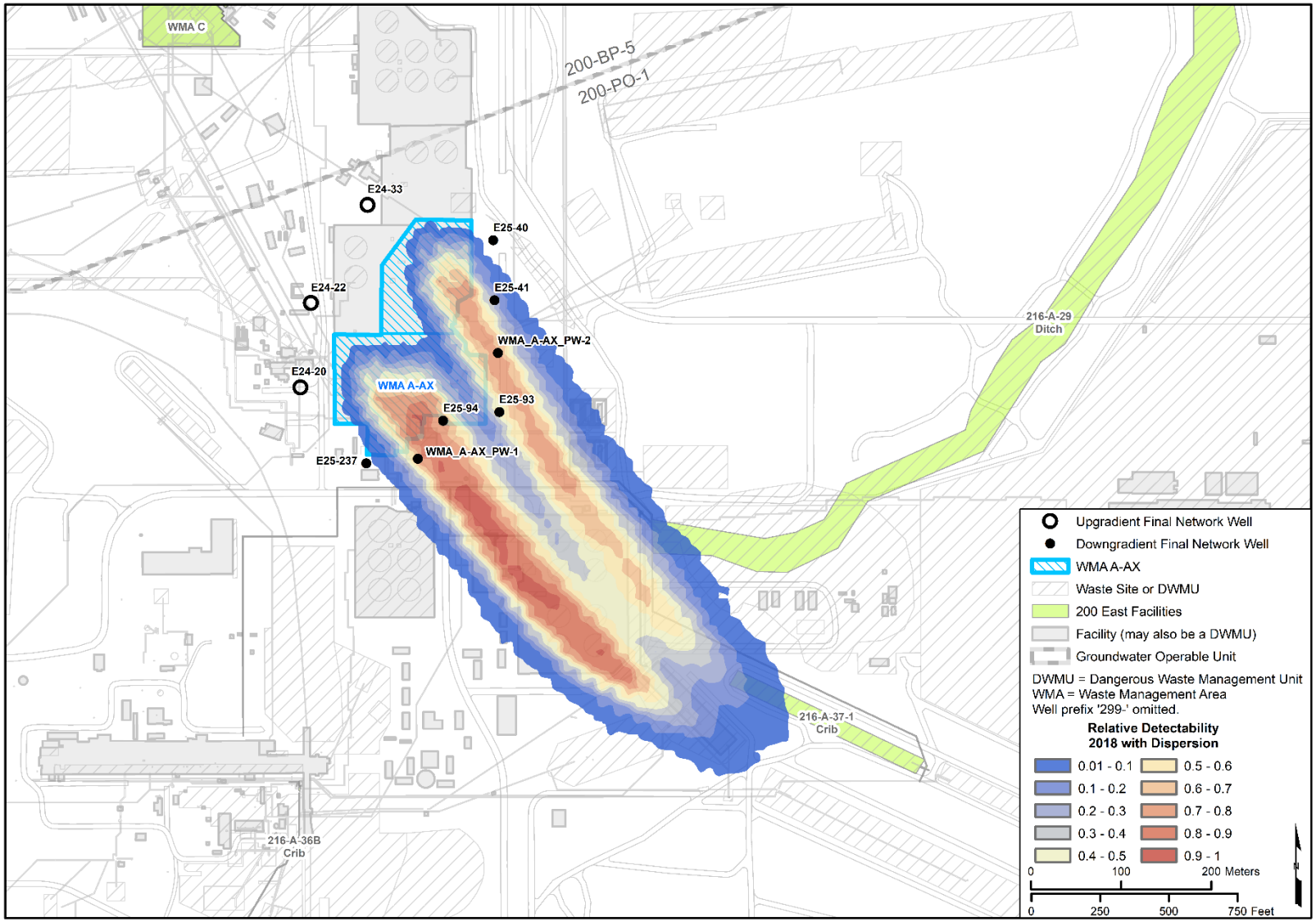


**Figure 7-34. Relative Detectability Map for SST WMA A-AX, 2018**

## 7.9 Single-Shell Tank Waste Management Area B-BX-BY Input and Results

Section 4.2 describes the general input for the calculations for SST WMA B-BX-BY. The following discussion describes the particle starting locations and calculational grid used. The results developed from the calculations specific to SST WMA B-BX-BY are also presented.

The SST WMA B-BX-BY, located in the northwestern part of the 200 East Area, consists of three tank farms: B Tank Farm, BX Tank Farm, and BY Tank Farm. The three tank farms encompass 40 SSTs and ancillary liquid-handling equipment, including diversion boxes, piping, sluice and valve pits, pump pits, and a waste transfer vault. The BX Tank Farm contains 12 large SSTs, the BY Tank Farm contains 12 large SSTs, and the B Tank Farm contains 12 large SSTs and 4 small SSTs.

Perched water is present in the deep vadose zone beneath WMA B-BX-BY and is estimated to extend from the central portion of the BX Tank Farm northeast to the 216-B-8 Crib, encompassing the northwest corner of B Tank Farm. The simulations performed herein do not address this perched water zone; instead, the simulations are focused on the groundwater conditions in the underlying unconfined aquifer.

The SST WMA B-BX-BY final status monitoring network (Figure 7-35) was determined in SGW-60587, *Engineering Evaluation Report for Single-Shell Tank Waste Management Area B-BX-BY Groundwater Monitoring*, and consists of 5 upgradient wells (existing wells 299-E33-31, 299-E33-32, 299-E33-38, 299-E33-42, and 299-E33-334) and 11 downgradient wells (existing wells 299-E33-20, 299-E33-41, 299-E33-44, 299-E33-47, 299-E33-48, 299-E33-49, 299-E33-335, 299-E33-337, 299-E33-338, 299-E33-339; and proposed well WMA B-BX-BY_PW-1).

### 7.9.1 Release Locations and Relative Detectability Grid for Single-Shell Tank Waste Management Area B-BX-BY

The starting locations for the particle-tracking calculations represent the area over which a potential release from a given facility would impact the underlying water table. The particle releases were located at plausible release sites throughout the facility. Twenty particles were released from each release location specified along the centerline of the unit (Figure 7-36) and tracked to provide the density of particles in space and time required for the calculations.

A contour map of relative detectability is generated by counting the number of particles that pass through a pre-defined uniform calculational grid (Figure 7-36). The grid used to develop the relative detectability maps is defined by 10 m by 10 m (33 ft by 33 ft) cells and is oriented to be parallel to the predominant groundwater flow direction at SST WMA B-BX-BY.

### 7.9.2 Results for Single-Shell Tank Waste Management Area B-BX-BY

The groundwater elevation contours shown in Figure 7-1 form the basis for the facility-specific calculations performed in this ECF. The elevations near SST WMA B-BX-BY for 2018 are shown in Figure 7-37, and the outputs of the particle tracking and relative detectability calculations are discussed in the following sections.

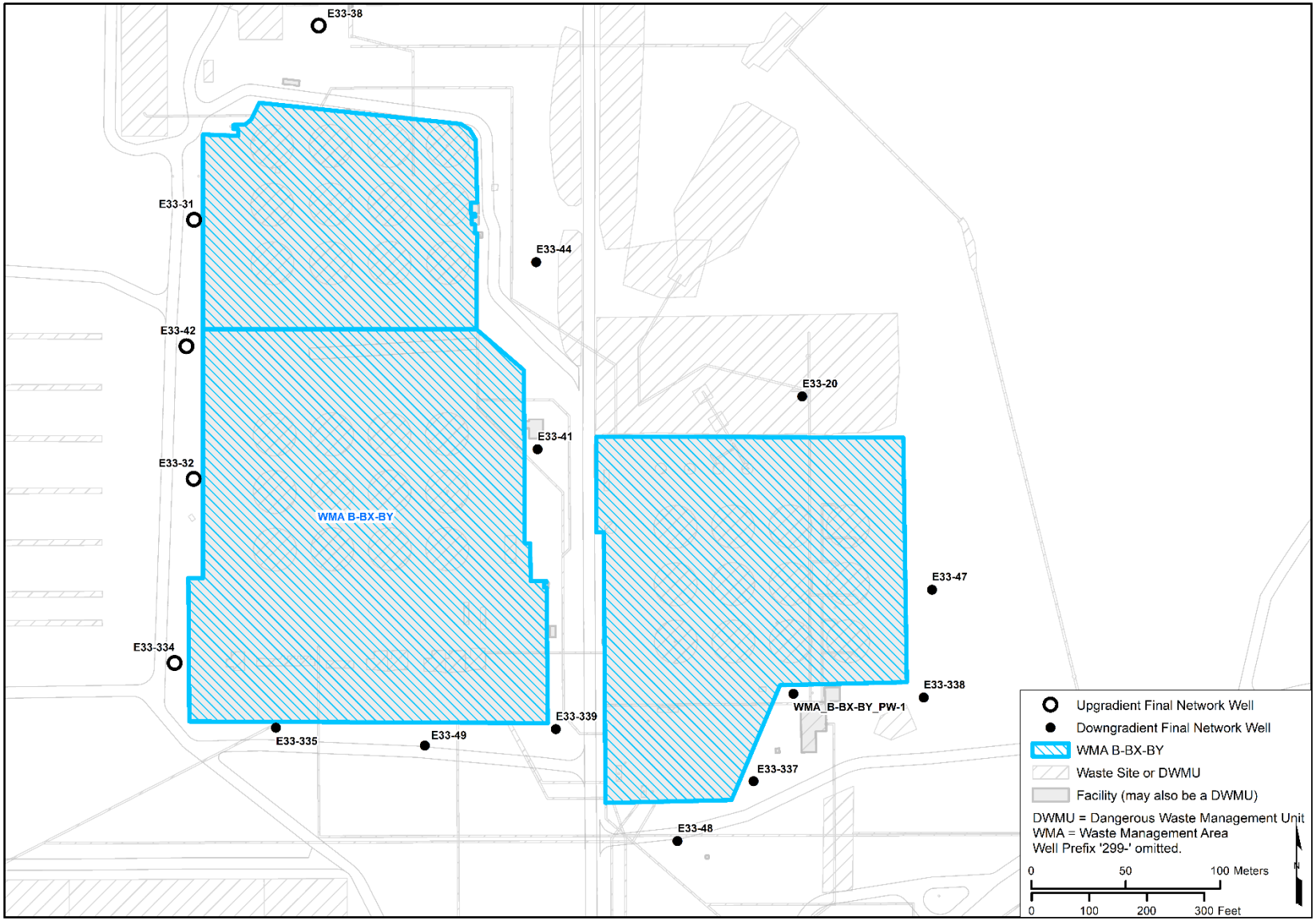


**Figure 7-35. Final Status Monitoring Network for SST WMA B-BX-BY**

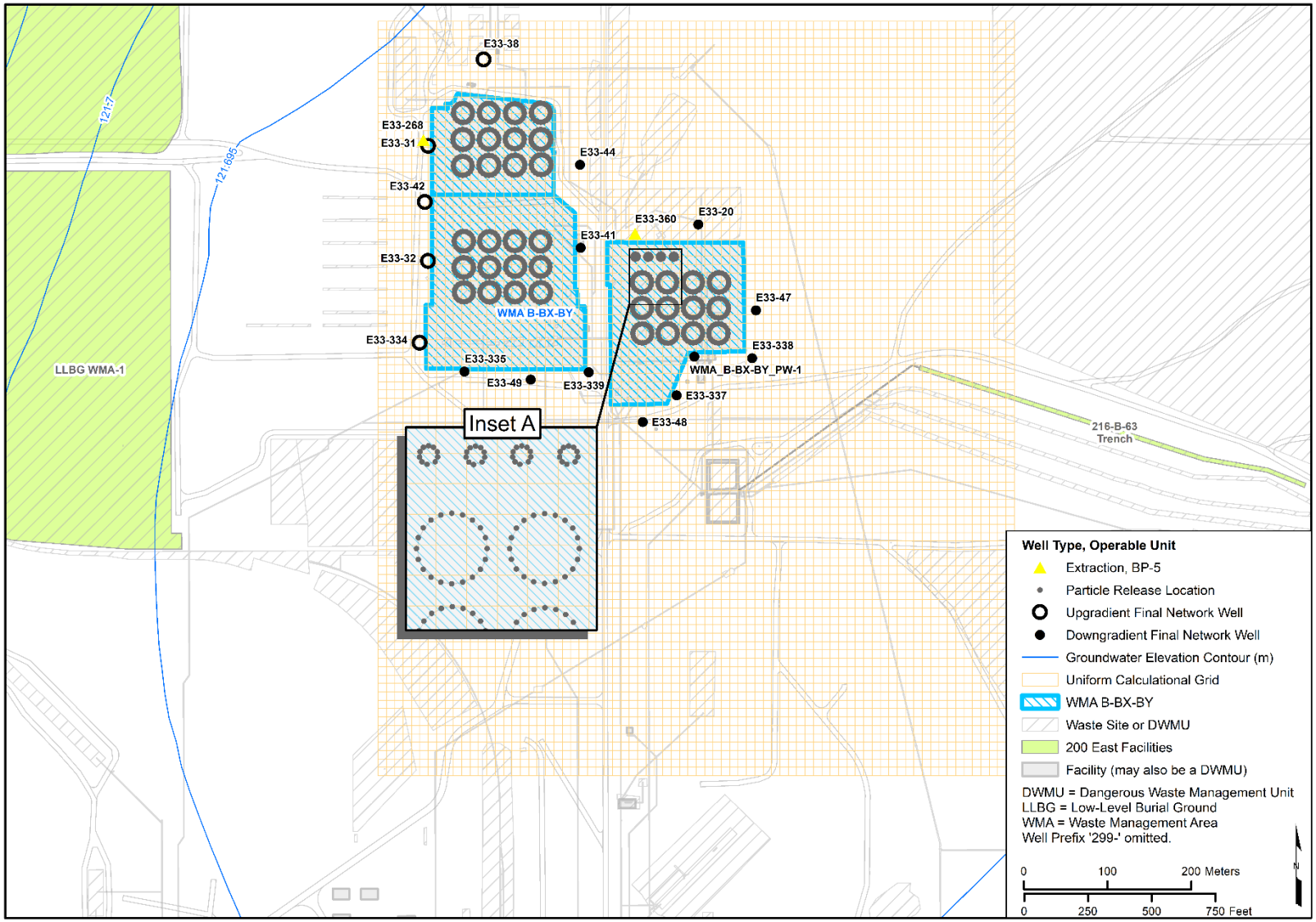


**Figure 7-36. Release Locations and Calculational Grid for SST WMA B-BX-BY**

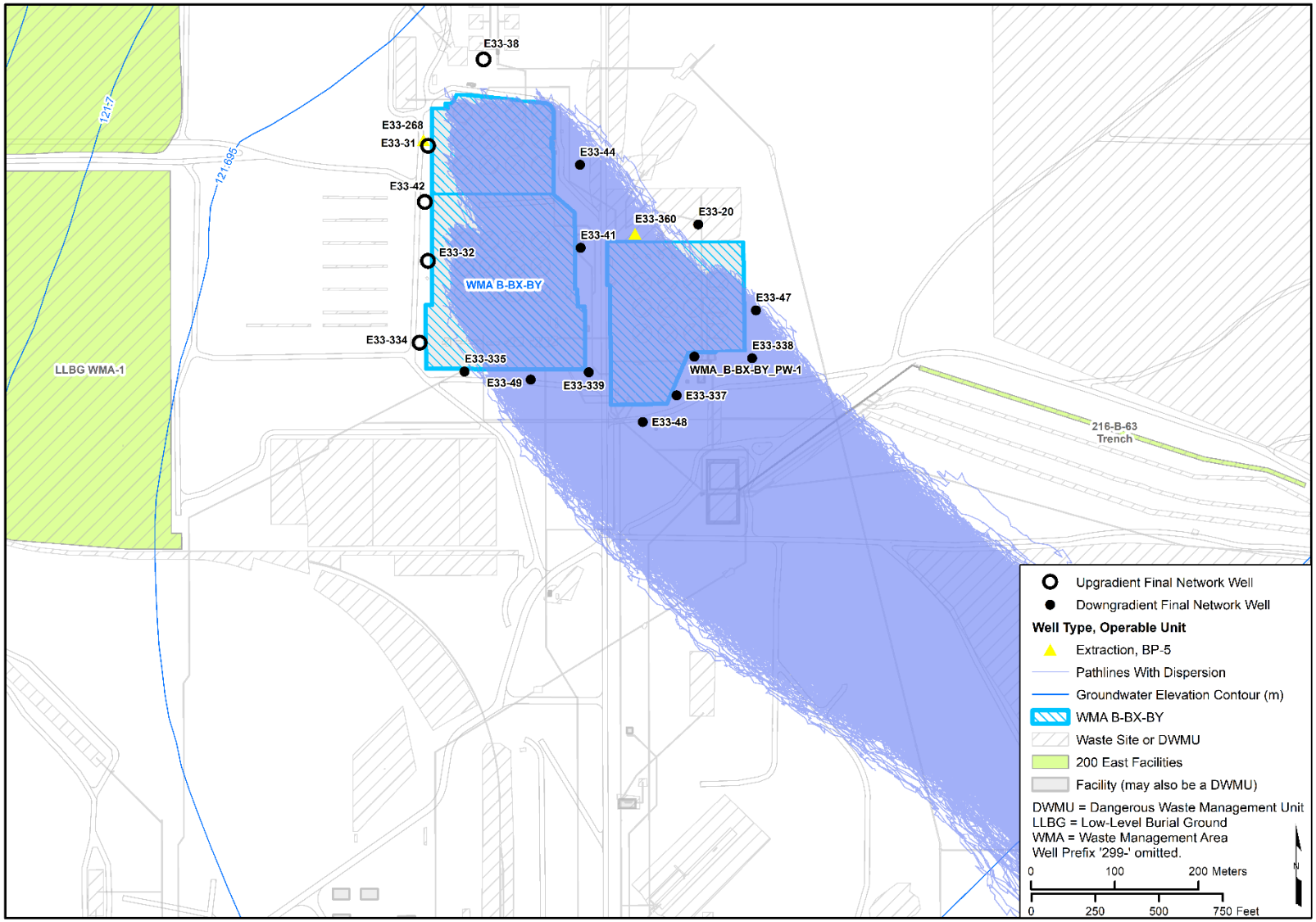


**Figure 7-37. Groundwater Elevations and Particle Pathlines for SST WMA B-BX-BY, 2018**

#### *7.9.2.1 Particle Tracking*

After the groundwater elevation contour maps and underlying piecewise continuous elevation grids were prepared using TRIM, particle tracking was implemented using both advection and dispersion. The particle pathlines that were produced depict the patterns of spreading that might accompany the contaminant migration near the unit for the flow conditions in 2018. Figure 7-37 shows the particle pathlines developed based on the groundwater elevations prepared throughout the 200 East Area using TRIM. The resulting maps were prepared based on the release of 20 particles from each starting location to provide the high density of particles in space and time required for these detailed facility-specific calculations. Figure 7-37 shows the particle pathlines calculated after 1,500 days of travel, by which time most of the particles would have arrived at or passed by the final status groundwater monitoring wells. Figure 7-37 depicts an instantaneous release to the water table from the release locations in SST WMA B-BX-BY to illustrate the adequacy of the well network for monitoring the entire facility.

#### *7.9.2.2 Relative Detectability Map*

To compare the relative density of the particles that pass by each monitoring well location, a relative detectability index was calculated at a subgrid level (described in Section 6.3) and a corresponding contour map was generated. Figure 7-38 shows the relative detectability map developed based on the instantaneous release of a large number of particles at the facility after 1,500 days of calculated travel, by which time all particles would have arrived at or passed by the final status groundwater monitoring wells. Figure 7-38 depicts areas of relatively higher and lower potential impact from a release at the facility that reaches the water table for conditions represented by 2018.

The goal of well placement is for well locations to span the range of detectable areas downgradient of SST WMA B-BX-BY. The relative detectability map shows that under the evaluated range of conditions, the final status well network continues to meet this goal.

## 7.10 Single-Shell Tank Waste Management Area C Input and Results

Section 4.2 describes the general input for the calculations for SST WMA C. The following discussion describes the particle starting locations and calculational grid used. The results developed from the calculations specific to SST WMA C are also presented.

The SST WMA C, located in the east-central part of the 200 East Area, consists of the C Tank Farm. The tank farm is composed of 16 SSTs and ancillary liquid-handling equipment including diversion boxes, a vault, a catch tank, a french drain, dry wells, and piping. The C Tank Farm contains 16 SSTs, 4 of which have smaller capacities.

The SST WMA C final status monitoring network (Figure 7-39) was determined in SGW-60588, *Engineering Evaluation Report for Single-Shell Tank Waste Management Area Groundwater Monitoring*, and consists of four upgradient wells (existing wells 299-E27-12, 299-E27-15, 299-E27-22, and 299-E27-26) and eight downgradient wells (existing wells 299-E27-13, 299-E27-14, 299-E27-21, 299-E27-23, 299-E27-24, 299-E27-155; and proposed wells WMA_C_PW-1 and WMA_C_PW-2).

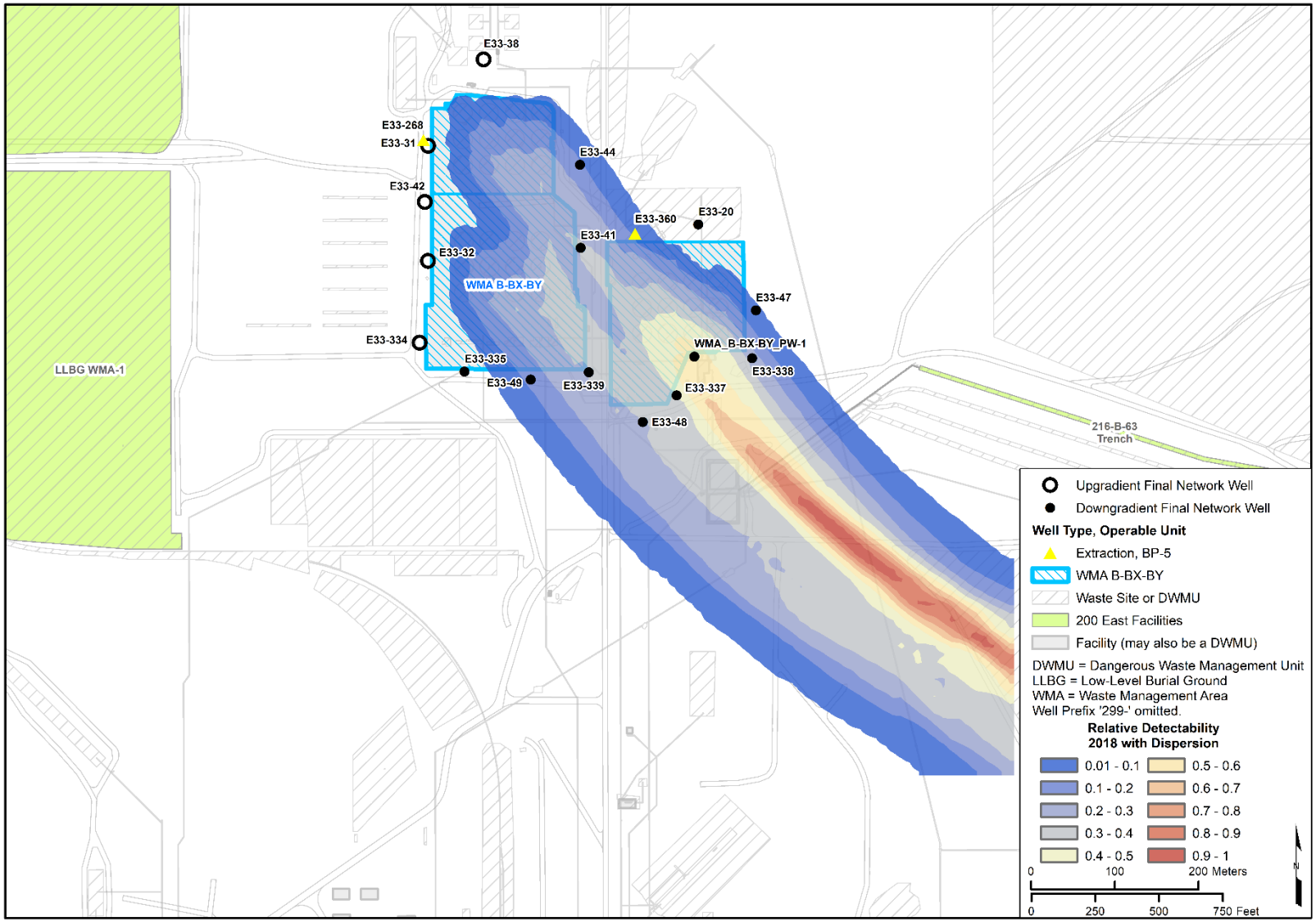


**Figure 7-38. Relative Detectability Map for SST WMA B-BX-BY, 2018**

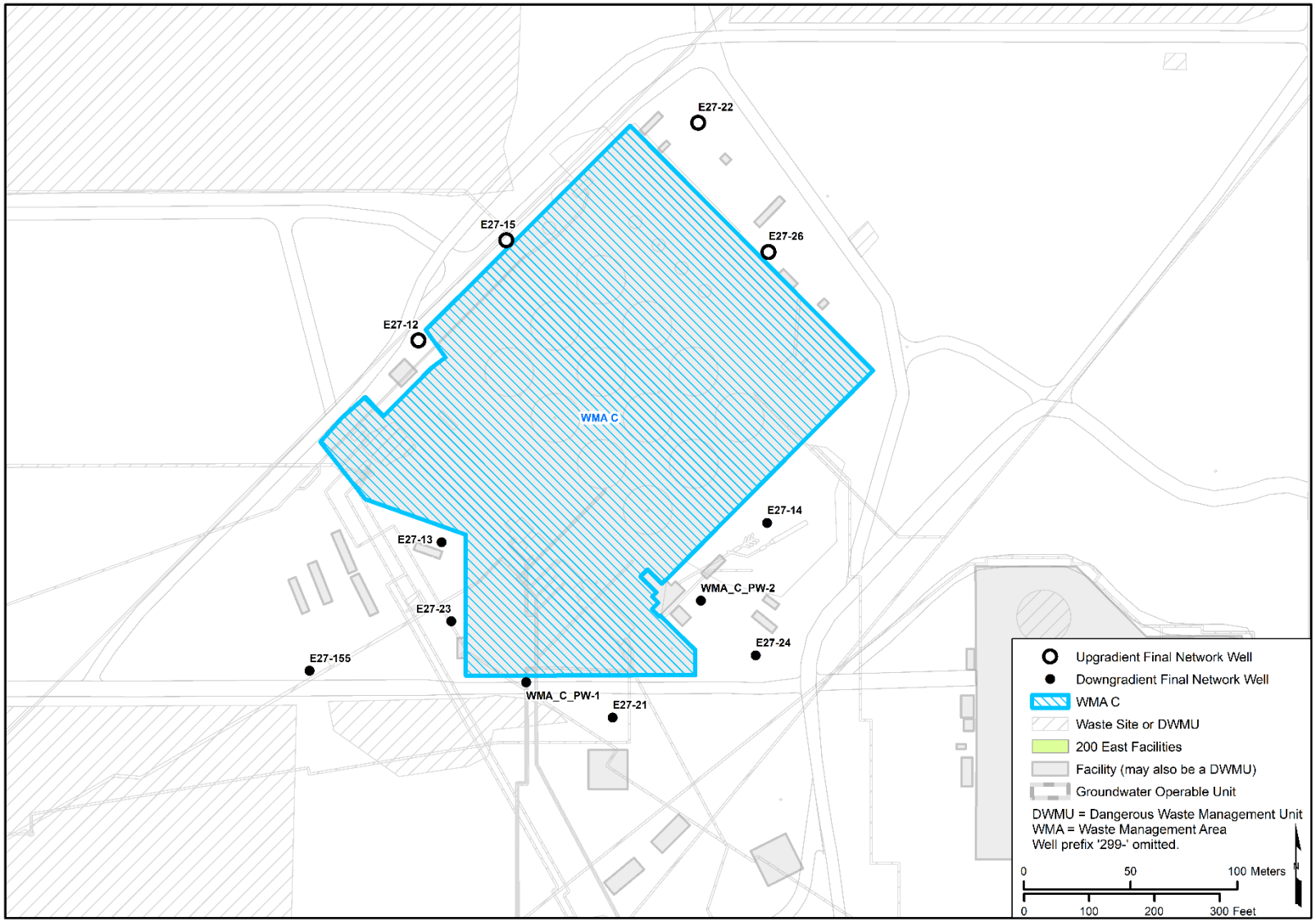


**Figure 7-39. Final Status Monitoring Network for SST WMA C**

### 7.10.1 Release Locations and Relative Detectability Grid for Single-Shell Tank Waste Management Area C

The starting locations for the particle-tracking calculations represent the area over which a potential release from a given facility would impact the underlying water table. The particle releases were located at plausible release sites throughout the facility. Twenty particles were released from each release location specified along the centerline of the unit (Figure 7-40) and tracked to provide the density of particles in space and time required for the calculations.

A contour map of relative detectability is generated by counting the number of particles that pass through a pre-defined uniform calculational grid (Figure 7-40). The grid used to develop the relative detectability maps is defined by 10 m by 10 m (33 ft by 33 ft) cells and is oriented to be parallel to the predominant groundwater flow direction at SST WMA C.

### 7.10.2 Results for Single-Shell Tank Waste Management Area C

The groundwater elevation contours shown in Figure 7-1 form the basis for the facility-specific calculations performed in this ECF. The elevations near SST WMA C for 2018 are shown in Figure 7-41, and the outputs of the particle tracking and relative detectability calculations are discussed in the following sections.

#### *7.10.2.1 Particle Tracking*

After the groundwater elevation contour maps and underlying piecewise continuous elevation grids were prepared using TRIM, particle tracking was implemented using both advection and dispersion.
The particle pathlines that were produced depict the patterns of spreading that might accompany the contaminant migration near the unit for the flow conditions in 2018. Figure 7-41 shows the particle pathlines developed based on the groundwater elevations prepared throughout the 200 East Area using TRIM. The resulting maps were prepared based on the release of 20 particles from each starting location to provide the high density of particles in space and time required for these detailed facility-specific calculations. Figure 7-41 shows the particle pathlines calculated after 200 days of travel, by which time most of the particles would have arrived at or passed by the final status groundwater monitoring wells. Figure 7-41 depicts an instantaneous release to the water table from the release locations in SST WMA C to illustrate the adequacy of the well network for monitoring the entire facility.

#### *7.10.2.2 Relative Detectability Map*

To compare the relative density of the particles that pass by each monitoring well location, a relative detectability index was calculated at a subgrid level (described in Section 6.3) and a corresponding contour map was generated. Figure 7-42 shows the relative detectability map developed based on the instantaneous release of a large number of particles at the facility after 200 days of calculated travel, by which time all particles would have arrived at or passed by the final status groundwater monitoring wells. Figure 7-42 depicts areas of relatively higher and lower potential impact from a release at the facility that reaches the water table for conditions represented by 2018.

The goal of well placement is for well locations to span the range of detectable areas downgradient of SST WMA C. The relative detectability map shows that under the evaluated range of conditions, the final status well network continues to meet this goal.

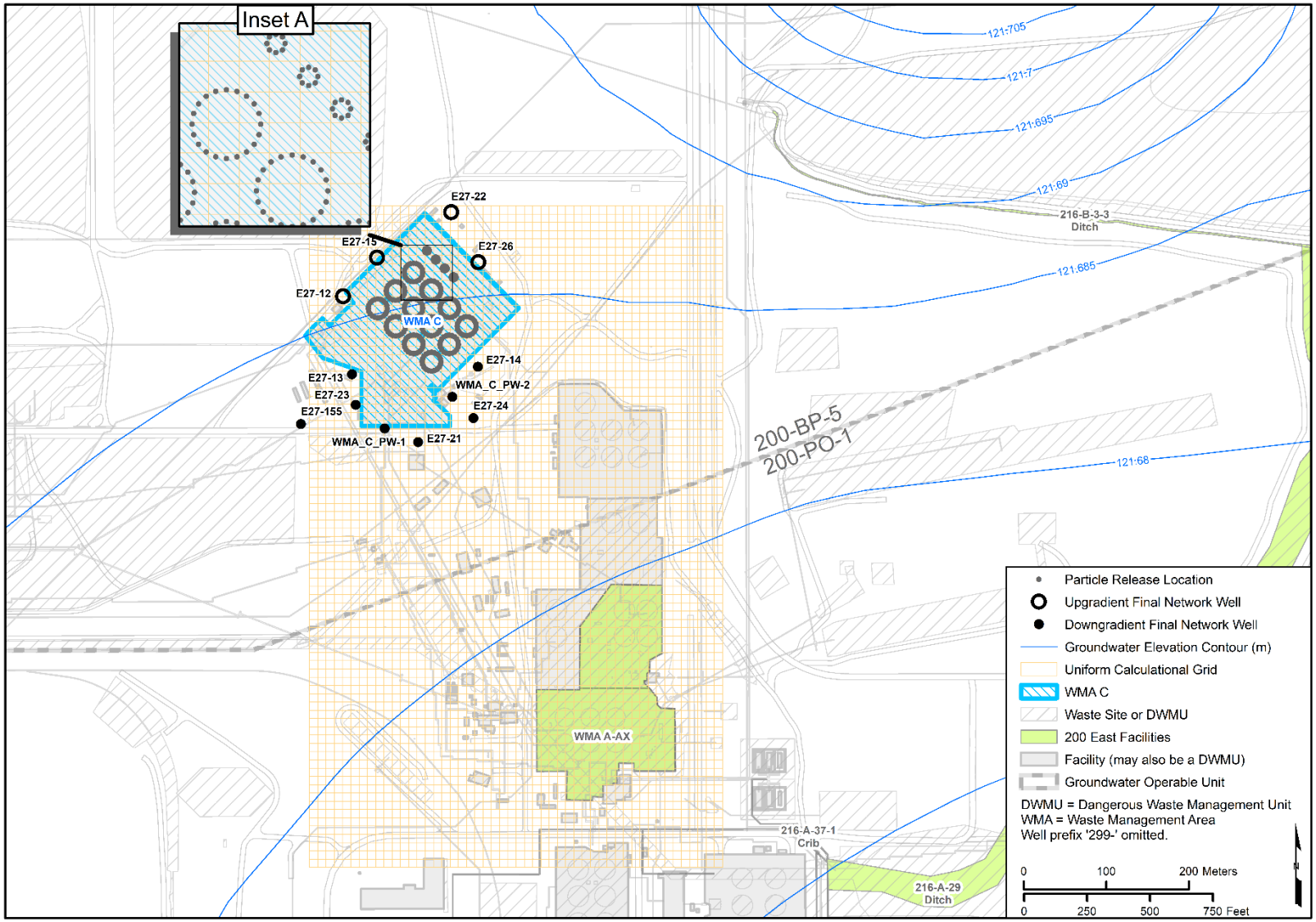


**Figure 7-40. Release Locations and Calculational Grid for SST WMA C**

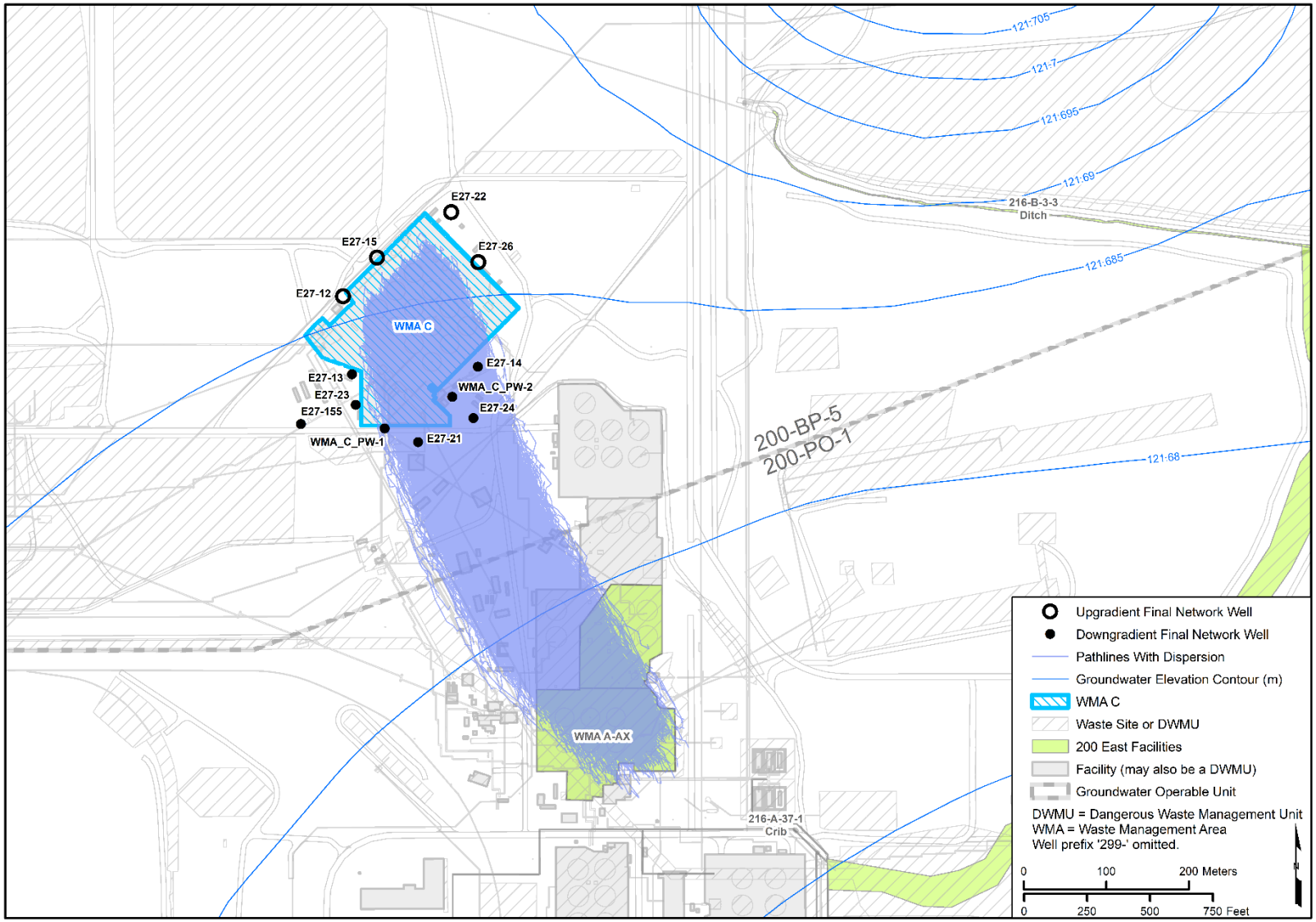


**Figure 7-41. Groundwater Elevations and Particle Pathlines for SST WMA C, 2018**

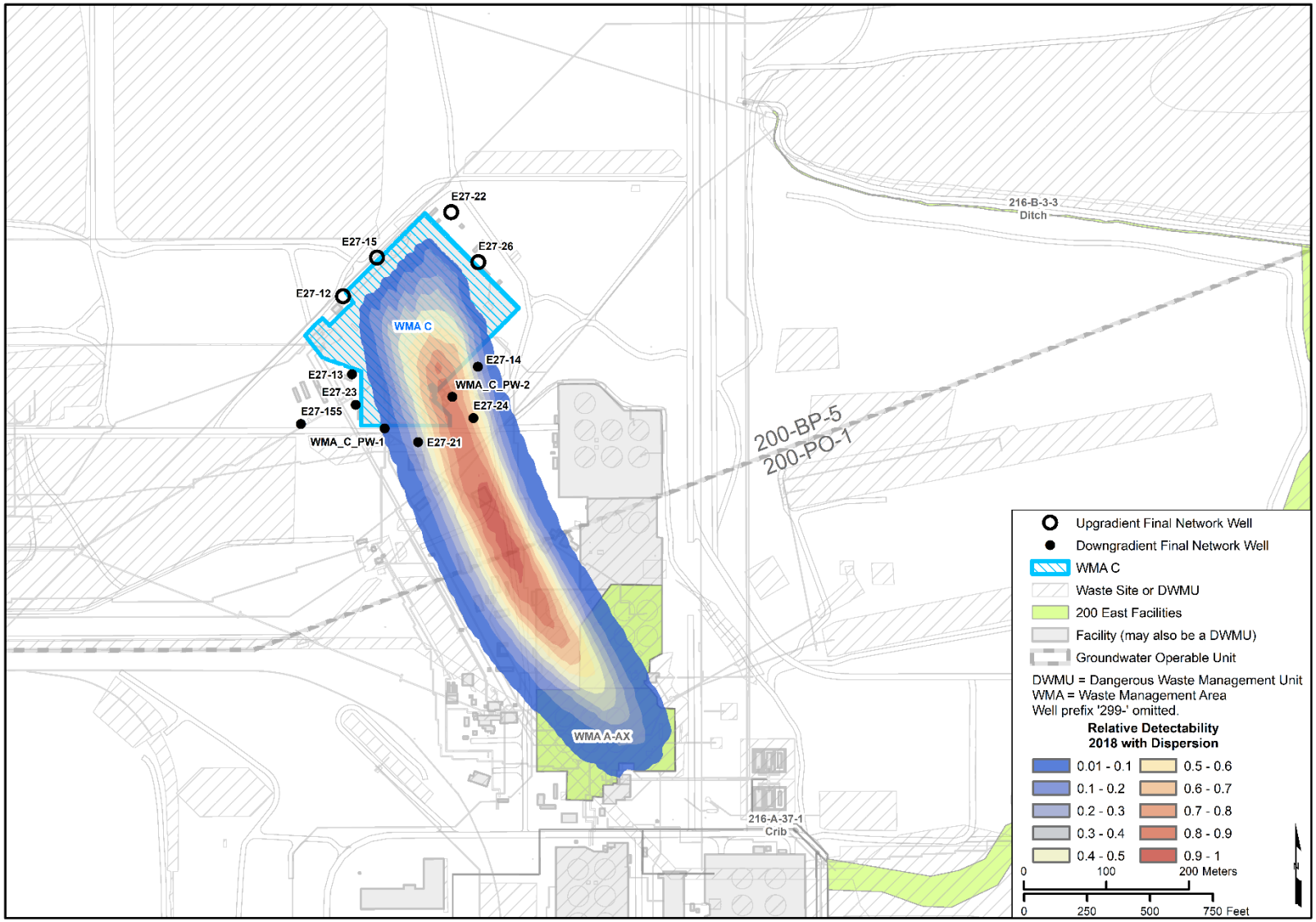


**Figure 7-42. Relative Detectability Map for SST WMA C, 2018**

# 8 References

CHPRC-00257, 2010, *MODFLOW and Related Codes Functional Requirements Document*, Rev. 1, CH2M HILL Plateau Remediation Company, Richland, Washington.

CHPRC-00258, 2015, *MODFLOW and Related Codes Software Management Plan*, Rev. 4, CH2M HILL Plateau Remediation Company, Richland, Washington.

CHPRC-00259, 2014, *MODFLOW and Related Codes Software Test Plan*, Rev. 3, CH2M HILL Plateau Remediation Company, Richland, Washington.

CHPRC-00260, 2014, *MODFLOW and Related Codes Requirements Traceability Matrix*, CHPRC Build 7, Rev. 7, CH2M HILL Plateau Remediation Company, Richland, Washington.

CHPRC-00261, 2014, *MODFLOW and Related Codes Acceptance Test Report*, CHPRC Build 7, Rev. 7, CH2M HILL Plateau Remediation Company, Richland, Washington.

CP-47631, 2018, *Model Package Report: Central Plateau Groundwater Model, Version 8.4.5*, Rev. 4, CH2M HILL Plateau Remediation Company, Richland, Washington. Available at: https://pdw.hanford.gov/arpir/pdf.cfm?accession=0066449H.

DOE, 2016, "Proposal to Address Mixed Waste Containers in the Low-Level Burial Grounds Operating Group," letter from Ray J. Corey to Alexandra K. Smith, Washington State Department of Ecology, U.S. Department of Energy, Richland Operations Office, Richland, Washington, dated December 28. Available at: https://pdw.hanford.gov/arpir/pdf.cfm?accession=0073186H.

DOE/RL-2008-56, 2012, *200 West Area Pre-Conceptual Design for Final Extraction/Injection Well Network: Modeling Analyses*, Rev. 0, U.S. Department of Energy, Richland Operations Office, Richland, Washington. Available at: https://pdw.hanford.gov/arpir/pdf.cfm?accession=0081011H.

DOE/RL-2008-59, 2017, *Interim Status Groundwater Monitoring Plan for the 216-B-3 Pond*, Rev. 2, U.S. Department of Energy, Richland Operations Office, Richland, Washington. Available at: https://pdw.hanford.gov/arpir/pdf.cfm?accession=0066771H.

DOE/RL-2010-92, 2017, *Interim Status Groundwater Monitoring Plan for the 216-A-37-1 PUREX Plant Crib*, Rev. 3, U.S. Department of Energy, Richland Operations Office, Richland, Washington. Available at: https://pdw.hanford.gov/arpir/pdf.cfm?accession=0066775H.

DOE/RL-2010-93, 2016, *Interim Status Groundwater Monitoring Plan for the 216-A-36B PUREX Plant Crib*, Rev. 2, U.S. Department of Energy, Richland Operations Office, Richland, Washington. Available at: https://pdw.hanford.gov/arpir/pdf.cfm?accession=0073381H.

DOE/RL-2012-57, 2012, *Annual Summary of the Integrated Disposal Facility Performance Assessment 2012*, Rev. 0, U.S. Department of Energy, Richland Operations Office, Richland, Washington. Available at: https://www.osti.gov/servlets/purl/1363963.

DOE/RL-2015-49, 2016, *Interim-Status Groundwater Quality Assessment Plan for the Single-Shell Tank Waste Management Area A-AX*, Rev. 0, U.S. Department of Energy, Richland Operations Office, Richland, Washington. Available at: https://pdw.hanford.gov/arpir/pdf.cfm?accession=0073187H.

DOE/RL-2016-66, 2017, *Hanford Site RCRA Groundwater Monitoring Report for 2016*, Rev. 0, U.S. Department of Energy, Richland Operations Office, Richland, Washington. Available at: https://pdw.hanford.gov/arpir/pdf.cfm?accession=0072146H.

Doherty, J., 2015, *Calibration and Uncertainty Analysis for Complex Environmental Models, PEST: Complete Theory and What it Means for Modelling the Real World*, Watermark Numerical Computing, Brisbane, Australia.

Doherty, J., 2016, *PEST Model-Independent Parameter Estimation User Manual Part I: PEST, SENSAN, and Global Optimisers*, Watermark Numerical Computing, Brisbane, Australia.

ECF-200E-18-0066, 2018, *Groundwater Flow and Migration Calculations to Assess Monitoring Networks in the 200 East Area Dangerous Waste Management Units*, Rev. 0, CH2M HILL Plateau Remediation Company, Richland, Washington. Available at: https://pdw.hanford.gov/arpir/pdf.cfm?accession=0064076H.

ECF-200E-18-0085, 2019, *Water Level Mapping and Hydraulic Gradient Calculations for 200 East Area RCRA Sites, 2018*, Rev. 0, CH2M HILL Plateau Remediation Company, Richland, Washington. Available at: https://pdw.hanford.gov/arpir/pdf.cfm?accession=AR-02370.

ECF-HANFORD-13-0029, 2018, *Development of the Hanford South Geologic Framework Model, Hanford Site, Washington*, Rev. 5, CH2M HILL Plateau Remediation Company, Richland, Washington. Available at: https://pdw.hanford.gov/arpir/pdf.cfm?accession=0064943H.

EPA, 2016, "Estimated Longitudinal Dispersivity," *EPA On-line Tools for Site Assessment*, modified February 23, 2016, U.S. Environmental Protection Agency, Washington D.C. Available at: https://www3.epa.gov/ceampubl/learn2model/part-two/onsite/longdisp.html.

Gelhar, Lynn W., Claire Welty, and Kenneth R. Rehfeldt, 1992, "A Critical Review of Data on Field-Scale Dispersion in Aquifers," *Water Resources Research* 28(7):1955-1974. Available at: http://www.cof.orst.edu/cof/fe/watershd/fe537/labs_2007/gelhar_etal_reviewfieldScaleDispersion_WRR1992.pdf.

Hansen, P.C., 2000, *The L-curve and its use in the numerical treatment of inverse problems*, Department of Mathematical Modelling, Technical University of Denmark, Lyngby, Denmark. Available at: https://www.sintef.no/globalassets/project/evitameeting/2005/lcurve.pdf.

HydroAlgorithmics, 2016, *AlgoMesh User Guide*, HydroAlgorithmics Pty Ltd, Canberra, Australia. Available at: https://static1.squarespace.com/static/569e33fad82d5e0d877c25d7/t/57b28ab6579fb3a225563e6e/1471318805055/AlgoMesh+User+Guide+v1.2.pdf.

Menke, William, 2018, *Geophysical Data Analysis: Discrete Inverse Theory*, Fourth Edition, Academic Press, Cambridge, Massachusetts.

Mitchell, Andy, 1999, *The ESRI Guide to GIS Analysis, Volume 1: Geographic Patterns & Relationships*, First Edition, Environmental Systems Research Institute, Inc., Redlands, California.

Muffels, Christopher, Leland Scantlelbury, Xiaomin Wang, Matthew Tonkin, Christopher Neville, Muhammad Ramadhan, and James R. Craig, 2018, *User's Guide for mod-PATH3DU, A Groundwater Path and Travel-Time Simulator*, S.S. Papadopulos & Associates, Inc., Bethesda, Maryland. Available at: http://mp3du.sspa.com/man/.

NAVD88, 1988, *North American Vertical Datum of 1988*, National Geodetic Survey, Federal Geodetic Control Committee, Silver Spring, Maryland. Available at: https://www.ngs.noaa.gov/datums/vertical/.

Nichols, Eric M. and Tracy L. Roth, 2006, *Downward Solute Plume Migration: Assessment, Significance, and Implications for Characterization and Monitoring of "Diving Plumes,"* API Soil and Groundwater Technical Task Force Bulletin 24, American Petroleum Institute, Washington, D.C. Available at: https://www.api.org/environment-health-and-safety/clean-water/ground-water/~/media/f1074760be2a4f769029349c81f8defd.ashx.

Panday, Sorab, Christian D. Langevin, Richard G. Niswonger, Motomu Ibaraki, and Joseph D. Hughes, 2013, "MODFLOW-USG Version 1: An Unstructured Grid Version of MODFLOW for Simulating Groundwater Flow and Tightly Coupled Processes Using a Control Volume Finite-Difference Formulation," *U.S. Geological Survey Techniques and Methods*, Book 6, Chap. A45, U.S. Geological Survey, Reston, Virginia.

PNNL-15479, 2005, *Groundwater Monitoring Plan for the Hanford Site 216-B-3 Pond RCRA Facility*, Pacific Northwest National Laboratory, Richland, Washington. Available at: https://pdw.hanford.gov/arpir/pdf.cfm?accession=DA01649608.

PRC-PRO-IRM-309, 2014, *Controlled Software Management*, Revision 5, Change 0, CH2M HILL Plateau Remediation Company, Richland, Washington.

*Resource Conservation and Recovery Act of 1976*, 42 USC 6901, et seq. Pub. L. 94-580, 90 Stat. 2795. Available at: https://elr.info/sites/default/files/docs/statutes/full/rcra.pdf.

Rumbaugh, J.O. and D.B. Rumbaugh, 2017, *Groundwater Vistas Version 7*, Environmental Simulations, Inc., Reinholds, Pennsylvania.

SGW-54165, 2014, *Evaluation of the Unconfined Aquifer Hydraulic Gradient Beneath the 200 East Area, Hanford Site*, Rev. 0, CH2M HILL Plateau Remediation Company, Richland, Washington. Available at: https://pdw.hanford.gov/arpir/pdf.cfm?accession=0085682.

SGW-60586, *Engineering Evaluation Report for Single-Shell Tank Waste Management Area A-AX Groundwater Monitoring*, Rev. 0 pending, CH2M HILL Plateau Remediation Company, Richland, Washington.

SGW-60587, *Engineering Evaluation Report for Single-Shell Tank Waste Management Area B-BX-BY Groundwater Monitoring*, Rev. 0 pending, CH2M HILL Plateau Remediation Company, Richland, Washington.

SGW-60588, *Engineering Evaluation Report for Single-Shell Tank Waste Management Area C Groundwater Monitoring*, Rev. 0 pending, CH2M HILL Plateau Remediation Company, Richland, Washington.

SGW-60590, *Engineering Evaluation Report for Low-Level Burial Grounds Waste Management Area-1 Green Islands Groundwater Monitoring*, Rev. 0 pending, CH2M HILL Plateau Remediation Company, Richland, Washington.

SGW-60591, *Engineering Evaluation Report for the 216-B-3 Main Pond Groundwater Monitoring*, Rev. 0 pending, CH2M HILL Plateau Remediation Company, Richland, Washington.

SGW-60592, *Engineering Evaluation Report for the 216-A-29 Ditch Groundwater Monitoring*, Rev. 0 pending, CH2M HILL Plateau Remediation Company, Richland, Washington.

SGW-60593, *Engineering Evaluation Report for the 216-A-37-1 Crib Groundwater Monitoring*, Rev. 0 pending, CH2M HILL Plateau Remediation Company, Richland, Washington.

SGW-60594, *Engineering Evaluation Report for the 216-B-63 Trench Groundwater Monitoring*, Rev. 0 pending, CH2M HILL Plateau Remediation Company, Richland, Washington.

SGW-60595, *Engineering Evaluation Report for the 216-A-36B Crib Groundwater Monitoring*, Rev. 0 pending, CH2M HILL Plateau Remediation Company, Richland, Washington.

SGW-62007, *Engineering Evaluation Report for the Integrated Disposal Facility Groundwater Monitoring*, Rev. 0 pending, CH2M HILL Plateau Remediation Company, Richland, Washington.

Tikhonov, A.N. and V.Y. Arsenin, 1977, *Solutions of Ill-Posed Problems*, Halsted Press, New York.

Tonkin, Matthew James and John Doherty, 2005, "A Hybrid Regularized Inversion Methodology for Highly Parameterized Environmental Models," *Water Resources Research* 41(10).

WAC 173-303, "Dangerous Waste Regulations," *Washington Administrative Code*, Olympia, Washington. Available at: https://apps.leg.wa.gov/WAC/default.aspx?cite=173-303

Xu, Moujin Jimmy and Yoram Eckstein, 1995, "Use of Weighted Least-Squares Method in Evaluation of the Relationship Between Dispersivity and Field Scale," *Groundwate*r 33(6):905-908. Available at: https://www.researchgate.net/publication/227611817_Use_of_Weighted_Least-Squares_Method_in_Evaluation_of_the_Relationship_Between_Dispersivity_and_Field_Scale.

Zheng, C. and P.P. Wang, 1999, *MT3DMS: A Modular Three-Dimensional Multispecies Transport Model for Simulation of Advection, Dispersion, and Chemical Reactions of Contaminants in Groundwater Systems; Documentation and User's Guide*, Contract Report SERDP-99-1, U.S. Army Engineer Research and Development Center, U.S. Army Corps of Engineers, Vicksburg, Mississippi. Available at: http://hydro.geo.ua.edu/mt3d/mt3dmanual.pdf.

# Appendix A

# Measured Water Levels Used as Inputs to the Groundwater-Level Analysis

This page intentionally left blank.

**Table A-1. Average Monthly and Annual Water Levels for 200 East Area Wells**

| Well Name | Average Monthly Measured Water Levels (NAVD88 [m]) | | | | | | | | | | | | CY 2018 Average |
|---|---|---|---|---|---|---|---|---|---|---|---|---|---|
| | Jan | Feb | Mar | Apr | May | Jun | Jul | Aug | Sep | Oct | Nov | Dec | |
| 299-E17-18 | NM | 121.661 | 121.662 | 121.632 | 121.664 | 121.675 | 121.682 | 121.655 | 121.653 | 121.634 | 121.652 | 121.659 | 121.657 |
| 299-E17-21 | 121.649 | 121.688 | 121.654 | NM | 121.710 | 121.711 | 121.724 | 121.705 | 121.685 | 121.670 | 121.706 | 121.664 | 121.688 |
| 299-E17-22 | NM | 121.679 | 121.684 | 121.676 | 121.687 | 121.696 | 121.703 | 121.683 | 121.666 | 121.650 | 121.686 | 121.687 | 121.682 |
| 299-E17-23 | NM | 121.684 | 121.684 | 121.647 | 121.682 | 121.697 | 121.702 | 121.704 | 121.669 | 121.606 | 121.667 | 121.603 | 121.668 |
| 299-E17-25 | NM | 121.696 | 121.698 | 121.661 | 121.691 | 121.707 | 121.714 | 121.692 | 121.677 | 121.616 | 121.719 | 121.695 | 121.688 |
| 299-E18-2 | 121.740 | 121.732 | 121.739 | NM | 121.753 | 121.737 | 121.766 | 121.755 | 121.727 | 121.708 | 121.768 | 121.732 | 121.742 |
| 299-E23-1 | 121.669 | 121.677 | 121.680 | 121.650 | 121.676 | 121.679 | 121.698 | 121.680 | 121.661 | 121.646 | 121.693 | 121.630 | 121.670 |
| 299-E24-16 | 121.704 | 121.698 | 121.705 | 121.682 | 121.708 | 121.701 | 121.721 | 121.700 | 121.725 | 121.662 | 121.722 | 121.705 | 121.703 |
| 299-E24-18 | NM | 121.672 | 121.666 | 121.656 | 121.674 | 121.687 | 121.692 | 121.666 | 121.662 | 121.642 | 121.663 | 121.673 | 121.668 |
| 299-E24-21 | NM | 121.682 | 121.681 | 121.668 | 121.684 | 121.693 | NM | 121.683 | 121.669 | 121.660 | 121.676 | 121.681 | 121.678 |
| 299-E24-22 | 121.723 | 121.672 | NM | NM | 121.679 | 121.679 | NM | 121.674 | 121.662 | 121.652 | 121.698 | 121.663[a] | 121.678 |
| 299-E24-24 | NM | 121.686 | 121.691 | 121.668 | 121.688 | 121.691 | NM | 121.687 | 121.677 | 121.657 | 121.695 | 121.649 | 121.679 |
| 299-E24-25 | 121.683 | 121.664 | 121.658 | 121.636 | 121.683 | 121.665 | 121.651 | 121.677 | 121.657 | 121.658 | 121.669 | 121.643 | 121.662 |
| 299-E24-33 | 121.727 | 121.676 | 121.674 | NM | 121.686 | 121.690 | NM | 121.678 | 121.668 | 121.652 | 121.702 | 121.700 | 121.685 |
| 299-E25-19 | 121.723 | 121.684 | 121.682 | 121.667 | 121.666 | 121.691 | 121.684 | 121.677 | 121.685 | 121.658 | 121.711 | 121.716 | 121.687 |
| 299-E25-24 | 121.719 | 121.686 | 121.691 | 121.669 | 121.676 | 121.685 | 121.686 | 121.674 | 121.687 | 121.666 | 121.704 | 121.714 | 121.688 |
| 299-E25-25 | NM | NM | NM | 121.681 | NM | NM | NM | NM | NM | 121.694 | NM | NM | 121.688 |
| 299-E25-34 | 121.693 | 121.668 | 121.675 | 121.672 | 121.675 | 121.685 | 121.677 | 121.690 | 121.676 | 121.668 | 121.693 | 121.685 | 121.680 |
| 299-E25-35 | 121.711 | 121.672 | 121.673 | NM | 121.681 | 121.679 | 121.674 | 121.671 | NM | 121.670 | 121.698 | 121.701 | 121.683 |
| 299-E25-93 | 121.700 | 121.669 | 121.668 | NM | 121.684 | 121.681 | NM | 121.675 | 121.666 | 121.650 | 121.694 | 120.663 | 121.676 |
| 299-E26-10 | 121.722 | 121.697 | 121.704 | 121.717 | 121.702 | 121.731 | 121.708 | NM | NM | NM | NM | NM | 121.712 |
| 299-E26-13 | 121.701 | 121.676 | 121.690 | 121.689 | 121.686 | 121.703 | 121.683 | 121.699 | 121.684 | 121.675 | 121.697 | 121.687 | 121.689 |
| 299-E26-14 | 121.799 | 121.778 | 121.782 | 121.772 | 121.789 | 121.797 | NM | NM | NM | 121.797 | 121.797 | 121.797 | 121.790 |
| 299-E26-15 | 121.730 | NM | 121.710 | NM | 121.679 | NM | NM | NM | 121.706 | 121.708 | 121.705 | NM | 121.706 |

**Table A-1. Average Monthly and Annual Water Levels for 200 East Area Wells**

| Well Name | Average Monthly Measured Water Levels (NAVD88 [m]) | | | | | | | | | | | | CY 2018 Average |
|---|---|---|---|---|---|---|---|---|---|---|---|---|---|
| | Jan | Feb | Mar | Apr | May | Jun | Jul | Aug | Sep | Oct | Nov | Dec | |
| 299-E26-4 | NM | NM | 121.673 | 121.687 | 121.682 | 121.696 | 121.678 | 121.691 | 121.682 | 121.666 | 121.693 | 121.688 | 121.684 |
| 299-E26-79 | 121.733 | 121.721 | 121.721 | 121.714 | 121.723 | 121.741 | NM | NM | NM | 121.736 | NM | NM | 121.727 |
| 299-E27-12 | 121.706 | 121.679 | 121.683 | NM | 121.674 | 121.687 | 121.674 | 121.683 | 121.678 | 121.661 | 121.707 | 121.683 | 121.683 |
| 299-E27-14 | 121.711 | 121.676 | 121.678 | 121.669 | 121.687 | 121.685 | 121.679 | 121.680 | 121.673 | 121.659 | 121.699 | 121.681 | 121.681 |
| 299-E27-15 | 121.705 | 121.681 | 121.680 | 121.669 | 121.675 | 121.688 | 121.682 | 121.685 | 121.676 | 121.663 | 121.698 | 121.688 | 121.682 |
| 299-E27-17 | 121.715 | 121.692 | 121.677 | 121.675 | 121.668 | 121.694 | 121.694 | 121.687 | 121.685 | 121.665 | 121.702 | 121.689 | 121.687 |
| 299-E27-18 | 121.716 | 121.693 | 121.690 | 121.676 | 121.754 | 121.697 | 121.693 | 121.703 | 121.693 | 121.677 | 121.696 | 121.703 | 121.699 |
| 299-E27-21 | 121.707 | 121.676 | 121.664 | 121.658 | NM | 121.677 | 121.675 | 121.663 | 121.657 | 121.649 | 121.695 | 121.676 | 121.672 |
| 299-E27-22 | 121.730 | 121.709 | 121.706 | 121.691 | 121.692 | 121.716 | 121.711 | 121.712 | 121.703 | 121.689 | 121.725 | 121.707 | 121.708 |
| 299-E27-23 | 121.712 | 121.674 | 121.677 | 121.658 | 121.679 | 121.684 | 121.678 | NM | 121.665 | 121.652 | 121.695 | 121.677 | 121.677 |
| 299-E27-7 | 121.722 | 121.684 | 121.682 | 121.670 | NM | 121.687 | 121.683 | 121.678 | NM | 121.657 | 121.973[b] | 121.674 | 121.682 |
| 299-E27-8 | 121.717 | 121.682 | 121.688 | 121.671 | 121.677 | 121.695 | 121.690 | 121.699 | 121.693 | 121.672 | 121.696 | 121.702 | 121.690 |
| 299-E27-9 | 121.713 | 121.682 | 121.688 | 121.673 | 121.701 | NM | 121.691 | 121.695 | NM | 121.671 | 121.700 | 121.696 | 121.691 |
| 299-E28-1 | 121.691[c] | 121.695 | 121.702 | 121.666 | 121.703 | 121.686 | NM | 121.735[c] | 121.682 | 121.656 | 121.689 | 121.661 | 121.682 |
| 299-E28-17 | 121.689 | 121.679 | 121.686 | 121.654 | 121.689 | 121.693 | 121.698 | 121.705 | 121.684 | NM | 121.712 | 121.711 | 121.691 |
| 299-E28-18 | 121.713 | 121.702 | 121.708 | 121.676 | 121.711 | 121.707 | 121.719 | NM | 121.700 | 121.685 | 121.721 | 121.715 | 121.705 |
| 299-E28-27 | 121.708 | 121.691 | 121.696 | 121.669 | 121.706 | 121.700 | NM | 121.701 | 121.696 | 121.676 | 121.706 | 121.702 | 121.696 |
| 299-E29-54 | NM | 121.680 | 121.685 | 121.652 | NM | NM | NM | NM | NM | NM | NM | NM | 121.672 |
| 299-E32-5 | 121.718 | 121.692 | 121.707 | 121.676 | 121.714 | 121.698 | NM | 121.713 | 121.710 | 121.689 | 121.720 | 121.715 | 121.705 |
| 299-E32-6 | 121.724 | 121.697 | 121.705 | 121.680 | 121.716 | 121.702 | 121.720 | 121.715 | 121.714 | 121.695 | 121.720 | 121.713 | 121.708 |
| 299-E32-8 | 121.731 | 121.703 | 121.712 | 121.688 | 121.719 | 121.707 | 121.726 | 121.722 | 121.719 | 121.705 | 121.727 | 121.718 | 121.715 |
| 299-E33-14 | 121.714 | 121.690 | 121.698 | 121.671 | 121.681 | 121.688 | 121.708 | 121.700 | 121.692 | 121.679 | 121.706 | 121.701 | 121.694 |
| 299-E33-267 | NM | 121.693 | NM | 121.676 | 121.688 | 121.689 | 121.716 | NM | NM | NM | NM | NM | 121.692 |
| 299-E33-28 | 121.701 | 121.691 | 121.697 | 121.678 | 121.694 | 121.700 | 121.710 | 121.708 | 121.698 | 121.686 | 121.707 | 121.703 | 121.698 |

## Table A-1. Average Monthly and Annual Water Levels for 200 East Area Wells

| Well Name | Average Monthly Measured Water Levels (NAVD88 [m]) | | | | | | | | | | | | CY 2018 Average |
|---|---|---|---|---|---|---|---|---|---|---|---|---|---|
| | Jan | Feb | Mar | Apr | May | Jun | Jul | Aug | Sep | Oct | Nov | Dec | |
| 299-E33-31 | 121.705 | 121.698 | 121.674 | 121.676 | 121.675 | 121.688 | 121.709 | NM | NM | NM | 121.697 | NM | 121.690 |
| 299-E33-32 | 121.707 | 121.691 | 121.687 | 121.670 | 121.685 | 121.687 | 121.706 | NM | NM | NM | 121.677 | NM | 121.689 |
| 299-E33-339 | 121.709 | 121.687 | 121.686 | 121.669 | 121.686 | 121.690 | 121.708 | 121.699 | 121.683 | 121.678 | 121.689 | 121.698 | 121.690 |
| 299-E33-34 | 121.720 | 121.701 | 121.709 | 121.684 | 121.697 | 121.702 | 121.719 | 121.717 | 121.704 | 121.695 | 121.720 | NM | 121.706 |
| 299-E33-342 | 121.712 | 121.688 | 121.692 | 121.658 | 121.687 | 121.692 | 121.709 | NM | NM | NM | 121.684 | NM | 121.690 |
| 299-E33-37 | 121.719 | 121.695 | 121.689 | 121.679 | 121.694 | 121.698 | 121.692 | 121.706 | 121.676 | 121.680 | 121.693 | NM | 121.693 |
| 299-E33-38 | 121.715 | 121.693 | 121.695 | 121.679 | 121.692 | 121.700 | 121.712 | 121.705 | 121.700 | 121.685 | 121.695 | NM | 121.697 |
| 299-E33-41 | 121.704 | 121.684 | 121.684 | 121.666 | 121.684 | 121.688 | 121.702 | NM | NM | NM | 121.672 | NM | 121.686 |
| 299-E33-42 | 121.709 | 121.692 | 121.686 | 121.684 | 121.685 | 121.690 | 121.709 | NM | NM | NM | 121.680 | NM | 121.692 |
| 299-E33-44 | 121.726 | 121.689 | 121.704 | NM | 121.672 | 121.695 | 121.710 | NM | NM | NM | NM | NM | 121.699 |
| 299-E34-10 | 121.722 | 121.691 | 121.693 | 121.680 | 121.690 | 121.695 | 121.695 | 121.706 | 121.695 | 121.678 | 121.799 | 121.707 | 121.704 |
| 299-E34-9 | 121.717 | 121.687 | 121.693 | 121.680 | 121.685 | 121.691 | 121.695 | 121.704 | 121.692 | 121.679 | 121.710 | 121.694 | 121.694 |
| 699-37-43 | 121.674 | 121.638 | 121.645 | 121.635 | 121.627 | 121.650 | 121.642 | 121.642 | 121.637 | 121.615 | 121.645 | 121.688 | 121.645 |
| 699-37-47a | 121.672 | 121.658 | 121.662 | 121.640 | 121.679 | 121.677 | 121.694 | 121.671 | 121.652 | 121.626 | 121.658 | 121.686 | 121.665 |
| 699-49-55a | 121.745 | 121.715 | 121.732 | 121.703 | 121.729 | 121.739[d] | 121.748 | 121.734 | 121.740 | 121.740 | 121.735 | 121.744 | 121.733 |
| 699-49-57a | 121.733 | 121.708 | 121.718 | 121.694 | 121.732 | 121.732[e] | 121.738[f] | 121.738 | 121.738 | 121.727 | 121.731 | 121.730 | 121.723 |

Reference: NAVD88, *North American Vertical Datum of 1988*.

a. For well 299-E24-22, December measured value was deemed to be an outlier and as such was not included in the annual average.

b. For well 299-E27-7, November measured value was deemed to be an outlier and as such was not included in the annual average.

c. For well 299-E28-1, January and August measured values were deemed to be outliers and as such were not included in the annual average.

d. For well 699-49-55a, water level was not measured in June 2018. As such, the average of measured water levels in May and July 2018 was used for the analysis.

e. For well 699-49-57a, water level was not measured in June 2018. As such, the average measured water level from May was used for the analysis.

f. For well 699-49-57a, water level was not measured in July 2018. As such, the average measured water level from August was used for the analysis.

CY = calendar year

NM = not measured

This page intentionally left blank.